Step-wise responses in mesoscopic glassy systems: a mean field approach

Hajime Yoshino[1,2] and Tommaso Rizzo[3,4]

[1]*Laboratoire de Physique Théorique et Hautes Énergies, Jussieu,*
5ème étage, Tour 25, 4 Place Jussieu, 75252 Paris Cedex 05, France
[2]*Department of Earth and Space Science, Faculty of Science, Osaka University, Toyonaka 560-0043, Japan*
[3]*Laboratoire de Physique Théorique de l'Ecole Normale Supérieure, 24 rue Lhomond, 75231 Paris, France*
[4]*"E. Fermi" Center, Compendio del Viminale, Via Panisperna 89 A, 00184, Rome Italy*
yoshino@ess.sci.osaka-u.ac.jp, tommaso.rizzo@inwind.it

We study statistical properties of peculiar responses in glassy systems at mesoscopic scales based on a class of mean-field spin-glass models which exhibit 1 step replica symmetry breaking. Under variation of a generic external field, a finite-sized sample of such a system exhibits a series of step wise responses which can be regarded as a finger print of the sample. We study in detail the statistical properties of the step structures based on a low temperature expansion approach and a replica approach. The spacings between the steps vanish in the thermodynamic limit so that arbitrary small but finite variation of the field induce infinitely many level crossings in the thermodynamic limit leading to a static chaos effect which yeilds a self-averaging, smooth macroscopic response. We also note that there is a strong analogy between the problem of step-wise responses in glassy systems at mesoscopic scales and intermittency in turbulent flows due to shocks.

I. INTRODUCTION

Glassy systems sometimes exhibit anomalously large macroscopic response to external perturbations. In the case of spin-glasses, the most well known effect is the so called *anomaly*: field cooled magnetization is significantly larger than zero field cooled magnetization [1]. Because of the anomaly, aging effects clearlly appear in the magnetization in spin-glasses [2, 3]. Another striking effect is the so called *rejuvenation*. For example spin-glasses aged (relaxed) for a long time can rejuvenate, i. e. restart aging, through small changes of the temperature [4] or of the applied magnetic field [5]. Similar phenomena have been observed in polymer glasses [6, 7, 8, 9], relaxor ferro-electrics [10], deutron glass [11] and other glassy systems.

In order to understand these anomalous macroscopic effects, it is desirable to study what is going on at *mesoscopic* length and time scales. Indeed there is a class of phenomenological theories which *assumes* that mesoscopic excitations called droplets dictate physical xoproperties of glassy systems [12, 13, 14, 15]. It remains as a challenge to find these droplets directly by experimental and theoretical studies. To this end, one must find sensible ways to work directly at mesoscopic scales escaping from the inevitable *self-averaging* mechanism working at larger scales.

Experimental studies of magnetoresistence in mesoscopic spin-glass samples [16] have proved that magnetoresistence provides a *fingerprint* of a given sample reflecting its frozen-in spin-pattern. Quite interestingly changes of statistical weights of a few low lying states under magnetic field has been observed [17], which suggests level crossings among low lying excited states due to the variation of the magnetic field. Mesoscopic measurements also appear promising for other glassy systems such as vorticies in super-conductors[18] and polymer glasses [19].

To make a step forward from a theoretical side, we study in the present paper statistical properties of responses in a class of mean field systems of *finite sizes N*. A great advantage of the mean field approach is that it allows us to obtain results analytically from a given microscopic hamiltonian. It will gives us a generic *mean-field* picture for peculiar properties at mesoscopic scales in glassy systems. The latter may provide us hints to develop *droplet pictures* for broader classes of glassy systems.

Somewhat surprisingly statistical properties of finite sized systems have not been explored extensively in the studies of mean-field models. The present work is motivated by an interesting numerical observation by Kirkpatrik and Young [20] who showed that the magnetization of a finite sized sample of the Sherrington-Kirkpatric (SK) model, that is given by a certain realization of random interaction bonds between the spins, grows in a step-wise manner as a function of the applied magnetic field. Note that in the thermodynamic limit the magnetization curve (per spin), which is a thermodynamic quantity, must converge to a unique limit independent samples. Later it was suggested by Young, Bray and Moore [21] that the fact that linear-susceptibilities are non self-averaging in mean-field models reflects the step-wise responses. Quite interestingly similar observation has been done numerically in directed polymer in random media [22] by Mézard, suggesting that the step-wise response is not a pathology only found in mean-field models. Our work is also motivated by a seminal work by Krzakala and Martin (KM) [24] who considered an extended version of Derrida's random-energy-model (REM) [25] to analyze chaotic resuffling of low lysing states under variation of a generic external field. An important basis of our present work is the idea of generalized complexity introduced in our previous work [26] which is motivated by the work by KM.

In the present paper we focus on a class of mean-field spin-glass models which exhibit 1 step replica symmetry breaking (RSB), which is analytically and physically more tractable than the systems with full RSB such as the SK model mentioned above. By a combination of a low temperature expansion approach and a replica approach we analyze statistical properties of the step-wise responses of finite sized systems. We will identify three characteristic scales for the steps, namely its height (per spin) $\Delta/\sqrt{N}$, width $h_{\rm w} \sim T/\Delta\sqrt{N}$ at temperature T and spacing $h_{\rm s} \sim T_c/\Delta\sqrt{N}$ with T_c being the critical temperature. In the thermodynamic limit $N \to \infty$, the steps become invisible leading to apparently smooth macroscopic response.

The static step-wise response reflects level crossings among low lying metastable-states, which are the solutions of the Thouless-Anderson-Palmer (TAP) equation [28] in the mean-field models, under variation of the external field. In the systems with 1 step RSB, the metastable states have zero overlap with respect to each other meaning that (spin) configurations are completely different on different metastable states. Thus variation of the external field completely change the energy-landscape, called the static chaos effect [12, 13, 34, 36]. It is worth to note that the static chaos effect, which appear at macroscopic scales [26, 35], emerge as step-wise, intermittent responses at mesoscopic scales. Actually step-wise response itself is not at all new in frustrated systesm which oftenly exibit sequence of phase transitions. Most well known example may be the Devil's stair cases in the magnetization curve of the ANNI (axial-next-nearest-neighbour Ising) models [29]. In this respect, a distinct feature of the case of static chaos effect is that there is a *continuous* sequence of steps (phase transitions) in the thermodynamic limit. It is also amusing to note that there is an intimate analogy among the present problem of step-wise responses in glassy systems at mesoscopic scales, jerky effective energy landscape of pinned elastic manifolds [30], and intermittency in turbulent flows due to shocks [31, 32, 33], as we explain in the end of the present paper.

The organization of the paper is as follows. In sec. II we introduce our models and sketch basic features of their step-wise responses. In sec. III we revisit the generalized complexity introduced in [26]. Based on the latter we first discuss macroscopic responses from a general point of view. Then we analyze statistical properties of low lying metastable states which will serve as a basis for the analysis of mesoscopic responses. In sec. IV we analyze statistical properties of the mesoscopic responses by a low temperature expansion scheme. Then in sec. V we analyze the problem again by a replica approach. In sec. VI we discuss connections between our problem and related problems including the intermittency in tubulent flows. In sec. VII we summarize our result and discuss some perspectives. In the appendices we report some details.

II. STEP-WISE RESPONSES IN FINITE SIZED MEAN-FIELD MODELS

In the present paper we consider a generic class of mean field spin-glass models which exhibit static glass transitions with 1 step RSB. By now it is well known that the generic phenology of such a class of models capure quite well static and dynamical properties of real glassy systems [38, 39, 40].

A. p-spin mean-field spin-glass model

As a representative model let us take the p-spin Ising mean-field spin-glass model [25, 44] whose hamiltonian is given by,

$$H = - \sum_{i_1 < i_2 < \ldots i_p} J_{i_1,\ldots,i_p} \sigma_{i_1} \ldots \sigma_{i_p} - h \sum_i \sigma_i. \tag{1}$$

Here σ_i $(i = 1, \ldots, N)$ are Ising variables which are coupled with each other by p-body random interactions $J_{i_1,\ldots,i_p}$ and subjected to an external field of strength h. The coupling $J_{i_1,\ldots,i_p}$ follows a Gaussian distribution with zero mean and variance $J\sqrt{\frac{p!}{2N^{p-1}}}$,

$$\left[J_{i_1,\ldots,i_p}\right] = 0 \qquad \left[J^2_{i_1,\ldots,i_p}\right] = J^2 \frac{p!}{2N^{p-1}} \tag{2}$$

Here and in the following we denote averages over different realizations of the quenched randomness as $[\![\ldots]\!]$.

For $p > 2$ the p-spin Ising model exhibists a static phase transition from the paramagnetic (liquid) phase to glassy phase characterized by 1 step RSB. We note the transition temperature, which is usually interperted as the so called Kauzmann temperature, as T_c in the present paper.

We wish to examine changes of the magnetization

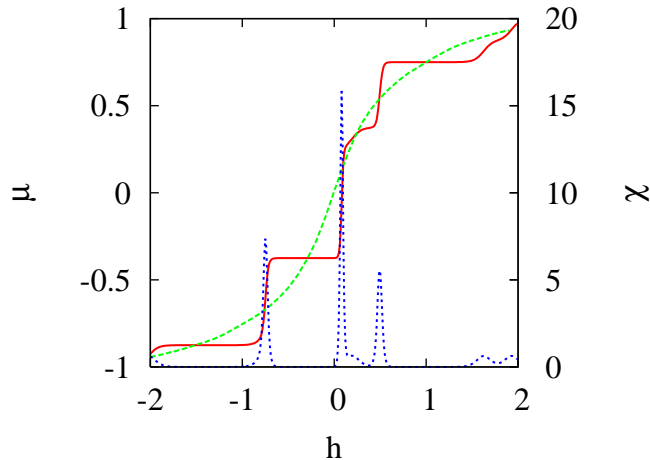$$\mu = \frac{1}{N} \sum_i \langle \sigma_i \rangle \tag{3}$$

FIG. 1: Magnetization curve in a small sample of a $p = 3$ Ising mean-field spin-glass model. The solid step-wise curve is the equilbrium values of the magnetization $m = (1/N) \sum_i \langle S_i \rangle_h$ at $T/J = 0.1$ and at various values of the external field h obained by an exact enumerations of the partition function of a $N = 16$ system. The S shaped line (cross) is obtained by taking averages over large number of samples, which actually has only very weak finite size effects so that it is very close to the thermodynamic one $N \to \infty$. The spiky curves is the linear susceptibility $\chi = (\beta/N) \sum_{ij} (\langle S_i S_j \rangle_h - \langle S_i \rangle_h \langle S_j \rangle_h)$ with $\beta = 1/T$. Similar features have been observed in the SK model ($p = 2$) see [20] and directed polymer in random media [22].

under variation of the extenral field h in *finite sized systems* of N spins at temperatures below T_c. Here and in the following we denote thermal avarages as $\langle \ldots \rangle$. In section V we derive the generating functional for the mesoscopic magnetic responses in this model.

For an illustration we show in Fig. 1 an example of magnetization curve observed numerically in a certain small sample of $p = 3$ model. By a *sample* we mean a specific realization of the J_{ij} bonds in Eq. (1). Note the step-wise increase of the magnetization μ under increase of the magnetic field h. The pattern of the steps depend on each realization of samples so that it can be regarded as a *fingerprint* of a given sample. Note also that the linear susceptibility χ is quite spiky and significant only in the visinity of the steps.

On the other hand we know that in the thermodynamic limit $N \to \infty$ the magnetization curve *must* converge to a unique limit independently of samples. Thus the steps obserbed in mesoscopic (finite sized) samples must somehow disappear in $N \to \infty$ limit. But how?

A similar observation has been made also in the SK model by Kirkpatrick and Young [20]. Young, Bray and Moore [21] have argued that 2the step-wise response reflects crossings of free-energies of low lying metastable states under variation of the magnetic field. Mézard has discussed similar phenomena in the directed polymer in random media [22].

In our present paper we consider the 1 step RSB mean-field models instead of the full RSB models like the SK model. The 1 step RSB models are techinically and conceptually much simpler than the full RSB models and allow us to perform much more detailed, direct analysis on the mesossopic responses.

B. effective random energy model

In most parts of the present paper we consider more simplied models called random energy models (REM) which are suited for our purposes for various reasons.

Formally, Derrida's original REM [25, 44] can be derived by considering the limiting case $p \to \infty$ of the p-spin model given above. In this limit the model allows analytical calucurations to a great extent.

Physically the mesoscopic step-wise response arise from jumps between different metastable states (inter-state response). In this respect, responses within each metastable states (intra-state response) are irrelvant from our point of view. In the REM the intra-state responses automatically vanish so that we can avoide to work hard to disentabgle intra-state and inter-state responses.

The partition function of the REM at temperature $T = \beta^{-1}$ under the field h can be written as,

$$Z_{\text{REM}} = \sum_{i=1}^{e^{Nc}} e^{-\beta(F_i - hY_i)}. \tag{4}$$

Here $i = 1 \ldots e^{Nc}$ $(c > 0)$ is the label for the metastable states. F_α is the free-energy of the metastable state α at $h = 0$ and Y_α is a variable which is conjugate to the external field h.

In the case of magnetic systems, as the original REM by Derrida [25], the variable Y corresponds to the magnetization which takes random values at different metastable states. However in the present paper we wish to leave it as a *generic* extensive random variable conjugated to a generic external field h, in the same sprit of the seminal work by Krzakala and Martin (KM) [24]. We may call such a model as an *effective* REM. As far as the inter-state responses are concerned, the effective REM should correctly simulate a given original model which exhibits 1 step RSB.

Then the eseential ingredient we need to know is the density of metastable states at a give value of the free-energy F and the variable Y. The metastable states are obtained as the solutions of the equation of states called Thouless-Anderson-Palmer (TAP) equations [28]. In a previous work [26] we have given an analytic recipe to compute the logarithm of such a density of states, which we called *generalized complexity* from the TAP equation of a given microscopic model.

In Fig. 2 a) we show an example of the profile of the response observed in a REM. In Fig. 2 b) it can be seen that free-energies of low lying states exhibit level crossings precisely at the 'critical fields' h_c corresponding to the edges of the staircases of the response curve $y(h) = \langle Y \rangle / N$.

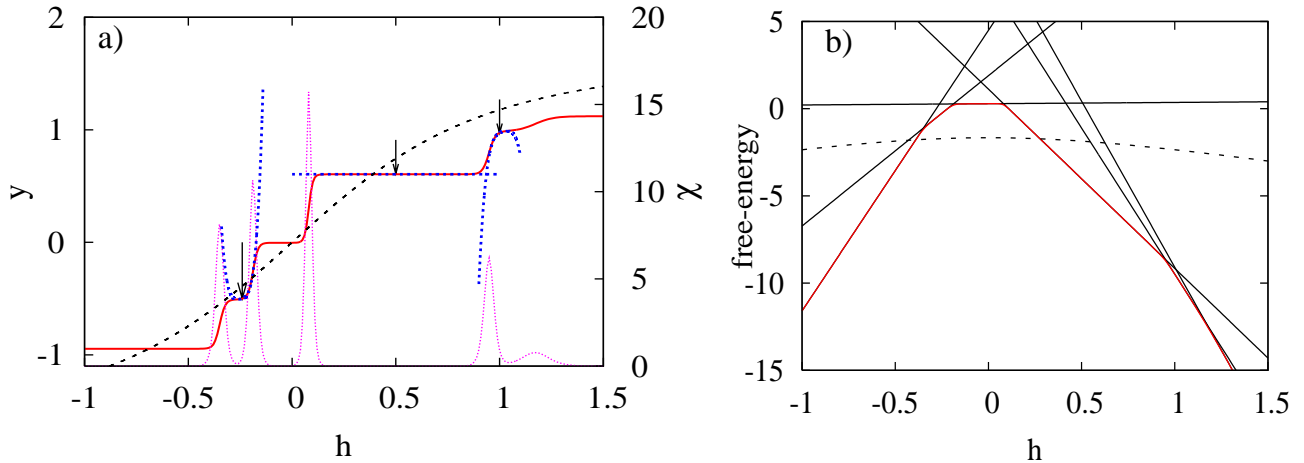### C. Some basic features of the step-wise responses

FIG. 2: Step wise responses and level-crossings of the free-energies in an effective REM. Here we used the toy model proposed by Krzakala and Martin [24]. (See sec. III and appendix B for the details.) In a) the solid (red) line which exhibits a sequence of steps is the response curve $y(h)$ computed numerically in a certain finite size ($N = 17$) sample of a model specified by the density of state Eq. (17) with $c = 2 \ln 2$, $\Delta = 1$ at temperature $T/T_c^0 = 0.1$. Here $T_c^0 = 1/\sqrt{2c}$ is the critical temperature of the model under $h = 0$ (See appendix B). The linear susceptibility $\chi(h)$, and all non-linear susceptibilities $\chi_n(h)$ with $n \geq 2$ (not shown), exhibit spikes at the edges of the staircases. The step-structures become finer as N is increased. The doted (blue) lines represent local Taylor expansions of the response curve $\text{const} + \chi_1 \delta h + \chi_2 (\delta h)^2 + \chi_2 (\delta h)^3 + \chi_2 (\delta h)^4$ wit δh being distances from the points indicated by the arrows. The (black) dashed line is the response curve in the thermodynamic limit obtained by taking first derivative of the total free-energy density in the thermodynamic limit $(f')^*(h)$ given in Eq. (B10) with respect to h. The qualitative difference between *thermodynamic susceptibilities* obtained by $\lim_{\delta h \to 0} \lim_{N \to \infty}$ and *susceptibilities associated with fluctuations* (FDT) obtained by $\lim_{N \to \infty} \lim_{\delta h \to 0}$ is clear. In b) the evolution of the free-energy densities $f'_l = f_l - hy_l$ under varying h for several low lying states are shown by solid (black) lines. The free-energy density of the total system is shown by the solid (red) line. The dashed line is the free-energy density in the thermodynamic limit $(f')^*(h)$ given in Eq. (B10).

In the present paper we wish to characterize statistical properties of the step-wise responses in *mesoscopic samples* explicitely. By *mesoscopic* we mean that N *is significantly larger than 1 but not infinitely large*. Our main result

is that there are three important characteristic scales of the steps in the 1 step RSB mean-field models: 1) typical height of a step ΔY , 2) typical spacing h_{s} between the steps and 3) typical width h_{w} of a step over which the step is rounded at finite temperatures T. Their orders of magnitudes are obtained as,

$$\Delta Y \sim \Delta_{\mathrm{eff}}(h)\sqrt{N} \qquad h_{\mathrm{s}} \sim \frac{T_c(h)}{\Delta_{\mathrm{eff}}(h)\sqrt{N}} \qquad h_{\mathrm{w}} \sim \frac{T}{\Delta_{\mathrm{eff}}(h)\sqrt{N}} \tag{5}$$

where $\Delta_{\mathrm{eff}}(h)$ characterize strength of the fluctuation of the quantity $Y = Ny$ conjugated to the external field h over different metastable states and $T_c(h)$ is the critical temperature under external field of strength h. In the thermodynamic limit $N \to \infty$, the spacing h_{s} between the steps vanish and the response curve converges to a unique limit.

We arrive at the above conclusion by analyzing anomalous scaling properties of thermal fluctuations associated with the steps, distribution function of the response in the zero temperature limit and decorrelation of two real replica systems subjected to different fields. We study these properties by two approaches : a low temperature expansion approach in section IV and a replica approach in section V.

1. Anomalous thermal fluctuations

A set of useful quantities which characterize the step-wise responses are linear and non-linear susceptibilities

$$\chi_n(h) = \left. \frac{\partial^n \langle y(h + \delta h) \rangle}{d\delta h^n} \right|_{\delta h=0} \qquad (n = 1, 2, \ldots,) \tag{6}$$

which exhibit series of spikes along the h axis as shown in Fig. 1 and Fig. 2. Note that the susceptibilities become significant only in close vicinities of the edges of the staircases,

$$\chi_n \sim O\left(\Delta Y h_{\mathrm{w}}^{-n}\right) \qquad \text{(around the edges of the steps)} \tag{7}$$

and remain almost zero elsewhere. Thus a given sample under a given value of h may or may not have large susceptibilities: it will have large susceptibilities only if it *happens* to have a 'critical field' h_c (edge of a step) close enough to h. Thus we naturally expect that linear and all non-linear susceptibilities are *not* self-averaging, as first pointed out by Young, Bray and Moore [21] in the SK model.

The susceptibilities are related to connected correlation functions of the Y variable through the static fluctuation dissipation theorem (FDT). FDT is derived by expanding the free-energy $Nf_J(T, h + \delta h)$ of a given sample, say J, in power series of an *infinitesimal* shift in the field δh,

$$-N\beta f_J(T, h + \delta h) - (-N\beta f_J(T, h)) = \ln\langle e^{\beta \delta h Y} \rangle = \beta \delta h \kappa_1(Y) + \frac{(\beta \delta h)^2}{2!}\kappa_2(Y) + \frac{(\beta \delta h)^3}{3!}\kappa_3(Y) + \ldots \tag{8}$$

where $\langle \cdots \rangle$ stands for weighted averages within the 'unperturbed system' ($\delta h = 0$). We denote the n-th thermal cumulant moments (or connected correlation functions) of the variable Y as $k_n(Y)$. The first few moments read as $\kappa_1(Y) = \langle Y \rangle$, $\kappa_2(Y) = \langle Y^2 \rangle - \langle Y \rangle^2$, $\kappa_3(Y) = \langle Y^3 \rangle - 3\langle Y^2 \rangle \langle Y \rangle + 2\langle Y \rangle^3$, $\kappa_4(Y) = \langle Y^4 \rangle - 4\langle Y \rangle \langle Y^3 \rangle + 6\langle Y \rangle^2 \langle Y^2 \rangle - 3\langle Y \rangle^4$. The above power series yields the usual *static* FDT; a change of Y induced by an infinitesimal increment of the field δh can be written as

$$\delta Y_J = \chi_1 \delta h + \chi_2 (\delta h)^2 + \chi_3 (\delta h)^3 + \ldots \tag{9}$$

with

$$\chi_1 = \beta \kappa_2(Y) \qquad \chi_2 = (\beta^2/2!)\kappa_3(Y) \qquad \chi_3 = (\beta^3/3!)\kappa_4(Y) \qquad \ldots \tag{10}$$

where χ_1 is the linear susceptibility and χ_2, χ_3 ,... are non-linear susceptibilities of a given sample J. If the thermal fluctuation of Y is Gaussian, as it happens at $T > T_c$, higher connected correlation functions vanishes $\kappa_n(Y) = 0$ for $n \geq 3$ and thus the non-linear susceptibilities vanish.

At around the edge of the steps where the response is significant (See Eq. (7)) the response may be described by a Taylor expansion,

$$\delta Y_J = \Delta Y \sum_{n=1}^{\infty} c_n \left(\frac{\delta h}{h_{\mathrm{w}}}\right)^n \tag{11}$$

with c_n being $O(1)$ numerical coefficients. Note that here the small parameter for the expansion is $h/h_{\rm w}$ with $h_{\rm w}$ being the width of the thermal rounding of the steps given in Eq. (5). This is indeed evident in the plot of Fig. 2 a) where we show some examples of truncated Taylor expansions of the response curve $y(h)$ at several points along the h axis (marked by arrows). Around the edges of the steps, the local Taylor expansion provides a good approximation only for sufficiently close neighbourhood of width $h_{\rm w}$. Thus "linear response theories" can *not* be invoked to estimate responses beyond the scale of a single step $h_{\rm s}$ which actually vanishes in the thermodynamic limit $N \to \infty$. (See Eq. (5))

Then one can notice that *thermodynamic susceptibilities* obtained in the limit $\lim_{\delta h \to 0} \lim_{N \to \infty}$ i.e. taking derivatives of 'smooth thermodynamic free-energy density', and *susceptibilities associated with fluctuations* (FDT) obtained in the other way around $\lim_{N \to \infty} \lim_{\delta h \to 0}$, which directly reflect 'rugged free-energy landscape', are completely different objects. In short the two limits are not commutative *everywhere* in the glass phase,

$$\lim_{\delta h \to 0} \lim_{N \to \infty} \neq \lim_{N \to \infty} \lim_{\delta h \to 0}. \tag{12}$$

The non-commutativity of the two limits signals the presence of the steps.

On passing let us note that *disorder-average* of the *linear* susceptibility defined via static fluctuation dissipation theorem (FDT) must agree with the 1st derivative of the thermodynamic response curve in a rather *accidental* manner as discussed in appendix A. Importantly the equivalence does *not* hold for the non-linear susceptibilities. Although the value of linear susceptibility obtained via FDT coincides, after averaging it over disorder, with the 'thermodynamic linear susceptibility', it must be emphasized that the meaning of 'linear responses' is totally different in the two cases. As can be seen in Fig. 2, linear response approximation is apparently not so bad for the thermodynamic response curve while we realize it is almost a nonsense in a given finite sized sample.

2. Sharp response in $T \to 0$ limit

The expansion of the response via FDT cannot go beyond the scale of a single step. In particular, in the close vicinity of the edges of the steps the Taylor expansion is valid only within the thermal width of the step $h_{\rm w}$ (See Eq. (11)). Moreover the thermal width $h_{\rm w}$ vanishes in the zero temperature limit $T \to 0$ at which the step structure becomes most clear. Thus it is tempting to look for another way to analyze the mesoscopic step-wise responses without relying on the FDT, which hopefully works at zero temperature.

By both the low temperature expansion method and the replica method, we will demonstrate that it is indeed possible to take $T \to 0$ limit *first* and study mesoscopic responses consisting of successive sharp steps within small increments of the field δh. Interestingly enough, we will otbain another series expansion of the mesoscopic response in which the relvant small parameter is $\delta h/h_{\rm s}$ instead of $\delta h/h_{\rm w}$ which appears in the FDT case (Note that $h_{\rm w} < h_{\rm s}$ since $T < T_c(h)$). Thus the two limts $T \to 0$ and $\delta h \to 0$ are not commutative,

$$\lim_{\delta h \to 0} \lim_{T \to 0} \neq \lim_{T \to 0} \lim_{\delta h \to 0}. \tag{13}$$

Somewhat unexpectedly, the approach $\lim_{T \to 0} \lim_{\delta h \to 0}$ allows us to go beyond the limit of single step. We will find that the $O(\delta h/h_{\rm s})$ term in the series corresponds to the case that only single step is present in a given interval δh, $O(\delta h/h_{\rm s})^2$ term to the case of two steps, and so on.

3. Cusp in the overlap: a mesoscopic aspect of the chaos effect

In addition to the response of the variable, say Y cojugated to a given external field h, we examine the change of the corelation function between two replicas subjected to slightly different fields,

$$C(\delta h) \equiv \frac{\big[\!\!\big[\langle Y(h - \delta h) \rangle \, \langle Y(h + \delta h) \rangle \big]\!\!\big]}{\big[\langle Y(h) \rangle^2 \big]} \tag{14}$$

under variation of δh. This kind of correlation function or *overlap* function is oftenly used to analyze the static chaos effects known in spin-glasses and related systems [12, 13, 14, 34, 36, 37, 47, 50].

We are sure that the correlation function must vanish $C \to 0$ for any small but finte variation of the field in the thermodynamic limit $N \to \infty$, i.e. chaos. This is because in such a circumstance there will certainly be level crossings between different metastable states which have zero overlap with respect to each other in 1 step RSB models [26].

Our interest here is to look at *how* it decays as δh is increased in mesoscopic (finite sized) samples. To this end we analyze Eq. (14) at finite temperatures using the FDT approach and also directly at $T \to 0$ limit without relying on the FDT. We will find that the overlap $C(\delta h)$ exhibists a *cusp* singularity at $\delta h = 0$ in $T \to 0$ limit, which is rounded at finite temperatures over the scale $h_{\rm w}$, and that the width of the cusp is given by $h_{\rm s}$ (See Eq. (5)). Somewhat unexpectedly, as we discuss in section VI, the overlap function has counterparts which describe the jerky effective energy landscape of pinned elastic manifolds [30] and intermittencies due to shocks in turbulence [32].

III.   GENERALIZED COMPLEXITY

Now let us discuss some generic features of the density of the metastablestates (TAP states). As we noted in in sec II B, the effective REM can be constracted based only on this information (See Eq. (4)).

We consider an ensemble of metastable states $i = 1, 2, \ldots$ each of which is a solution of the TAP equations of states at a given temperature T and an external field h. We denote the free-energy of a TAP state, say α, as $F_\alpha = N f_\alpha$ and the extensive variable conjugated to h as $Y_\alpha = N y_\alpha = -N \partial f_\alpha / \partial h$.

We rewrite the partition function of a given sample of the effective REM Eq. (4) at temperature T and under slightly shifeted external field $h + \delta h$ with small enough δh as [35, 45],

$$Z_{\rm REM}(T, h + \delta h) = \sum_\alpha e^{-N\beta(f_\alpha - \delta h y_\alpha)} = \int df \, dy \, e^{N[\Sigma(f,y) - \beta(f - \delta h y)]} \tag{15}$$

where $\beta = 1/T$. Here $\Sigma(f, y)$ is the generalized complexity [26] defined as the logarithm of the density of states with respect to the two variables f and y,

$$\Sigma(f, y) = \frac{1}{N} \log \sum_\alpha \delta(f - f_\alpha) \delta(y - y_\alpha). \tag{16}$$

In general [26] we expect that the generalized complexity $\Sigma(f, y)$ can be presented as a surface $\Sigma = \Sigma(f, y)$ which is convex upward as shown schematically in Fig. 3. See [26] for an analytical recipe to compute the generalized
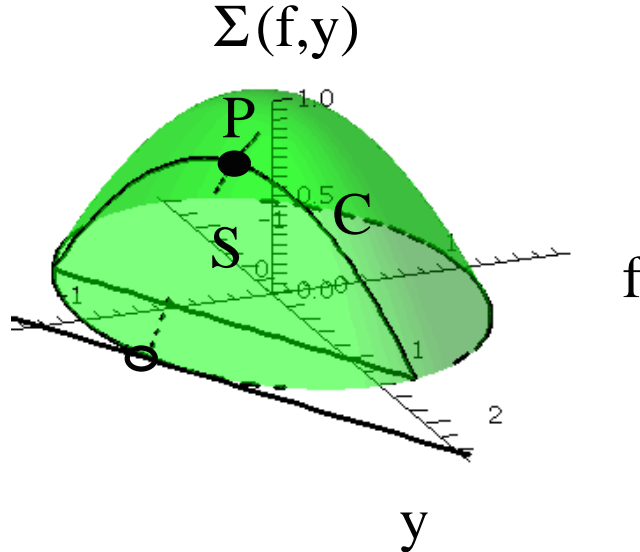

FIG. 3: The generalized complexity $\Sigma = \Sigma(f, y)$ have a shape like a surface of a bell cut by $\Sigma = 0$ plane. The dashed line on the $\Sigma = 0$ plane is the zero complexity curve $\Sigma(f, y) = 0$. The surface $S(f')$ is normal to the axis of the 'total free-energy' $f - \delta h y$ and cut the latter at $f' = f - \delta h y$. Cross section between the plane $S(f')$ and the complexity surface $\Sigma = \Sigma(f, y)$ defines a curve C on which the complexity is maximized at a peak $P = P(f')$.

complexity of a given microscopic model. Note that in general $\Sigma(f,y)$ can depend both on the temperature T and external field h.

As a toy model we can use the model propose by Krzakala and Martin (KM) [24] in which the generaized complexity takes a particulary simple form,

$$\Sigma(f,y) = c - \frac{f^2}{2} - \frac{y^2}{2\Delta^2}, \tag{17}$$

which depends neither on the temperautre T nor the field h. In appendix B we summarize some basic properties of the model. We will find that it gives generic results concerning inter-state responses common for all 1 step RSB models in the glass phase.

A. Thermodynamic response

In the thermodynamic limit $N \to \infty$, at a given temperature T and under an external field $h + \delta h$, the partition function Eq. (15) is dominated by contribution from a certain saddle point (f^*, y^*) which parametrize a particular set of TAP states. Then thermodynamic value of Y variable is given by $Y = Ny^*$ and the thermodynamic free-energy is given by $F' = N(f^* - \delta h y^*)$.

The saddle point (f^*, y^*) can be located as the following. Let us consider the three-dimensional space (f, y, Σ) as shown in Fig. 3. Consider a plane $S = S(f')$ on which the total free-energy density takes a constant value $f - \delta h y = f'$. Cross section between $S(f')$ and the complexity surface $\Sigma = \Sigma(f, y)$ defines a line $C = C(S)$ along which the complexity takes a maximum value at a certain point $P = P(C)$. Then for each value of f' we have a unique point $P = P(f')$ associated with it. Now we look for a special point $P^* = (f^*, y^*, \Sigma^*)$ such that it satisfies,

$$\left. \frac{\partial \Sigma(f,y)}{\partial f'} \right|_{P=P^*} = \frac{1}{T}. \tag{18}$$

It is easy to verify that (f^*, y^*) is the saddle point which dominates the partition function Eq. (15) and Σ^* is the value of the complexity at the saddle point.

As the temperature T is lowered under a fixed value of the external field h, the point P^* moves downward on the complexity surface. At a certain critical temperature $T = T_c(h)$, the value Σ^* of the complexity at the point P^* becomes 0. As the temperatures is lowered further the point P^* remains pinned there. Thus the system is understood to be in the glass phase where $\Sigma^* = 0$ at lower temperatures $T < T_c(h)$.

Within the glass phase $T < T_c$, the saddle point moves smoothly along the zero complexity line $\Sigma(f,y) = 0$ under variation of the extenal field h. The equilibrium values of the parameters $(f^*(h + \delta h), y^*(h + \delta h))$ under a given external field $h + \delta h$ is simply obtained by looking for a line $f - \delta h y = f'$ with slope δh which is tangent to the zero complexity curve $\Sigma(f,y) = 0$. The touch point is nothing but the saddle point $(f^*(h + \delta h), y^*(h + \delta h))$ [26].

By varing h, the equilbrium value of $y^*(h)$ will change smoothly. Consequently all linear and non-linear suscepibilities

$$\chi_n(h) = \left. \frac{d^n y^*(h + \delta h)}{d\delta h^n} \right|_{\delta h = 0} \tag{19}$$

will be smooth functions of h. Note that these are *thermodynamic susceptibilities* which are obtained by taking thermodynamic limit $N \to \infty$ *before* taking derivatives with respect to h.

The fact that (f^*, y^*) varies with h means that strong chaos is induced by extensive level crossings in the 1 step RSB systems [26]: a set of TAP states which dominates the equilibrium states at a given value of h becomes completely out-of-equilibrium at $h + \Delta h$. However, thermodynamic response itself is completely smooth and featureless, which ironically provides us no hint of the underlying chaos effect. Thus we are naturally lead to go down to smaller scales to look for some traces of the chaos effect.

In appendix B we rephrase the above discussion based on the toy model Eq. (17).

B. Low lying states close to $\Sigma = 0$ line

We are interested in the glassy phase $T < T_c(h)$ so that the shape of the complexity around the saddle point $(f^*(h), y^*(h))$ on the zero complexity line $\Sigma = 0$ will be particularly important. A generic shape around the saddle
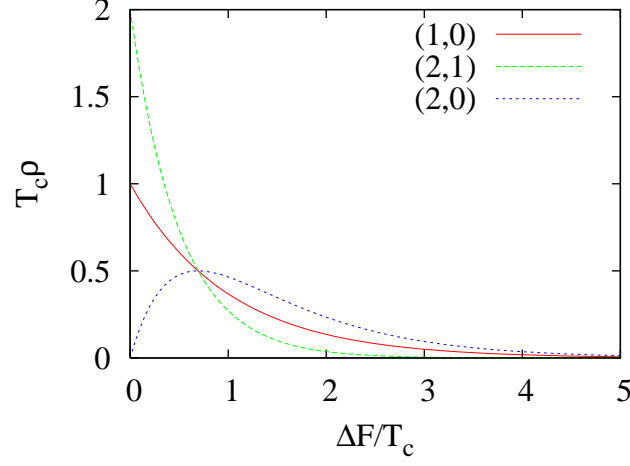
FIG. 4: Spacing between low lying states. Adjacent free-energy levels $(1,0),(2,1),...$are *not* repulsive to each other. More generically, free-energies of l-th and m-th states with $|l - m| > 1$ are "repulsive" to each other.

point close to $\Sigma = 0$ may be cast into a form like,

$$\Sigma(f,y) \simeq \frac{f - f^*(h)}{T_c(h)} - \frac{(y - y_P(f))^2}{2\Delta_{\text{eff}}(h)^2} \tag{20}$$

where $y_P(f)$ describes the position of the peak P (see Fig. 3) at a given value of f. The latter may be described by a Taylor expansion,

$$y_P(f) = y^*(h) - a(h)(f - f^*(h)) + O((f - f^*(h))^2). \tag{21}$$

with $a(h)$ being a certain constant.

The functional form Eq. (20) suggests us to introduce a new variable $\tilde{Y}$,

$$\tilde{Y} = N\tilde{y} \qquad \tilde{y} \equiv y - y_p(f). \tag{22}$$

Then we can rewrite the generalized complexity Eq. (20) as,

$$N\Sigma \simeq \frac{F - F^*(h)}{T_c(h)} - \frac{\tilde{Y}^2}{2N\Delta_{\text{eff}}(h)^2} \tag{23}$$

Note that this means the density of states $e^{N\Sigma(\Xi)}$ is decoupled into two parts: exponential distribution function for the free-energy and Gaussian distribution function for the transverse variable $\tilde{Y}$. In the present paper we call $\tilde{Y}$ as *transverse variable*.

In appendix B we rephrase the above discussion based on the toy model Eq. (17). In particular we find that the complexity of the model behaves as Eq. (23) close to the $\Sigma = 0$ plane so that it should give generic results common in all 1 step RSB models concerning inter-state responses below $T_c(h)$.

1. Level spacings among the low-lying states

From Eq. (23) we find that the total free-energy F of low lying states $(F - F^*)/T_c(h) \approx O(1)$ follow an exponential distribution [46],

$$\rho(F) \simeq \exp((F - F^*)/T_c(h)). \tag{24}$$

Now let us order the states as $l = 0, 1, 2, \ldots$ according to the value of their total free-energies F_l such that $F_0 \leq F_1 \leq F_2 \ldots$. We will need in particular the information of the statistics of level-spcacings: differences between free-energies,

$$\Delta F_{(l,m)} \equiv F_l - F_m \qquad l > m. \tag{25}$$

Recently Bertin [54] have shown that spacing between random numbers drawn from an exponential distribution function exactly obey a class of exponential distribution laws. Following his proof we find from Eq. (24) that free-energy gaps of adjacent levels $\Delta F_{(l,l-1)}$ follow an l-dependent exponential distribution[60],

$$\rho_{(l,l-1)}(\Delta F_{(l,l-1)}) = \frac{l}{T_c} e^{-l\frac{\Delta F_{(l,l-1)}}{T_c}}. \qquad (26)$$

The exponential form Eq. (26) implies absence of repulsions between adjacent levels in the sense that $\lim_{x\to 0} \rho_{(l,l-1)}(x) > 0$ (See Fig. 4). On the other hand we find distribution of the free-energy difference between $l+1$-th and $l-1$-th states using Eq. (26) as,

$$\rho_{(l+1,l-1)}(\Delta F_{(l+1,l-1)}) = \frac{l(l+1)}{T_c} e^{-(l+1)\frac{\Delta F_{(l+1,l-1)}}{T_c}} \left(1 - e^{-l\frac{\Delta F_{(l+1,l-1)}}{T_c}}\right). \qquad (27)$$

This implies a certain *effective* level repulsion between $l-1$-th and $l+1$-th states in the sense that $\lim_{x\to 0} \rho_{(l+1,l-1)}(x) = 0$. (See Fig. 4). Thus the free-energy levels are not *too much* degenerate: only a few low lying states dominate the static properties in the glassy phase in contrast the liquid phase $T > T_c(h)$ where exponentially many states contribute.

2.   Distribution of the transverse variable $\tilde{Y}$

A remarkable feature of the transverse variable $\tilde{Y}$ is that *it is statistically independent from the free-energy*. From Eq. (23), we find $\tilde{Y}_l$ follows a simple Gaussian distribution,

$$P(\tilde{Y}_l) = \frac{1}{\sqrt{2\pi N(\Delta_{\text{eff}})^2}} \exp\left(-\frac{\tilde{Y}_l^2}{2N(\Delta_{\text{eff}}(h))^2}\right). \qquad (28)$$

which is independent of l, i. e. independent of the free-energy.

The original Y variable depends both on the transverse variable $\tilde{Y}$ and the free-energy F,

$$Y - Y^* = \tilde{Y} + a(h)(F - F^*) \qquad (29)$$

which follows from Eq. (22). Here it is evident that thermal fluctuations and responses to the field of Y is dominated by that of $\tilde{Y}$.

Thus for the rest of this paper we will focus on thermal fluctuations of the variable $\tilde{Y}$ instead of Y. Correspondintly we will consider to apply a fictitious field conjugated to the tranverse variable $\tilde{Y}$ and examine its response. We will frequently denote $\tilde{Y}$ simply as Y for simplicity.

3.   Discussions

The most important features of the density of states specified by the generalized complexity Eq. (23) are the following two points: 1) In a finite fraction of samples low lying states are almost degenerate and 2) Existence of the transverse variable. The combination of the two points yield the step-wise responses in the glass phase at mesoscopic scales: a fraction samples can make a large response of order $\Delta_{\text{eff}}\sqrt{N}$ even by an infinitesimally small variation of the field. Note that the situation must be distiguished from that in the liquid phase $T > T_c(h)$ where *all* samples respond. In contrast the response is *intermittent* in the glass phase because only some *finite fraction* of the samples are ready to respond to infenitesimal fields.

While the thermal fluctuations of the free-energy F is necessarily of $O(T)$, thermal fluctuations of the transverse variable $\tilde{Y}$ can be of order $O(\Delta_{\text{eff}}(h)\sqrt{N})$. Thus $\tilde{Y}$ is reminiscent of the Goldstone modes in the sense that it can make large thermal fluctuations and also large respons to small variations of the external field even at very low temperatures. (See [22, 23] for related discussions in the problem of directed polymer in random media.)

In the case of the magnetic perturbation, the variance Δ_{eff} of the magnetization is related to the Edwards-Anderson (EA) order parameter q_{EA} as $\Delta_{\text{eff}} = \sqrt{q_{\text{EA}}}$ under zero external magnetic field $h = 0$ [26]. The latter has been also noticed by Franz and Virasoro [55] in the context of dynamics.

The situation will change qualitatively if there are level-repulsions between adjacent free-energy levels as in the familiar Wigner's distribution. It will also depend on the the parameter Δ_{eff}. Chaos will be absent for a perturbation with $\Delta_{\text{eff}} = 0$.

Interestingly enough quite similar properties as 1) 2) are *assumed* and plays prominent roles in the phenomenological Imry-Ma type droplet scaling arguments for glassy systems [12, 13, 14, 22, 47] which assume thermally active *rare* low-energy excitations called *droplet excitations*. The difference between the present mean field theory is that the characteristic energy scale T_c is replaced by typical energy scale of droplet excitations which grows with the system size L,.

$$T_c \quad \text{``mean field''} \quad \rightarrow \quad \Upsilon(L/L_0)^\theta \quad \text{``droplet''}$$

Here the exponent $\theta > 0$ is usually called stiffness exponent and L_0 is a certain length scale beyond which the power law behaviour holds. Such an intriguing analogy has been pointed out in some literatures [30, 41].

IV.   LOW TEMPERATURE EXPANSION APPROACH ON MESOSCOPIC RESPONSES

We now analyze responses at mesoscopic scales by a low temperature expansion approach on the effective REM. To this end, it is convenient to rewrite the partition function Eq. (4) of a given sample as,

$$Z_J = e^{-\beta F_0} \sum_{l=0}^{M-1} \exp\left(-\beta \sum_{k=1}^{l} \Delta F_k + \beta \delta h Y_l\right). \tag{30}$$

Here the index $l = 0, 1, \ldots, M-1$ label the states in an ascending order of the values of their free-energies, i.e $F_0 \leq F_1 \leq \ldots \leq F_{M-1}$. The free-energy gaps $\Delta F_l = F_{l+1} - F_l$ follow the l-dependent exponential distribution Eq. (26). The variables Y_l are understood as the *transverse variable* which is statistically independent from the free-energy at $\delta h = 0$. For simplicity we denote it as Y.

A.   A first look by a simple two-level model

First let us look at a simple two-level model to get some basic insights. The two-level model is defined such that it consists of only the two lowest levels in a given sample disregarding higher levels: the sum over the states $l = 1, 2, \ldots, M$ in the partition function Eq. (30) is truncated at $l = 2$. In the next section we will actually find that this simple two-level model gives quantitatively correct results up to $O(T/T_c(h))$ which is a good approximation at low enough temperatures. Contributions from higher levels give only moderate correction terms of higher order in $T/T_c(h)$.

Let us consider a two-level system at temperature T and under external field h_0. It is easy to see that the response $\langle y \rangle_h - \langle y \rangle_{h_0}$ by varitaion of the field can be expanded in power series of $\delta h = h - h_0$ as

$$\frac{\langle y \rangle_h - \langle y \rangle_{h_0}}{\Delta Y} = \sum_{n=0}^{\infty} \left(\frac{\delta h}{h_w}\right)^n \tilde{\chi}_n\left(\frac{h - h_c}{h_w}\right) \tag{31}$$

with $\Delta F \equiv F_1 - F_0$, $\Delta Y \equiv Y_1 - Y_0$, $\tilde{\chi}_n(y) \equiv \frac{\partial^n}{\partial y^n}\frac{1}{1+e^{-y}}$, and

$$h_c \equiv h_0 + \frac{\Delta F}{\Delta Y} \qquad h_w \equiv \frac{T}{\Delta Y}. \tag{32}$$

The above observation readily suggests the three important characteristic scales of steps announced in Eq. (5). First, the scale of a single step is given by ΔY whose typical magnitude is,

$$\Delta Y \sim \sqrt{N}\Delta_{\text{eff}}. \tag{33}$$

as Eq. (28) implies. Second, the distance from a given h_0 to the nearby 'critical field' h_c where a level crossing take place is given by $h_c - h_0 = \Delta F/\Delta Y$. Typical order of magnitude of the latter is,

$$h_s \sim \frac{T_c(h)}{\sqrt{N}\Delta_{\text{eff}}}. \tag{34}$$

This follows from Eq. (26) which implies typically $\Delta F \sim T_c(h)$. Lastly h_w introduced in Eq. (32) defines the scale of *thermal width* over which which the edge of a step is *rounded* at temperature T. We readily find,

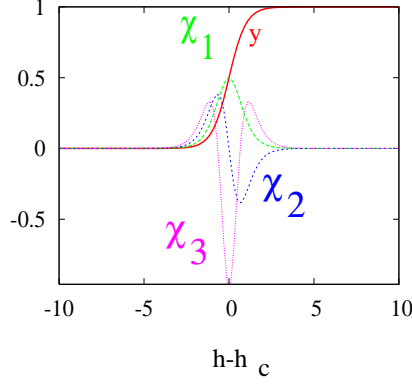$$h_w \sim \frac{T}{\sqrt{N}\Delta_{\text{eff}}}. \tag{35}$$

FIG. 5: Profiles of linear and non-linear susceptibilities associated with a step. The solid (red) line represents a model function of a step $\langle y \rangle / \Delta Y = [1 + e^{-(h-h_c)/h_{\mathrm{w}}}]^{-1}$ with $h_{\mathrm{w}} = 0.5$. The others are susceptibilities $\chi_n / \Delta Y = \partial^n (\langle y \rangle / \Delta Y)/\partial h^n$ which have significant amplitudes only in a narrow region of the *thermal width* h_{w} around the critical field' h_c. Note also that sings of the non-linear susceptibilities oscillate.

Note that h_{w} is the scale up to which a local Taylor expansions of the response around the edges of the steps converge as noted in Eq. (11).

From Eq. (31) the susceptibilities are obtained as

$$\chi_n(h) = \Delta Y \frac{1}{h_{\mathrm{w}}^n} \tilde{\chi}_n \left(\frac{h - h_{\mathrm{c}}}{h_{\mathrm{w}}} \right) \tag{36}$$

which are displayed in Fig. 5. Note that they are significant only within the thermal width h_{w} around the critical field h_{c}. Since ΔF and ΔY fluctuate from sample-to-sample, a given sample will have significant susceptibilities under a given external field h_0 *only if the distance to the critical field $h_{\mathrm{s}} = h_c - h_0$ happens to be smaller than the thermal width h_{w}.* A simple minded estimate of the probably to actually have such a sample is,

$$\frac{h_{\mathrm{w}}}{h_{\mathrm{s}}} = O \left(\frac{T}{T_{\mathrm{c}}(h)} \right) \tag{37}$$

which becomes small at low temperatures $T \ll T_{\mathrm{c}}(h)$. With such a small probability the susceptibility of a given sample take significantly large values,

$$\chi_n \sim \Delta Y h_{\mathrm{w}}^{-n} \sim (\Delta_{\mathrm{eff}})^{1+n} N^{(1+n)/2} \tag{38}$$

while they remain negligible otherwise.

From Eq. (37) and Eq. (38) we find sample-average of p-th moment of χ_n is dominated by the *rare sample* and behave as,

$$[\![\chi_n^p]\!] \sim (\Delta Y h_{\mathrm{w}}^{-n})^p \frac{h_{\mathrm{w}}}{h_{\mathrm{s}}} \sim \left[(\Delta_{\mathrm{eff}})^{1+n} N^{(1+n)/2} \right]^p \frac{T}{T_{\mathrm{c}}(h)}. \tag{39}$$

Thus the sample-to-sample fluctuations of the susceptibilities are very far from Gaussian and non-self averaging. For instance we find,

$$\frac{[\![\chi_n^4]\!]}{([\![\chi_n^2]\!])^2} \sim \left(\frac{T}{T_{\mathrm{c}}(h)} \right)^{-1}. \tag{40}$$

The above argument based on the two-level model is surprisingly similar to the typical Imry-Ma type scaling arguments in the droplet phenomenology [13, 14]. Indeed let us note that a very similar Imry-Ma type scaling argument has been constracted for directed polymer in random media subjected to tilt field [22].
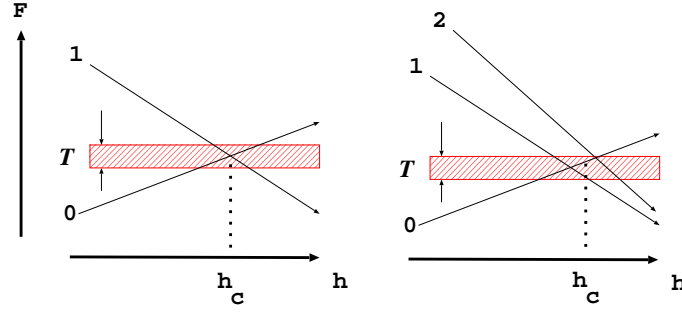
FIG. 6: Schematic pictures of free-energy levels close to a 'critical field' h_c. (Left) A case when lowest two levels $l = 0, 1$ come close to each other with a separation of only $O(T)$. Rare samples which realize such a situation under a given h make $O(T/T_c(h))$ contributions to the thermal cumulants under the given h. 2-level models take into account such samples correctly. (Right) A case when lowest three levels $l = 0, 1, 2$ come close to each other simultaneously. Such rare samples make $O(T/T_c(h))^2$ contributions. 3-level models are needed to take into account such samples correctly.

B. Sample-to-sample fluctuations of linear and non-linear susceptibilities

Now we study thermal fluctuations associated with the steps more systematically. Our task is to compute k-th thermal cumulants of Y (more precisely $\tilde{Y}$) and examine its moments,

$$\left[\kappa_{k_1}^{p_1}(Y)\kappa_{k_2}^{p_2}(Y)\cdots\right] = \left[\left(\frac{\partial^{k_1}}{\partial(\beta\delta h)^{k_1}}\ln Z(h+\delta h)\right)^{p_1}\left(\frac{\partial^{k_2}}{\partial(\beta\delta h)^{k_2}}\ln Z(h+\delta h)\right)^{p_2}\cdots\Bigg|_{\delta h=0}\right]. \tag{41}$$

where $Z((h+\delta h)$ is the partition function and $[\cdots]$ denotes the average over different realizations of samples. Here we compute them by a low temperature expansion approach. Later in section V B we confirm the results by a replica approach.

Omitting the global factor $e^{-\beta F_0}$ in Eq. (30) which is irrelevant for our purposes, the partition function can be formally rewritten as,

$$Z(\{O_l, X_l\}) = O_0 + \sum_{l=1}^{M-1} O_l \prod_{k=1}^{l} X_k, \tag{42}$$

with

$$X_l \equiv e^{-\beta\Delta F_l} \qquad O_l \equiv e^{\beta\delta h\tilde{Y}_l}. \tag{43}$$

The exponential distribution of ΔF_k given in Eq. (26) implies power law distribution of X_k,

$$p_k(X_k) = X_k^{k\frac{T}{T_c(h)}-1}k\frac{T}{T_c(h)} = k\frac{T}{T_c(h)}\left\{1 + \frac{T}{T_c(h)}\log X_k + O\left(\frac{T}{T_c(h)}\right)^2\right\} \tag{44}$$

defined in the range $0 \le X_k \le 1$. Now the sample average of the p-th moment of k-th thermal cumulant given by Eq. (41) can be expressed as,

$$\left[\kappa_{k_1}^{p_1}(\tilde{Y})\kappa_{k_2}^{p_2}(\tilde{Y})\cdots\right]$$
$$= \left[\prod_{r=1}^{p_1}\left\{\left(\sum_{l=0}^{M-1}Y_l O_{lr}\frac{\partial}{\partial O_{lr}}\right)^{k_1}\ln Z(\{O_{lr}, X_l\})\right\}\prod_{r=p_1+1}^{p_1+p_2}\left\{\left(\sum_{l=0}^{M-1}Y_l O_{lr}\frac{\partial}{\partial O_{lr}}\right)^{k_2}\ln Z(\{O_{lr}, X_l\})\right\}\cdots\Bigg|_{O=1}\right] \tag{45}$$

Let us emphasize that a M-th level model, which only takes into account the lowest M levels, gives correct results of the moments up to order $O(T/T_c)^{M-1}$. We report the proof in appendix C 1. This justifies the use the simple two-level model discussed in the previous subsection IV A at low enough temperatures and guarantees that correction terms at high orders in $T/T_c(h)$, if needed, can be obtained systemacially by considering 3,4,..-level models.

Now let us examine explicitly a few moments of $\kappa_2(Y)$ and $\kappa_3(Y)$ which are related to the linear $\chi_1 = \beta\kappa_2(Y)$ and the 1st non-linear susceptibilities $\chi_2 = \beta^2/2!\kappa_3(Y)$. The details of the computation are reported in appendix C and we quote the results below.

For the linear susceptibility, we obtain by using a 3-level model,

$$\llbracket\kappa_2(Y)\rrbracket = (\sqrt{N}\Delta_{\text{eff}})^2 \left\{ \frac{T}{T_{\text{c}}(h)} + O\left(\frac{T}{T_{\text{c}}(h)}\right)^3 \right\} \tag{46}$$

$$\left[\kappa_2^2(Y)\right] = (\sqrt{N}\Delta_{\text{eff}})^4 \left\{ \frac{T}{T_{\text{c}}(h)} + O\left(\frac{T}{T_{\text{c}}(h)}\right)^3 \right\}. \tag{47}$$

These results demonstrates that the linear susceptibility is not self-averaging, i.e. $\left[\chi_1^2\right] \neq (\llbracket\chi_1\rrbracket)^2$ as expected. In sec. IV A we have argued that probability to have a rare sample which happens to have a critical field h_c close enough to a given h is $O(T/T_{\text{c}}(h))$ Eq. (37). Indeed in the above results we see that both the 1st and 2nd moment of the 2nd thermal cumulant are proportional to $T/T_{\text{c}}(h)$ and agree with the expected scaling form Eq. (39).

The sample average of the 1st moment of the 3rd thermal cumulant is zero $\llbracket\kappa_3(Y)\rrbracket = 0$ simply due to the symmetry reason. (We again remind the readers that we are actually studying the fluctuations of the transverse variable $\tilde{Y}$.) However its 2nd moment $\left[\kappa_3^2(Y)\right]$ is non-zero. Following the same steps as before we find after a lengthy algebra,

$$\left[\kappa_3^2(Y)\right] = (\sqrt{N}\Delta_{\text{eff}})^6 \; 2 \left\{ \frac{T}{T_{\text{c}}(h)} - \left(\frac{T}{T_{\text{c}}(h)}\right)^2 + O\left(\frac{T}{T_{\text{c}}(h)}\right)^3 \right\}. \tag{48}$$

The result means that the non-linear susceptibility χ_2 is strongly non-self averaging. The result agrees again with the expected scaling Eq. (39) at low enough temperatures $T \ll T_{\text{c}}(h)$. A remarkable feature is that it is *super* extensive,

$$\frac{\sqrt{\llbracket\chi_2^2\rrbracket}}{N} \sim \sqrt{N}(\Delta_{\text{eff}})^3 \tag{49}$$

which diverges in the thermodynamic limit $N \to \infty$. Thus the non-linear susceptibility can be divergingly large either positively or negatively in a given sample. This is an ambiguous signature of anomaly the associated with step-wise responses which is invisible in thermodynamic susceptibilities.

C. Distribution of mesoscopic responses in the zero temperature limit

Here we take a different route to study the mesoscopic response by taking the zero temperature limit $T \to 0$ first. As noted in II C 2, in this limit $h_{\text{w}} \to 0$, meaning that the steps become maximally sharp, so that the FDT approach cannot be invoked anymore. While the FDT approach is limitted to desribe response only within the scale of single steps, here we will find that we can actually go beyond this limit.

For each sample, we consider response at $T = 0$ induced by the field increased from h to $h + \delta h$ with $\delta h > 0$. At the beginning the system stays at the ground state under h. By increasing the field by δh there may be level crossings by which the variable Y jump abruptly. Thus at $T = 0$ the induced response can be written simply as

$$\psi \equiv Y(h + \delta h) - Y(h) \tag{50}$$

where $Y(h)$ is the value of the Y variable of the ground state at h and $Y(h + \delta h)$ is that under $h + \delta h$. We are especially interested in the distribution function of the induced response Eq. (50) over different realizations of the samples,

$$p(\delta h, \psi) \equiv \llbracket\delta(\psi - (Y(h + \delta h) - Y(h)))\rrbracket. \tag{51}$$

Fortunately we have complete information of the low lying states: Y_l (more precisely $\tilde{Y}_l$) follows the Gaussian distribution given by Eq. (28) and the free-energy difference $\Delta F_{l,m}$ between l-th and m-th states follow the distributions discussed in sec. III B 1.
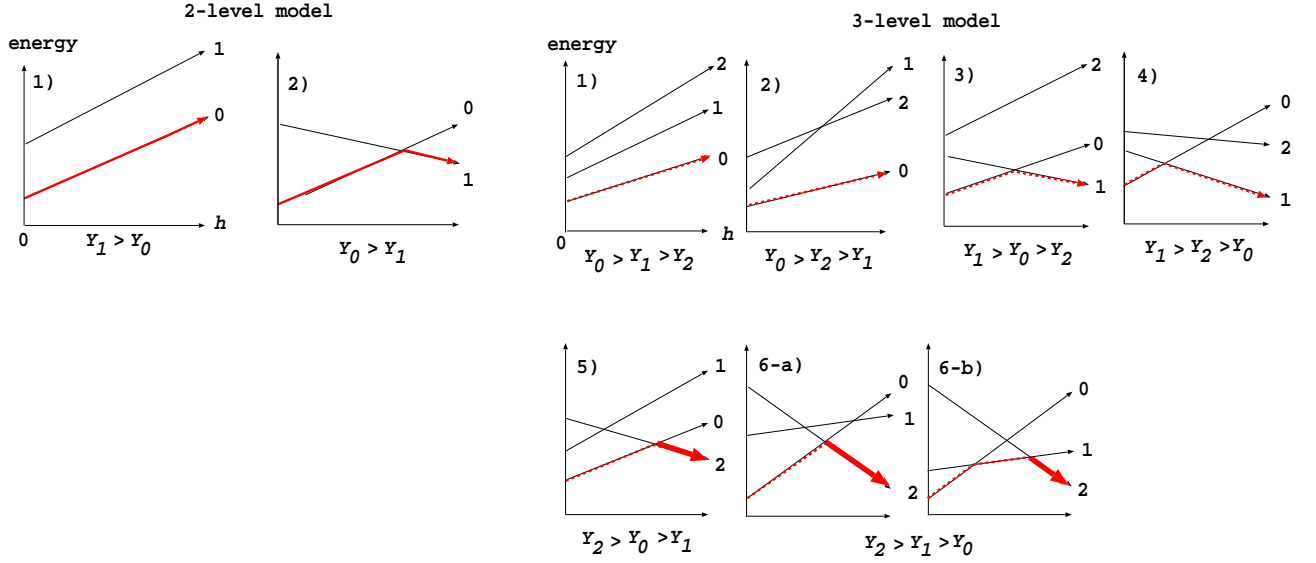
FIG. 7: (Left) Level crossing in the two-level system. In the case 1) $Y_1 > Y_0$ the two levels do not make a level crossing for $h > 0$ so that there are no induced response $\psi = 0$. On the other hand for the case 2) $Y_1 < Y_0$ the two levels make a level crossing by which a step of the response $\psi = Y_1 - Y_0$ is induced. (Right): Level crossing in the three-level systems. The cases 1)-4) are already included in the two-level model (See Fig. 7). In the cases 5),6-a) and 6-b), the third level comes into play in the last stages represented by thick arrows.

1. Two-level model

Let us start from the two-level model. First we note that the case 1) $Y_1 > Y_0$ and 2) $Y_1 < Y_0$ must be distinguished. As shown in Fig. 7 there are no level crossing and thus no response in the case 1) for $\delta h > 0$. In the case 2) the response remains zero $\psi = 0$ until the applied field reaches a critical field,

$$h_c = \frac{\Delta F_{(1,0)}}{Y_1 - Y_0}$$

at which the free-energy level of the two states become the same and then jumps to $\psi = Y_1 - Y_0$. The distribution of the response ψ may be decomposed

$$p^{2-\text{level}}(\psi, \delta h) = p_0^{2-\text{level}}(\psi, \delta h) + p_1^{2-\text{level}}(\psi, \delta h) \tag{52}$$

where $p_0(\psi)$ is the contribution from the cases that the ground state remains to be '0' and $p_1(\psi)$ is the case that it is shifted to '1'. One can easily find (see appendix D),

$$p_0^{2-\text{level}}(\psi, \delta h) = \delta(\psi) \left\{ 1 - \int_0^\infty d\psi' \frac{e^{-\frac{(\psi')^2}{4N\Delta_{\text{eff}}}}}{\sqrt{4\pi N\Delta_{\text{eff}}^2}} (1 - e^{-\frac{\delta h}{T_c(h)}\psi'}) \right\} \qquad p_1^{2-\text{level}}(\psi, \delta h) = \frac{e^{-\frac{\psi^2}{4N\Delta_{\text{eff}}}}}{\sqrt{4\pi N\Delta_{\text{eff}}^2}} (1 - e^{-\frac{\delta h}{T_c(h)}\psi}). \tag{53}$$

If we take $N \to \infty$ limit with fixed δh in Eq. (52) and Eq. (53), the distribution function reduces to a single delta function $\delta(\psi)$. On the other hand, the result also suggests us to consider the distribution of a scaled variable,

$$\tilde{\psi} \equiv \frac{\psi}{\Delta Y} \qquad \Delta Y = \sqrt{N}\Delta_{\text{eff}} \tag{54}$$

where ΔY is the scale of typical height of a step given in Eq. (33). Its distribution function reads as,

$$\tilde{p}^{2-\text{level}}(\tilde{\psi}, \delta h/h_{\text{s}}) = \tilde{p}_0^{2-\text{level}}(\tilde{\psi}, \delta h/h_{\text{s}}) + \tilde{p}_1^{2-\text{level}}(\tilde{\psi}, \delta h/h_{\text{s}}) \tag{55}$$

with

$$\tilde{p}_0^{2-\text{level}}(\tilde{\psi}, \delta h/h_{\text{s}}) = \delta(\tilde{\psi})\left[1 - \int_0^\infty d\tilde{\psi}\frac{e^{-\frac{\tilde{\psi}^2}{4}}}{\sqrt{4\pi}}\left(1 - e^{-\frac{\delta h}{h_{\text{s}}}\tilde{\psi}}\right)\right] = \delta(\tilde{\psi})\left(1 - \frac{\delta h}{h_s}\right) + O\left(\frac{\delta h}{h_s}\right)^2$$

$$\tilde{p}_1^{2-\text{level}}(\tilde{\psi}, \delta h/h_{\text{s}}) = \frac{e^{-\frac{\tilde{\psi}^2}{4}}}{\sqrt{4\pi}}\left(1 - e^{-\frac{\delta h}{h_{\text{s}}}\tilde{\psi}}\right) = \frac{\delta h}{h_s}\frac{e^{-\frac{\tilde{\psi}^2}{4}}}{\sqrt{4\pi}}\tilde{\psi} + O\left(\frac{\delta h}{h_s}\right)^2 \tag{56}$$

where we find a natural scale of the field,

$$h_{\text{s}} = \frac{T_{\text{c}}}{\sqrt{N}\Delta}. \tag{57}$$

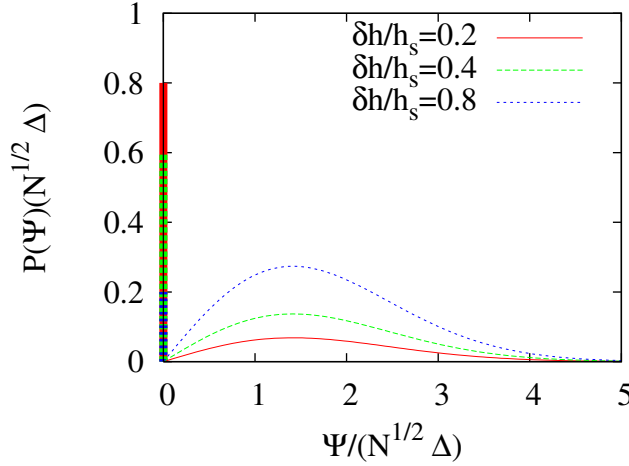Note that this is nothing but the scale of the typical spacing between steps given in Eq. (34).

FIG. 8: Plot of the distribution function $\tilde{P}(\tilde{\psi})$ of the scaled response $\tilde{\psi} = \psi/\sqrt{N}\Delta$. Here contributions from the terms up to $O(\delta h/h_s)$ in Eq. (56) are displayed. For small fields $\delta h/h_{\text{s}} \ll 1$, most of the sample remain intact by the presence of the field while *rare samples* of a fraction of order $O(\delta h/h_{\text{s}})$ make large jumps of order $\sqrt{N}\Delta$.

A notable feature of Eq. (56) is that it is an *analytic* function of the scaled field $\delta h/h_{\text{s}}$. For sufficiently small field $\delta h/h_{\text{s}} \ll 1$, the terms up to $O(\delta h/h_{\text{s}})$ will be sufficient. In Fig. 8 we display the distribution function using the terms up to $O(\delta h/h_{\text{s}})$ in Eq. (55)-Eq. (56). We can understand the physical meaning of the profile as the following. The term $\tilde{p}_1^{2-\text{level}}(\delta h/h_{\text{s}}, \tilde{\psi})$, which is $O(\delta h/h_{\text{s}})$, represent *rare samples* which jump by very small field while the other term $\tilde{p}_0^{2-\text{level}}(\delta h/h_{\text{s}}, \tilde{\psi})$ represent majority of the samples which remain intact by the presence of the field. Thus the distribution function describes the intermittency of the mesosocpic response.

2. Three-level model

Now we extend the analysis including the 3rd lowest state and consider a three-level model, which consists of the ground state 0, 1st excited state 1 and the 2nd excited state 2 under h. The pattern of level crossings can be classified into $3! = 6$ cases depending on the ordering of Y_0, Y_1 and Y_2 as shown in Fig. 7. In this model there can be at most 2 level crossings within a given interval δh while only 1 level crossing was allowed in the two-level model.

Similarly to Eq. (55), it is natural to decompose the scaled probability distribution function as,

$$\tilde{p}^{3-\text{level}}(\tilde{\psi}, \delta h/h_{\text{s}}) = \tilde{p}_0^{3-\text{level}}(\tilde{\psi}, \delta h/h_{\text{s}}) + \tilde{p}_1^{3-\text{level}}(\tilde{\psi}, \delta h/h_{\text{s}}) + \tilde{p}_2^{3-\text{level}}(\tilde{\psi}, \delta h/h_{\text{s}}) \tag{58}$$

where the 1st, 2nd and 3rd terms in r.h.s. corresponds to the cases that the ground state at $h + \delta h$ is at '0', '1' and

'2' respectively. They are computed in the appendix D. The results read as,

$$\tilde{p}_0^{3-\text{level}}(\tilde{\psi}, \delta h/h_\text{s}) = \delta(\tilde{\psi})\left[1 - \int_0^\infty d\tilde{\psi}\left(\tilde{p}_1^{3-\text{level}}(\tilde{\psi}) + \tilde{p}_2^{3-\text{level}}(\tilde{\psi})\right)\right]$$

$$\tilde{p}_1^{3-\text{level}}(\tilde{\psi}, \delta h/h_\text{s}) = \frac{e^{-\frac{\tilde{\psi}^2}{4}}}{\sqrt{4\pi}}\left(1 - e^{-\frac{\delta h}{h_\text{s}}\tilde{\psi}}\right)\left[1 - \int_{-\infty}^\infty \frac{dz_1}{\sqrt{4\pi}}e^{-\frac{z_1^2}{4}}\int_{\frac{z_1+\tilde{\psi}}{2}}^\infty \frac{dz_2}{\sqrt{2\pi}}e^{-\frac{z_2^2}{2}}\left(1 - e^{-\frac{1}{2}\frac{\delta h}{h_\text{s}}(z_2 - \frac{z_1+\tilde{\psi}}{2})}\right)\right]$$

$$\tilde{p}_2^{3-\text{level}}(\tilde{\psi}, \delta h/h_\text{s}) = \left(1 - 2e^{-\frac{\delta h}{h_\text{s}}\tilde{\psi}} + e^{-2\frac{\delta h}{h_\text{s}}\tilde{\psi}}\right)\int_{-\infty}^\infty \frac{dz_1}{\sqrt{4\pi}}e^{-\frac{z_1^2}{4}}\int_{\frac{z_1-\tilde{\psi}}{2}}^\infty \frac{dz_2}{\sqrt{2\pi}}e^{-\frac{z_2^2}{2}}$$

$$+ \left(1 - 2e^{-\frac{\delta h}{h_\text{s}}\tilde{\psi}} + e^{-2\frac{\delta h}{h_\text{s}}\tilde{\psi}}\right)\int_{-\infty}^\infty \frac{dz_1}{\sqrt{2\pi}}e^{-\frac{z_1^2}{2}}\int_{z_1}^\infty \frac{dz_2}{\sqrt{2\pi}}e^{-\frac{z_2^2}{2}}\left(1 - e^{-2X}\right)_{X=\frac{\delta h}{h_\text{s}}(\tilde{\psi}-(z_2-z_1))}$$

$$+ \int_{-\infty}^\infty \frac{dz_1}{\sqrt{2\pi}}e^{-\frac{z_1^2}{2}}\int_{z_1}^\infty \frac{dz_2}{\sqrt{2\pi}}e^{-\frac{z_2^2}{2}}\left[-(1 - e^{-2X}) + \frac{4}{3}(1 - e^{-3X}) - \frac{1}{2}(1 - e^{-4X})\right]_{X=\frac{\delta h}{h_\text{s}}(\tilde{\psi}-(z_2-z_1))} . \tag{59}$$

Comparing Eq. (59) and Eq. (56) we find that following. First $p_2(\psi, \delta h/h_\text{s})$, which is absent in the 2-level model, is $O((\delta h/h_\text{s})^2)$. Second, $p_0(\psi, \delta h/h_\text{s})$ and $p_1(\psi, \delta h/h_\text{s})$ of the 3-level model agree with those of 2-level model up to $O(\delta h/h_\text{s})$. The situation is reminiscent of the low temperature expansion where we found that M-level model give correct results up to $O((T/T_c)^{M-1})$ as we prooved in section C 1. In the present context we do not have an equivalent proof but we believe that M-level model gives correct results up to $O((\delta h/h_\text{s})^{M-1})$. By this way, we can go beyond the limit of single steps and access successive steps.

3. Discussions

The above results suggest that distribution of ths scaled variable $\tilde{\psi}$ follows a generic scaling form,

$$\tilde{P}(\tilde{\psi}, \delta h/h_\text{s}) = \delta(\tilde{\psi})\left(1 - \int_0^\infty d\tilde{\psi}\tilde{P}_\text{jump}(\tilde{\psi}, \delta h/h_\text{s})\right) + \tilde{P}_\text{jump}(\tilde{\psi}, \delta h/h_\text{s})$$

$$\tilde{P}_\text{jump}(\tilde{\psi}, \delta h/h_\text{s}) \equiv \sum_{n=1}^\infty \left(\frac{\delta h}{h_\text{s}}\right)^n f_n(\tilde{\psi}) \qquad \text{for} \qquad \delta h/h_\text{s} \ll 1 \tag{60}$$

The term $\tilde{P}_\text{jump}(\tilde{\psi}, \delta h/h_\text{s})$ represent contributions of the samples in which the ground state changes responding to the field. We expect correct value of the coefficient f_n will be obtained by considering $n + 1$-level model, which can take into account possible n successive jumps in a given internal δh. We expect that the qualitative feature is explained well by Fig. 8 and higher order terms of $\delta h/h_\text{s}$ give only mild modifications without changing very much the shape of the distribution function.

The distribution function of the response is a *smooth* function of the scaled field $\delta h/h_\text{s}$ in spite of the fact that the underlying responses in each sample are highly non-linear processes. It must be contrasted with the expansion of the *response itself* in a given sample in power series of $\delta h/h_\text{w}$ (See Eq. (31)). The static FDT relies on the latter kind of expansion and thus it can *not* be applied beyond the scale of a single step h_s. On the other hand, it must be noted that the power series of $\delta h/h_\text{s}$ will converge only for sufficiently small $\delta h/h_\text{s}$. Since h_s given in Eq. (57) (or Eq. (34)) vanishes in the thermodynamic limit $N \to \infty$, the new power series also describes not macroscopic but mesoscpic responses.

Let us call the regime $\delta h \ll h_\text{s}$, where the expansion converges, as *weakly perturbed regime*, and the other regime $\delta h \gg h_\text{s}$ as *strongly perturbed regime* following [47].

- An important generic feature in the weakly perturbed regime is that even with such a small field $\delta h \ll h_\text{s}$, where most of the samples do not respond at all, there are a fraction of 'fragile' samples of order $\delta h/h_\text{s}$ which are able to respond strongly chaging its own ground state. Although they are *rare*, they dominate average behaviours. This means, static chaos effect does not appear all of a sudden at certain large sizes (or strong enough field) but appear strongly on rare samples even at small sizes (or weak field) and thus appear gradually in the averaged quantities. The weakly perturbed regime is examined numerically in detail in the static chaos problems of directed polymer in random media in [47]. Recently it was also examined in detail in a study of bond-chaos effect in the Edwards-Anderson spin-glass model [48]. The weakly perturbed regime is also proposed to explain some features observed in temperature-shift experiments on spin-glasses [51, 52].

- In the strongly perturbed regime $\delta h \gg h_{\mathrm{s}}$, where most of the samples will respond, we still expect the distribution function of the repsonse ψ follows the generic scaling form as Eq. (60) but with a different functional form,

$$\tilde{P}(\tilde{\psi}, \delta h/h_{\mathrm{s}}) \sim \frac{\exp\left(-\frac{(\tilde{\psi}-\delta h/h_{\mathrm{s}})^2}{4}\right)}{\sqrt{4\pi}} \qquad \text{for} \qquad \delta h/h_{\mathrm{s}} \gg 1 \tag{61}$$

which means

$$P(\psi, \delta h) \sim \frac{\exp\left(-\frac{(\psi-N\delta h/T_c(h))^2}{4N(\Delta_{\mathrm{eff}}(h)^2)}\right)}{\sqrt{4\pi N(\Delta_{\mathrm{eff}}(h))^2}} \qquad \text{for} \qquad \delta h/h_{\mathrm{s}} \gg 1. \tag{62}$$

in terms of the original unscaled variable $\psi = Y(h+\delta h) - Y(h)$.

The reason for the above functional form is the following. Since there will be large number of steps $\delta h/h_{\mathrm{s}} \sim O(\sqrt{N}) \gg 1$ witin a fixed interval δh, each step with an increment of order $\Delta Y \sim \Delta_{\mathrm{eff}}(h)\sqrt{N}$, the total response within δh will be $O(N)$. This is consistent with the fact that the response must be *extensive* in the thermodynamic sense. Since the total response is the sum of suc a large number of steps, we expect its sample-to-sample fluctuation follows the Gaussiandistribution due to the central limit theorem. From the thermodynamic calcurations we know that

$$[\![\psi]\!] = [\![Y]\!]_{h+\delta h} - [\![Y]\!]_h = N\frac{(\Delta_{\mathrm{eff}}(h))^2 \delta h}{T_c(h)} \tag{63}$$

as given in Eq. (B10). Since there will be for sure some steps in the strongly perturbed regime, Y varianle of the ground state at h and that at $h+\delta h$ must be uncorrelated. Thus the squared-variance of ψ will be just the sum of those at h and $h+\delta h$, which amounts to $2N\Delta_{\mathrm{eff}}(h)^2$. In short, in the strongly perturbed regime we observe thermodynamic response which is *self-averaging*, while in the weakly perturbed regime, we observer mesoscopic response which is *non-self averaging*.

Lastly it is interesting to note that *average* response, obtained in the weakly perturbed regime, matches precisely with that in the strongly perturbed regime Eq. (63). From Eq. (55)-Eq. (56) we find

$$[\![\psi]\!] = \frac{\delta h}{h_{\mathrm{s}}} + O\left(\frac{\delta h}{h_{\mathrm{s}}}\right)^2 \tag{64}$$

which means,

$$[\![\psi]\!] = N\frac{(\Delta_{\mathrm{eff}}(h))^2 \delta h}{T_c(h)} + O\left(\frac{\delta h}{h_{\mathrm{s}}}\right)^2. \tag{65}$$

This agrees with the average in the strongly perturbed regime Eq. (63). Both are linear in δh so that they yeild the same linear susceptibility. This coincidence is consistent with the expectation that disorder-average of the linear susceptibility and 1st derivative of thermodynamic response should agree (See appendix A).

D. Cusp in the overlap

Finally we analyze the overlap function, given by Eq. (14), between two replicas subjected to slightly differnt fields which reads as,

$$C(\delta h) = \frac{[\![\langle Y(h+\delta h)\rangle \langle Y(h-\delta h)\rangle]\!]}{\left[\!\left[\langle Y(h)\rangle^2\right]\!\right].} \tag{66}$$

1. FDT approach

Let us consider a Taylor expansion of the correlation function $\langle Y(h+\delta h)\rangle \langle Y(h-\delta h)\rangle$ in power series of δh,

$$\langle Y(h+\delta h)\rangle \langle Y(h-\delta h)\rangle = (\kappa_1(Y))^2 - (\beta\delta h)^2((\kappa_2(Y))^2 - \kappa_3(Y)\kappa_1(Y)) + O(\beta\delta h)^4 \tag{67}$$
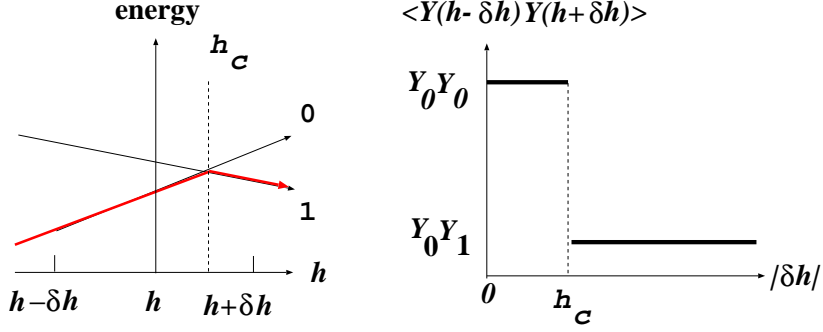
FIG. 9: Level crossing and decay of the overlap between 2-replicas subjected to $h - \delta h$ and $h + \delta h$. Here an example of the case $Y_0 > Y_1 > 0$ is shown.

Note that terms of odd powers of δh are absent smiply due to the symmetry of the correlation function under $\delta h \leftrightarrow -\delta h$.

We have obtained $\kappa_2^2(Y)$ up to $O(T/T_c)^3$ as Eq. (47). To the same order we find,

$$
[\kappa_1^2(Y)] = (\Delta\sqrt{N})^2 \left\{ 1 - \frac{T}{T_c} + O\left(\frac{T}{T_c}\right)^3 \right\} \qquad [\![\kappa_3(Y)\kappa_1(Y)]\!] = -(\Delta\sqrt{N})^4 \left\{ \frac{T}{T_c} - \left(\frac{T}{T_c}\right)^2 + O\left(\frac{T}{T_c}\right)^3 \right\} \qquad (68)
$$

as reported in Appendix C. Combining these results we obtain,

$$
C(\delta h) = 1 + O\left(\frac{T}{T_c}\right)^3 - \left(\frac{\delta h}{h_w}\right)^2 \left\{ 2\frac{T}{T_c} + \left(\frac{T}{T_c}\right)^2 + O\left(\frac{T}{T_c}\right)^3 \right\} + O\left(\frac{\delta h}{h_w}\right)^4 \qquad (69)
$$

where $h_w = T/(\Delta\sqrt{N})$ as given by Eq. (5). As shown in Fig. 10, the series Eq. (69) describes the thermally rounded region of the correlation function around $\delta h = 0$.

We know that the thermal cumulants which appear Eq. (67) are non-self averaging. Thus the overlap must be non-self averaging as well.

2. Zero temperature limit

Now we turn to the case of zero temperature limit where the FDT approach breaks down since $h_w \to 0$. For simplicity we only consider the 2-level model. As sohwn in Fig. 9, the overlap between the two replicas remains Y_0^2 in the range $0 < |\delta h| < h_c$ and becomes $Y_0 Y_1$ at $|\delta h| > \delta h_c$. The critical field is given by $\delta h_c = \Delta F/(Y_0 - Y_1)$.

Considering the cases $Y_0 > Y_1$ and $Y_1 > Y_0$, we obtain

$$
\lim_{T \to 0} [\![\langle Y(h - \delta h)Y(h + \delta h)\rangle]\!] = \int_{-\infty}^{\infty} dY_0 \int_{Y_0}^{\infty} dY_1 P(Y_0)P(Y_1) \left[Y_0^2 \int_{|\delta h|(Y_1 - Y_0)}^{\infty} d\Delta F \rho(\Delta F) + Y_0 Y_1 \int_{-\infty}^{|\delta h|(Y_1 - Y_0)} d\Delta F \rho(\Delta F) \right]
$$

$$
+ \int_{-\infty}^{\infty} dY_0 \int_{-\infty}^{Y_0} dY_1 P(Y_0)P(Y_1) \left[Y_0^2 \int_{|\delta h|(Y_0 - Y_1)}^{\infty} d\Delta F \rho(\Delta F) + Y_0 Y_1 \int_{-\infty}^{|\delta h|(Y_0 - Y_1)} d\Delta F \rho(\Delta F) \right]
$$

$$
= N\Delta^2 \left[1 - \frac{\delta h}{h_s} \left(\int_{-\infty}^{\infty} \frac{dy_0}{\sqrt{2\pi}} \int_{-\infty}^{y_0} \frac{dy_1}{\sqrt{2\pi}} y_0(y_0 - y_1)^2 - \int_{-\infty}^{\infty} \frac{dy_0}{\sqrt{2\pi}} \int_{y_0}^{\infty} \frac{dy_1}{\sqrt{2\pi}} y_0(y_0 - y_1)^2 \right) + O\left(\frac{\delta h}{h_s}\right)^2 \right] \qquad (70)
$$

from which we find,

$$
\lim_{T \to 0} C(\delta h) = 1 - \frac{4}{\sqrt{\pi}} \frac{|\delta h|}{h_s} + O\left(\frac{|\delta h|}{h_s}\right)^2 . \qquad (71)
$$

A remarkable feature of the correlation function at $T = 0$ is that it exhibits a cus singurality at $\delta h = 0$. In Fig. 9 it is evident that the cusp is strongly non-self averaging. The linear $|\delta h|$ profile is due to the presence of *rare samples* which have critical fields δh_c close to $\delta h = 0$.

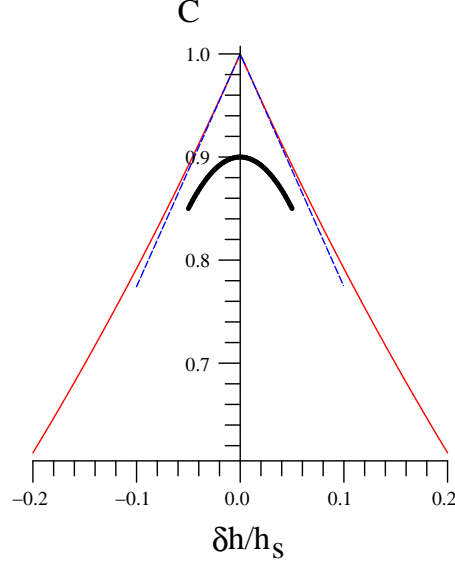FIG. 10: The profile of the overlap function. It exhibits a cusp at $T = 0$, which is rounded at finite temperatures. The doted line is Eq. (71) obtained at zero temperature with the two-level model, which correctly captures the feature around the top of the cusp. The solid line is the result obtained by the replica method at $T = 0$ which yeilds the full profile. (See sec. V C.) The dashed line is the curve at $T/T_c = 0.1$ Eq. (69) obtained by the FDT approach (using the 2-level model), which describes thermally rounded region of wdith h_w around the center.

V. REPLICA APPROACH

In this section we analyze the mesoscopic responses by a replica approach. This complements the low temperature exapnsion approach discussed in the previous section. We construct a generating functional from which various correlation functions associated with the mesoscopic responses can be computed exactly.

A. Generating functional

To analyze statistical properties of mesoscopic static responses it is useful to consider the following object:

$$\frac{\partial^{k_1}}{\partial(\beta\delta h)^{k_1}} \frac{\partial^{k_2}}{\partial(\beta\delta h)^{k_2}} \cdots \frac{\partial^{k_p}}{\partial(\beta\delta h)^{k_p}} [\![(-\beta F(\delta h_1))(-\beta F(\delta h_2))\ldots(-\beta F(\delta h_p))]\!] \tag{72}$$

with $k_1 \geq 1$, $k_2 \geq 1$,...,$k_p \geq 1$. Here $F(\delta h)$ is the free-energy of a system sujected to a small probing field δh. The derivatives with respect to the probing fields yeild disorder averages of various kinds of correlation functions of our interests. Using the replica formalism the product of the free-energies $[\![F(\delta h_1)F(\delta h_2)\ldots F(\delta h_p)]\!]$ in the above expression can be replaced by

$$\lim_{n_1, n_2, \ldots, n_p \to 0} \frac{1}{n_1 n_2 \cdots n_p} \overline{Z^{n_1}(\delta h_1) Z^{n_2}(\delta h_1) \ldots Z^{n_p}(\delta h_p)} \tag{73}$$

where $Z(\delta h)$ is the partition function of the system. Thus we need to consider *real* replicas $r = 1, 2, \ldots, p$ which are subjected to different probing fields $\delta h_1, \delta h_2, \ldots, \delta h_p$ and replicated further into $n_1, n_2, \ldots, n_r$ replicas.

1. p-spin Ising model and REM

To be specific, let us consider the p-spin Ising mean-field spin-glass model [25, 44] given Eq. (1). Following the standard steps [44] we obtain the replicated partition function of n-replicas,

$$[\![Z^n]\!] = \mathrm{Tr}_\sigma \left[e^{-\beta \sum_{a=1}^n H(\{\sigma_i^a\})} \right] = e^{nN(\beta J)^2/4} \int \prod_{a<b} dQ_{ab} \int \prod_{a<b} \frac{d\lambda_{ab}}{2\pi} e^{-NG(\{Q_{ab}\},\{\lambda_{ab}\})} \tag{74}$$
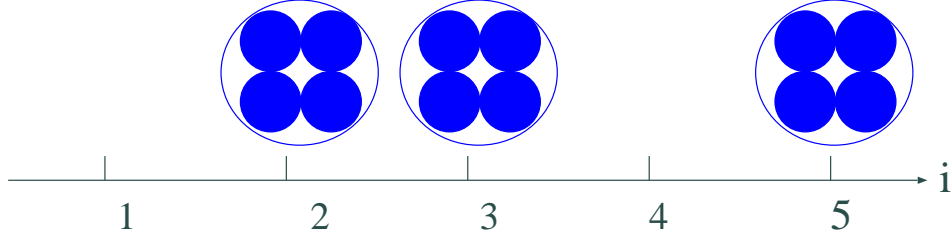
FIG. 11: A schematic representation of an 1 step RSB ansatz. n replicas ('atoms') are grouped in n/m clusters ('molecules') of size m. Different clusters occupy different metastable states i.
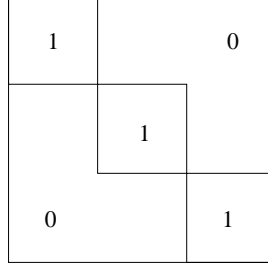

FIG. 12: Parisi's matrix I for a 1 step RSB solution of size $n \times n$. The size of the blocks are $m \times m$. Different solutions, corresponding to different grouping of the atoms in Fig. 11, are obtained by permutations of the lows and columns.

where

$$G(\{Q_{ab}, \lambda_{ab}\}) = -\frac{(\beta J)^2}{4} \sum_{a \neq b} Q_{ab}^p + \frac{1}{2} \sum_{a \neq b} \lambda_{ab} Q_{ab} - \ln \mathrm{Tr}_\sigma e^{\mathcal{L}} \tag{75}$$

with

$$\mathcal{L} = \frac{1}{2} \sum_{a \neq b} \lambda_{ab} \sigma_a \sigma_b + \sum_a \beta(h + \delta h_a)\sigma_a \tag{76}$$

Here λ_{ab} are Lagrangian multipliers introduced to define the overlap,

$$Q_{ab} = \frac{1}{N} \sum_{i=1}^{N} \sigma_i^a \sigma_i^b. \tag{77}$$

The integrals over Q_{ab} and λ_{ab} are evaluated using the saddle point method.

Note that we have added small perturbing field δh_a applied on each replica in addition to the uniform external field h. *We suppose that the perturbing fields are infenitesimally small such that they do not change the saddle point itself.*

Now we consider a particular 1 step RSB saddle point in which the n replicas are groupd into clusters $\mathcal{C} = 1, 2, \ldots, n/m$ of size m. (see Fig. 11.) The parameter m is known to depend on the temperature as (See Eq. (B20) for the case of the REM),

$$m = \frac{T}{T_{\mathrm{c}}(h)}. \tag{78}$$

For such a saddle point the $n \times n$ matricies Q_{ab} and λ_{ab} can be put into block-diagonal forms with block size m (see Fig. 12). We denote the matrix elements in the block diagonal parts as q_1, λ_1 and the others as q_0 and λ_0. Then one obtains for sufficiently small n,

$$\ln \mathrm{Tr}_\sigma e^{\mathcal{L}} = -n\frac{\lambda_1}{2} + \int Dz_0 \sum_{\mathcal{C}=1}^{n/m} \ln \int D_{z_{1\mathcal{C}}} \prod_{a \in \mathcal{C}} (2 \cosh \Xi(h + \delta h_a)) \tag{79}$$

with $\int Dz \ldots \equiv \int_{-\infty}^{\infty} \frac{dz}{\sqrt{2\pi}} e^{-z^2/2} \ldots$ and

$$\Xi(h) = \beta h + \sqrt{\lambda_0} z_0 + \sqrt{\lambda_1 - \lambda_0} z_{1\mathcal{C}}. \tag{80}$$

Making an exansion about the perturbing field δh_a, we obtain

$$\ln \mathrm{Tr}_\sigma e^{\mathcal{L}} = (\ln \mathrm{Tr}_\sigma e^{\mathcal{L}})_{\delta h=0} + \mu \sum_{a=1}^{n} \beta \delta h_a + T\chi^{\mathrm{EA}} \sum_{a=1}^{n} \frac{(\beta \delta h_a)^2}{2} + \frac{\Delta^2}{2} \sum_{\mathcal{C}=1}^{n/m} \sum_{a \in \mathcal{C}, b \in \mathcal{C}} \beta \delta h_a \beta \delta h_b + O(\delta h)^3 \tag{81}$$

with

$$\mu = \int D_{z_0} \frac{\int D_{z_1} \cosh^m(h) \tanh \Xi(h)}{\int D_{z_1} \cosh^m(h)} \qquad T\chi_{\mathrm{EA}} = 1 - \int D_{z_0} \left\{ \frac{\int D_{z_1} \cosh^m(h) \tanh \Xi(h)}{\int D_{z_1} \cosh^m(h)} \right\}^2 \tag{82}$$

and

$$(\Delta_{\mathrm{eff}})^2 = \int D_{z_0} \left[\frac{\int D_{z_1} \cosh^m(h) \tanh^2 \Xi(h)}{\int D_{z_1} \cosh^m(h)} - \left\{ \frac{\int D_{z_1} \cosh^m(h) \tanh \Xi(h)}{\int D_{z_1} \cosh^m(h)} \right\}^2 \right]. \tag{83}$$

The replicated parition function Eq. (74) contains contributions from other 1 step RSB solutions obtained by permutations of replicas. One must also integrate over fluctuations around saddle points. Then the replicated partition function is obtained as,

$$[\![Z^n]\!] = c \sum_{\mathrm{SP}} \exp \left[N\mu \sum_{\alpha=1}^{n} \beta \delta h_\alpha + NT\chi^{\mathrm{EA}} \sum_{\alpha=1}^{n} \frac{(\beta \delta h_\alpha)^2}{2} + \frac{(\sqrt{N}\Delta_{\mathrm{eff}})^2}{2} \sum_{\mathcal{C}=1}^{n/m} \sum_{\substack{\alpha \neq \beta \\ \alpha,\beta \in \mathcal{C}}} \beta \delta h_\alpha \beta \delta h_\beta + O(\delta h)^3 \right] \tag{84}$$

where $\sum_{\mathrm{SP}}$ stands for summation over all possible permutations of replicas, i.e. different ways of grouping the n replicas into n/m clusters of size m. The factor c stands for a common factor which does not depend on the probing field δh's. Then for the case that we have p replicas (See Eq. (73)) we obtain the following expression,

$$\begin{aligned}
\left[Z_1^{n_1} Z_2^{n_2} \ldots Z_p^{n_p} \right] = \quad & c \sum_{\mathrm{SP}} \exp \left[\mu \sum_{a=1}^{n} \beta \delta h_a + T\chi^{\mathrm{EA}} \sum_{a=1}^{n} \frac{(\beta \delta h_a)^2}{2} \right. \\
& \left. + \frac{(\sqrt{N}\Delta_{\mathrm{eff}})^2}{2} \sum_{r,s=1}^{p} \beta \delta h_r \beta \delta h_s \sum_{\beta=(r,1)}^{(r,n_r)} \sum_{\beta=(s,1)}^{(s,n_s)} \delta_{i_\alpha,i_\beta} + O(\delta h)^3 \right].
\end{aligned} \tag{85}$$

Here we have p groups of replicas. We labeled the groups as $r = 1, 2, \ldots, p$. r-th group consists of n_r replicas which we labeled as $(r,1), (r,2), \ldots, (r,n_r)$. The total number of replicas is

$$n_{\mathrm{tot}} = \sum_{r=1}^{p} n_r. \tag{86}$$

Let us explain the physical meaning of the terms in the argument of the exponential function in Eq. (85).

- It is easy to veryfy that the parameter μ for the terms at order $O(\delta h)$ represents the expectation value of the magnetization $\mu = [\![\langle \sigma \rangle]\!]$.

- We have devided the $O(\delta h)^2$ terms into two parts: one which involves single replicas and the other which envolves pairs of replicas. Physically we understand the former as due to *intra-state response* and the latter as due to *inter-state response*. As is well known, in the limit $p \to \infty$ the p-spin model reduces to the REM [25, 44] in which the *intra-state* linear-suscepibility χ_{EA} is zero by construction of the model.

Here let us note that the evaluations of the $O(\delta h)^2$ terms must be done carefully. Actually the expressions for the parameters χ_{EA} and Δ_{eff} Eq. (82) and Eq. (83) are valid only for zero external field $h = 0$. This is because for $h \neq 0$, the magnetization μ is non-zero so that integrations over fluctuations around the saddle points yield additional $O(\delta h)^2$ terms. Such calcurations are very difficult to perform in general. An exception is the case of REM ($p \to \infty$ limit) in which we only need to consider fluctuation of the *size* of the clusters m in the 1 step RSB solutions. as we report in appendix G.

For the rest of the present section we consider the case of REM $p \to \infty$ which allows us to neglect intra-state responses. As we noted in section II B, REM can be regarded as an effective model for a generic 1 step RSB systems.

B.   Sample-to-sample fluctuations of linear and non-linear susceptibilities

We now analyze the statistics of the susceptibilities using the replica approach to confirm the results obtained by the low temperature expansion approach in sec. IV B. As we show below we obtain presumably exact results for the sample average of the p-th moment of the thermal cumulants $[\![\kappa_k^p(Y)]\!]$ given by Eq. (41). Interestingly the results are expressed in power series of the parameter $m = T/T_c(h)$ (sed Eq. (78)) which can actually be viewed as expansions in power series of T, i.e. low temperature expansion.

Sample-average of p-th moment of the thermal cumulant $\kappa_k(Y)$ given by Eq. (41) can be computed as,

$$[\![\kappa_k^p(Y)]\!] = \lim_{n_1,n_2,\ldots,n_p \to 0} \frac{\partial^k}{\partial(\beta\delta h_1)^k} \frac{\partial^k}{\partial(\beta\delta h_2)^k} \cdots \frac{\partial^k}{\partial(\beta\delta h_p)^k} \left. \frac{\left[Z_1^{n_1} Z_2^{n_2} \ldots Z_p^{n_p}\right]}{n_1 n_2 \cdots n_p}\right|_{\delta h=0}$$

$$= (\sqrt{N}\Delta_{\text{eff}})^{kp} \lim_{n_1,n_2,\ldots,n_p \to 0} \frac{1}{n_1 n_2 \cdots n_p} \frac{\partial^k}{\partial x_1^k} \frac{\partial^k}{\partial x_2^k} \cdots \frac{\partial^k}{\partial x_p^k} \left\langle \left. \exp\left[\frac{1}{2}\sum_{r,s=1}^p x_r x_s A_{rs}\right]\right|_{x=0}\right\rangle_{\text{SP}} \tag{87}$$

where we introduced a scaled variable x_r defined as

$$x_r = \frac{\beta\delta h_r}{\Delta_{\text{eff}}\sqrt{N}} = \frac{\delta h_r}{h_{\text{w}}} \tag{88}$$

with h_{w} given in Eq. (5) and

$$A_{rs} \equiv \sum_{\alpha=(r,1)}^{(r,n_r)} \sum_{\beta=(s,1)}^{(s,n_s)} \delta_{i_\alpha,i_\beta} \tag{89}$$

and the bracket $\langle\ldots\rangle_{\text{SP}}$ means to take an average over all possible partitions of n_{tot} replicas into n_{tot}/m clusters of size m.

Let us begin from the linear susceptibility. As in the approach by the low temperature expansion we study 1st and 2nd moment of the 2nd thermal cumulant $\kappa_2(Y)$. Using the prescription Eq. (87) for the sample-average of the 1st moment of the 2nd thermal cumulant $\kappa_2(Y)$ we find,

$$[\![\kappa_2(Y)]\!] = (N(\Delta_{\text{eff}})^2) \lim_{n\to 0} \frac{1}{n} \langle A\rangle_{\text{SP}} \tag{90}$$

where

$$A = \sum_{\alpha,\beta}^n \delta_{i_\alpha,i_\beta} = n + \sum_{\alpha\neq\beta}^n \delta_{i_\alpha,i_\beta} \tag{91}$$

We now need to evaluate $\langle\delta_{i_\alpha,i_\beta}\rangle_{\text{SP}}$ for $\alpha = \beta$ which is the probability that two distinct replicas belong to a common cluster. It is evaluated as,

$$\langle\delta_{i_\alpha,i_\beta}\rangle_{\text{SP}} = \frac{(n/m)\cdot m(m-1)\cdot(n-2)!}{n!} = \frac{m-1}{n-1}.$$

Here the denominator $n!$ is the total number of solutions and the numerator is the number of solutions in which two distinct replicas belong to a common cluster. The first factor n/m in the numerator is the number of ways to choose a cluster among n/m clusters. The 2nd factor $m(m-1)$ is the number of ways to choose two replicas out of m replicas belonging to the cluster. The last factor $(n-2)!$ is the number of ways to put the rest of replicas in the remaining $n-2$ seats. Then we obtain

$$\left\langle \sum_{\alpha\neq\beta}^n \delta_{i_\alpha,i_\beta}\right\rangle_{\text{SP}} = n(n-1)\langle\delta_{i_\alpha,i_\beta}\rangle_{\text{SP}} = n(m-1).$$

Using the above results we finally obtain a very simple result,

$$[\![\kappa_2(Y)]\!] = (\sqrt{N}(\Delta_{\text{eff}}))^2 m. \tag{92}$$

Since $m = T/T_c(h)$ as given in Eq. (78), this result agrees with that obtained by the low temperature expansion given by Eq. (46) obtained in sec IV B. There we have found that $O(T^2)$ term is zero. The above result means that actually all higher order terms are zero.

Next let us evaluate the sample-average of the 2nd moment of the 2nd thermal cumulant $\kappa_2(Y)$. Using Eq. (87) we find,

$$\left[\kappa_2^2(Y)\right] = (N(\Delta_{\rm eff})^2)^2 \lim_{n_1,n_2\to 0} \frac{1}{n_1 n_2}(2\left\langle A_{12}^2\right\rangle_{\rm SP} + \left\langle A_{11}A_{22}\right\rangle_{\rm SP}). \tag{93}$$

We report the details of the computations in appendix E. Here we only quote the result,

$$\left[\kappa_2^2(Y)\right] = (\sqrt{N}(\Delta_{\rm eff}))^4 m, \tag{94}$$

which again agree with the result obtained by the low temperature expansion given by Eq. (47). In sec IV B we have found that $O(T^2)$ term is zero. The above result means again that actually all higher order terms are zero.

Last let us study the non-linear susceptibility χ_2. As in the approach by the low temperature expansion we analyze the 2nd moment of the 3rd thermal cumulant $\kappa_3(Y)$. We report the details of the computations in appendix E. The result reads as,

$$\left[\kappa_3^2(Y)\right] = (\sqrt{N}(\Delta_{\rm eff}))^6 \lim_{n_1,n_2\to 0} \frac{1}{n_1 n_2}(9\left\langle A_{11}A_{12}A_{22}\right\rangle_{\rm SP} + \left\langle A_{12}^3\right\rangle_{\rm SP}) = (\sqrt{N}(\Delta_{\rm eff}))^6 2m(1-m), \tag{95}$$

which agrees with Eq. (48).

C. Cusp in the overlap

Finally let us study the overlap Eq. (14) between two real replicas, '1' and '2', subjected to slightly different fields $h_0 + \delta h_1$ and $h_0 + \delta h_2$ by the replica approach. As we discussed using the low temperature exapnsion approach in sec IV D, the correlation between the two real replicas,

$$\langle Y(h_0 + \delta h_1)Y(h_0 + \delta h_2)\rangle = \frac{\partial^2}{\partial(\beta h_1)\partial(\beta h_2)} \left[\!\left[\log Z(h_1)\log Z(h_2)\right]\!\right]\bigg|_{h_1=h_0+\delta h_1,h_2=h_0+\delta h_2} \tag{96}$$

should strongly fluctuate from sample-to-sample. Using the replica method its sample average can be expressed formally as,

$$\left[\!\left[\langle Y(h_0 + \delta h_1)Y(h_0 + \delta h_2)\rangle\right]\!\right] = \frac{\partial^2}{\partial(\beta h_1)\partial(\beta h_2)} \lim_{n_1,n_2\to 0} \frac{1}{n_1 n_2} \left[\!\left[Z^{n_1}(h_1)Z^{n_2}(h_2)\right]\!\right]\bigg|_{h_1=h_0+\delta h_1,h_2=h_0+\delta h_2}$$

$$= \frac{\partial^2}{\partial(\beta h_1)\partial(\beta h_2)} \lim_{n\to 0} \frac{4}{n^2} \sum_{\rm SP} \exp\left(\frac{(\sqrt{N}\Delta_{\rm eff})^2}{2} \sum_{r,s=1}^{2} \beta\delta h_r \beta\delta h_s \sum_{\alpha=(1,1)}^{(1,n/2)} \sum_{\beta=(2,1)}^{(2,n/2)} \delta_{i_\alpha,i_\beta}\right). \tag{97}$$

In the last equation $\sum_{\rm SP}$ stands for the summation over all 1RSB solutions. For simplicity we chose $n_1 = n_2 = n/2$ which will not change the result.

As in our previous analysis based on the low temperature expansion, here we can again analyze the correlation function in two ways 1) FDT approach and 2) $T \to 0$ limit approach.

For the 1) FDT approah it is useful to rewrite Eq. (97) rescaling the fields by the width of the steps $h_{\rm w} = T/\sqrt{N}\Delta_{\rm eff}$ as we did in Eq. (88);

$$\frac{\left[\!\left[\langle Y(h_0 + \delta h_1)Y(h_0 + \delta h_2)\rangle\right]\!\right]}{(\sqrt{N}\Delta_{\rm eff}(h_0))^2} = \frac{\partial^2}{\partial\left(\frac{\delta h_1}{h_{\rm w}}\right)\partial\left(\frac{\delta h_2}{h_{\rm w}}\right)} \lim_{n\to 0} \frac{4}{n^2} \sum_{\rm SP} \exp\left(\frac{1}{2} \sum_{r,s=1}^{2} \frac{\delta h_r}{h_{\rm w}}\frac{\delta h_s}{h_{\rm w}} \sum_{\alpha=(1,1)}^{(1,n/2)} \sum_{\beta=(2,1)}^{(2,n/2)} \delta_{i_\alpha,i_\beta}\right). \tag{98}$$

On the other hand, for 2) $T \to 0$ approach we may rewrite it rescaling the fields by the spacing between the steps $h_{\rm s} = T_c(h_0)/\sqrt{N}\Delta_{\rm eff}$,

$$\lim_{T\to 0} \frac{\langle Y(h_0 + \delta h_1)Y(h_0 + \delta h_2)\rangle}{(\sqrt{N}\Delta_{\rm eff}(h_0))^2} = \lim_{m\to 0} \frac{\partial^2}{\partial\left(\frac{\delta h_1}{h_{\rm s}}\right)\partial\left(\frac{\delta h_2}{h_{\rm s}}\right)} \lim_{n\to 0} \frac{4}{n^2} \sum_{\rm SP} m^2 \exp\left(\frac{1}{2m^2} \sum_{r,s=1}^{2} \frac{\delta h_r}{h_{\rm s}}\frac{\delta h_s}{h_{\rm s}} \sum_{\alpha=(1,1)}^{(1,n/2)} \sum_{\beta=(2,1)}^{(2,n/2)} \delta_{i_\alpha,i_\beta}\right). \tag{99}$$

Here we used $m = T/T_c(h_0)$ given by Eq. (78).

1. FDT approach

In the FDT approach we exapnd Eq. (98) in power series of $\delta h_1/h_{\rm w}$ and $\delta h_2/h_{\rm w}$ around $\delta h_1/h_{\rm w} = \delta h_2/h_{\rm w} = 0$. We find for the case $\delta h_1 = -\delta h_2 = -\delta h$,

$$\frac{[\langle Y(h_0 - \delta h)Y(h_0 + \delta h)\rangle]}{(\sqrt{N}\Delta_{\rm eff}(h_0))^2} = \frac{[\kappa_1^2(Y)]}{(\sqrt{N}\Delta_{\rm eff}(h_0))^2} - \left(\frac{\delta h}{h_{\rm w}}\right)^2 \frac{[\kappa_2^2(Y)] - [\kappa_3(Y)\kappa_1(Y)]}{(\sqrt{N}\Delta_{\rm eff}(h_0))^4} + O\left(\frac{\delta h}{h_{\rm w}}\right)^4$$

$$= (1 - m) - m(2 - m)\left(\frac{\delta h}{h_{\rm w}}\right)^2 + O\left(\frac{\delta h}{h_{\rm w}}\right)^4 \tag{100}$$

using $[\kappa_2^2(T)] = (\sqrt{N}\Delta_{\rm eff}(h))^4 m$ given in Eq. (94), $[\kappa^2(Y)] = (\sqrt{N}\Delta_{\rm eff})^2(1 - m)$ and $[\kappa_3(Y)\kappa_1(Y)] = -(\sqrt{N}\Delta_{\rm eff})^4 m(1 - m)$ reported in appendix E. Thus we find the overlap function Eq. (14) as,

$$C(\delta h) = 1 - \frac{m(2 - m)}{1 - m}\left(\frac{\delta h}{h_{\rm w}}\right)^2 + O\left(\frac{\delta h}{h_{\rm w}}\right)^4. \tag{101}$$

Indeed the result agrees with that by the low temperature expansion appraoch given in Eq. (69).

2. Zero temperature limit

Techincal difficulty with the 2) $T \to 0$ approah is that we have to express the result of the summation over all 1RSB solutions $\sum_{\rm SP}$ in a closed analytic form so that we can take the $m \to 0$ limit analytically [61]. We report the calucrations in appendix F. The results reads,

$$\lim_{T \to 0}\frac{C(\delta h)}{(\sqrt{N}\Delta_{\rm eff}(h))^2} = \sqrt{\frac{2}{\pi}}e^{-\frac{l^2}{8}}\int_0^\infty dx \frac{e^{-\frac{x^2}{2}}(x^2 - \frac{l^2}{4})}{e^{-\frac{|l|}{2}}M_0(x - \frac{|l|}{2}) + e^{\frac{|l|}{2}}M_0(-x - \frac{|l|}{2})}$$

$$- \frac{|l|}{\pi}e^{-\frac{l^2}{4}}\int_0^\infty dx \frac{e^{-x^2}e^{-x|l|}}{\left\{e^{-\frac{|l|}{2}}M_0(x - \frac{|l|}{2}) + e^{\frac{|l|}{2}}M_0(-x - \frac{|l|}{2})\right\}^2}$$

$$= 1 - \frac{4}{\sqrt{\pi}}\frac{|\delta h|}{h_{\rm s}} + O\left(\frac{|\delta h|}{h_{\rm s}}\right)^2 \tag{102}$$

with $l = 2\delta h/h_{\rm s}$. Thus the overlap function exhibists a cusp as shown in Fig. 10 in agreement with the result obtained by the low temperature exapnsion approach.

To derive the above result in appendix F, we used the approach of [32, 33] which study statistical properties of turbulant flows obeying the Burgers equation. In the next section we discuss the intriguing connection between the intermittency in the turbulant flows and step-wise responses in mesoscopic glassy systems.

VI. MAPPING TO A PINNED ELASTIC MANIFOLD PROBLEM AND A TURBULENCE PRPBLEM

In this section we discuss the connecton between the present problem of mesoscopic responses in glassy systems, the problem of jerky effective energy landscape of pinned elastic manifolds [30] and intermittency in turbulent flows due to shocks [31, 32, 33].

Let us consider a simple pinned elastic manifold problem, namely a particle on a one dimensional space connected to a Hookian spring and subjected to a radom potential [42]. The partitoin function and the Hamiltonian is defined as,

$$Z(Y_0) = \int_{-\infty}^\infty \frac{dY}{\sqrt{2\pi/(\beta\kappa)}}e^{-\beta U(Y,Y_0)} \qquad U(Y, Y_0) = \frac{\kappa}{2}(Y - Y_0)^2 + F(Y). \tag{103}$$

One end of the Hookian spring of spring constant κ is connected to the particle at Y and the other end is fixed at Y_0. $F(Y)$ is a random potential whose values are drawn from a Gaussian distribution with zero mean and a short-ranged spatial correlation,

$$[F(Y)F(Y')] = Nc(|Y - Y'|). \tag{104}$$

Here $c(y)$ is a certain rapidly decaying function. Comparing with the random energy model given by Eq. (15) with the simplest generalized complexity of the form Eq. (17), we find the two models are related as,

- The extensive variable Y becomes a *coordinate* of an one-dimensional space.

- The Gaussian distribution of the Y variables over differnt metastable states with variance $\Delta\sqrt{N}$ amounts to an effective *entropic* spring force with spring constant,

$$\kappa = \frac{T}{\Delta\sqrt{N}} = h_{\mathrm{w}} \tag{105}$$

- The random (free) energy F at different metastable states amounts to a random potential $F(Y)$ with short-ranged correlation.

- The external field h is equivalent to,

$$Y_0 = \frac{h}{\kappa}. \tag{106}$$

The *effective force* that the system yeilds can be defined as,

$$f(Y_0) \equiv -T\frac{\partial \ln Z(Y_0)}{\partial Y_0} = \kappa(\langle Y\rangle - Y_0) \tag{107}$$

By moving the end point Y_0 of the spring, the position of the particle $\langle Y\rangle$ in equilibrium changes elastically up to a certain point beyond which it exibit a sudden jump to a different energy minimum. Such a process was studied in detail by Bouchaud and Mézard [33]. The jump is of couse rounded at finite temperatures. This is what corresponds to the step-wise response we have discussed so far in the present paper. At such a jump, the effective force $f(Y_0)$ also changes discontnuously. Thus the *effective energy landscape* $-T\ln Z(Y_0)$ consists of parabolic wells matching with each other at singular poionts where the effective force (slope) is discontinuous. Note that the overlap function Eq. (14) we studied, which exhibit the same cusp as shown in Fig. 10, corresponds to the correlation function of the effective force $[\![f(0)f(Y_0)]\!]$.

As pointed out by Bouchaud and Mézard [33], the toy model Eq. (103) can be mapped to a yet another problem of a one dimensional tubulent flow. By the so called Cole-Hopf transformation,

$$v(Y_0, t) = -\beta\frac{\partial \ln Z(Y_0)}{\partial Y_0} \qquad \beta = \frac{1}{2\nu} \qquad \kappa = \frac{1}{t} \tag{108}$$

we obtain the Burgers equatrion for the velocity field $v(Y_0, t)$ at time t,

$$\frac{\partial v}{\partial t} + v\frac{\partial v}{\partial Y_0} = \nu\frac{\partial^2 v}{\partial Y_0^2} \tag{109}$$

where η is understood as the viscosity of the fluid. The initial condition at time $t = 0$ specified by,

$$v(Y_0, 0) = \frac{\partial E(Y_0)}{\partial Y_0}, \tag{110}$$

so that the velocity field is completely randon at $t = 0$.

The velocity field $v(Y, t)$ changes discontinuously at certain points in the space, namely *shocks*. The intermittency of the flow due to the presence of the shock is manifested in the velocity-velocity correlation function, which corresponds to the overlap function Eq. (14) in our probelm, as the cusp-like simgularity shown in Fig, 10. To observe well defined shocks (steps) one need to consider fluid of high enough viscosity η (low enough temperature T). The spacing between the shocks (spacing between the steps h_{s}) decreases as the time t (system size N) increases.

The toy model Eq. (103) is the simplest 0 dimensional version of the broad class of systems called *elastic manifolds in random media*. The cusp like singularity of the force-force correlation function is predicted for such a broad class of systems by a mean-field theoretical approach based on the replica method and also by a functional renormalization group approach [30]. The thermally rounded region of width h_{w} around the top of a cusp in called *thermal boundary layer* [41]. Indeed the cusp is confirmed by a recent extensive numerical study [43]. These problems can be mapped to turbulent flows under continous random forcing [32].

VII.   CONCLUSIONS

In the present paper we studied the statistical properties of mesoscopic responses in glassy systems from a mean-field theoretical point of view. More specifically we have studied a generic class on mean field models which exhibit 1 step replica symmetry breaking. We conclude that the mesoscopic response consistes of step-wise responses with typical height $\sqrt{N}\Delta_{\text{eff}}$, spacing $h_{\text{s}} \sim T_{\text{c}}(h)/(\sqrt{N}\Delta_{\text{eff}})$ and width $h_{\text{w}} \sim T/(\sqrt{N}\Delta_{\text{eff}})$. This conclusion follows from observations of the mesosocpic response in two different ways. One is based on the FDT: we studied statistic of sample-to-sample fluctuations of the linear and non-linear susceptibilities related to the spontaneous thermal fluctuations. The latters are significant only in narrow regions of width h_{w} around steps so that the averages of their moments are dictated by contributions from such rare regions. Our result proves the intuitions developed by the pioneering works in the SK model a long time ago [20, 21]. We conclude that the FDT approach amounts to describe mesosocpic responses under variation of the external field δh by power series of $\delta h/h_{\text{w}}$. In the second approach we did not rely on the FDT. Working directly at $T = 0$ we obtained series expansions of the mesoscopic response in power series of $\delta h/h_{\text{s}}$ going beyond the scale of single steps. The presence of mesoscopic response means that the thermodynamic limit $N \to \infty$ and $\delta h \to 0$ limit do not commute: one observs thermodynamic susceptibilities by $\lim_{\delta h \to 0} \lim_{N \to \infty}$ and mesoscopic responses by $\lim_{N \to \infty} \lim_{\delta h \to 0}$. Furthermore, the presence of the two expansions $\delta h/h_{\text{w}}$ and $\delta h/h_{\text{s}}$ means the two limits $\lim T \to 0$ and $\lim \delta h \to 0$ do not commute either. The the non-commutativities of the limits reflect the step (or cusp) singularity at mesoscopic scales.

We note that a techincal challenge remains to evaluate the parameter Δ_{eff} for a given perturbation from a given microscopic Hamiltonian. It quantifies the strength of a given perturbation. Since it conceres with the *inter-state* responses, one must find ways to disentangle intra-state and inter-state responses in a given response. For example, for the p-spin Ising model discussed at the begining of sec. V, we could evaluate Δ_{eff} for general p only under zero field. For non-zero field, we could evaluate it in the $p \to \infty$ limit by considering the fluctuaion of the size of clusters m of the 1 step RSB solutions as explained in Appendix. G but remains as a challenge for $p < \infty$.

Many features we obtained in the present paper can be rephrased by Imry-Ma type scaling argument, for instance the droplet theory for spin-glasses [13] and directed polymer in random media [14] proposed by Fisher and Huse, as we noted from time to time in the present paper. In short, a low energy excitation of a mesoscopic scale L behaves much as a sample of a mean field model of size N. In finite dimensions, not only thermodynamic responses but also susceptibilities related to spontaneous thermal fluctuations via static FDT should become self-averaging thanks to the central limit theorem: independent mesoscopic excitations scattered over a given macroscopic sample contribute simultaneously and independently from each other to the total susceptibility. However it is of great interest to understand better properties at mesoscopic scales such as statistics of droplet-to-droplet fluctuations of the droplet excitations. We expect that our mean-field approach may be useful to obtain *meanf field* approximations of such kind of statistical properties.

In Imry-Ma type arguments one can incorporate some refined knowledge of realistic low dimensional systems obtained by other means. For example, our results can be refined by the following adjustments. First the characteristic energy scale T_{c} may be replace by $\Upsilon(L/L_0)^{\theta}$ where L_0 is a certain unit length scale, Υ is the stiffness constant and $\theta > 0$ is the stiffness exponent. Then the variance of the random variable Y may be generalized as $A(L/L_0)^{\alpha}$ with $\alpha > 0$ replacing the simple $\Delta\sqrt{N}$ scaling. Then one finds $h_{\text{w}} \sim (T/A)(L/L_0)^{-\alpha}$, $h_{\text{s}} \sim (\Upsilon/A)(L/L_0)^{-\zeta}$ where $\zeta = \alpha - \theta$ is the so called chaos exponent [12, 13]. If the chaos exponent is positive $\zeta > 0$, the spacing between the steps vanishes in the limit $L \to \infty$ leading to static chaos. An interesting consequence is that the thermal width h_{w} vanishes *faster* than the spacing h_{s} as $L \to \infty$ since $\theta > 0$. It will be very interesting to develop futher the replica approach in order to verify these points theoretically.

APPENDIX A: ON THE MESOSCOPIC AND MACROSCOPIC LINEAR-SUSCEPTIBILITY

For a given sample, say J, of a finite size N we can write,

$$y_J(h) = \int_0^h dh' \frac{\partial y_J(h)}{\partial h} \tag{A1}$$

where we put the subscript J in order to remind us that it is associated with a single sample J. The *differential susceptibility* which appears on the r. h. s. can be identified with the correlation function through the static FDT,

$$\frac{\partial y_J(h)}{\partial h} = \beta(\langle y_J^2(h) \rangle - \langle y_J(h) \rangle^2). \tag{A2}$$

Taking average over different realizations of samples of both sides of Eq. (A1) we obtain,

$$\llbracket y_J(h) \rrbracket = \int_0^h dh' \left[\frac{\partial y_J(h')}{\partial h'} \right] \qquad \text{or} \qquad \frac{\partial \llbracket y_J(h) \rrbracket}{\partial h} = \left[\frac{\partial y_J(h)}{\partial h} \right]. \tag{A3}$$

On the other hand we have

$$\lim_{N \to \infty} y_J(h) = \lim_{N \to \infty} \llbracket y_J(h) \rrbracket \tag{A4}$$

since $Y_J = N y_J$ is a thermodynamic and thus self-averaging quantity. Thus we obtain

$$\frac{\partial}{\partial h} \lim_{N \to \infty} y_J(h) = \lim_{N \to \infty} \beta \left[(\langle y_J^2(h) \rangle - \langle y_J(h) \rangle^2) \right]. \tag{A5}$$

at any h. Thus 1st derivative of the thermodynamic response curve, say 'thermodynamic linear susceptibility' and sample-average of the linear susceptibility obtained via static FDT must coincide. Note that the above argument cannot be repeated for non-linear susceptibilities since linear-susceptibility may *not* be self-averaging, i.e. in general $\lim_{N \to \infty} \partial y_j(h)/\partial h \neq \llbracket \partial y_J(h)/\partial h \rrbracket$.

APPENDIX B: AN EFFECTIVE REM

We summarize below some basic properties of an effective REM with the simplest form of the generalized complexity given by Eq. (17)

$$\Sigma(f, y) = c - \frac{f^2}{2} - \frac{y^2}{2\Delta^2} \tag{B1}$$

where $c (\geq 0)$ is a constant which fixes the total number of states as,

$$M = e^{Nc}. \tag{B2}$$

The complexity can be cast into the form like Eq. (20) as a function of the "total" free-energy $f' = f - hy$ and the transver variable $\tilde{y}$ given by Eq. (22),

$$\Sigma(\tilde{f}, \tilde{y}) = c - \frac{\tilde{f}^2}{2} - \frac{\tilde{y}^2}{2(\Delta_{\text{eff}})^2} \tag{B3}$$

where we introduced a 'renormalized variance',

$$\Delta_{\text{eff}} \equiv \frac{\Delta}{\sqrt{1 + (h\Delta)^2}} \tag{B4}$$

and new variables defined as,

$$\tilde{f} \equiv f' \sqrt{1 - (h\Delta_{\text{eff}})^2} \qquad \tilde{y} \equiv y + h(\Delta_{\text{eff}})^2 f'. \tag{B5}$$

In Eq. (B3) it is evident that $\tilde{f}$ and $\tilde{y}$ are statistically independent from each other. In the present paper the variable like $\tilde{y}$ which is statistically independent from the free-energy is called as *transverse variable* (see Eq. (22)).

The shape of the generalized complexity close to the $\Sigma = 0$ plane can be obtained by rewriting Σ as,

$$N\Sigma = \frac{F' - (F')^*(h)}{T_c(h)} - \frac{1}{2cN} \left(\frac{F' - (F')^*}{T_c(h)} \right)^2 - \frac{\tilde{Y}^2}{2N(\Delta_{\text{eff}})^2}. \tag{B6}$$

Here $F' = Nf'$, $\tilde{Y} = N\tilde{y}$ and $(F')^* = -2cNT_c(h)$ with T_c being the critical temperatrure obtained below as Eq. (B8). At large enough system sizes N the 2nd term on the r.h.s becomes negligible compared with the 1st term and the functional form of the generalized complexity converges to the expected generic form given by Eq. (20) close to the $\Sigma = 0$ plane. Thus this effective REM should give generic results common in all 1 step RSB models concerning inter-state responses.

It is straight forward to consider a slightly more generalized version of the complexity including also an off-diagonal term like $-Kf\frac{y}{\Delta}$ in Eq. (B1). The latter represents a possible correlation between f and y of strength $\sim K$ for small enough K. One can find again that the complexity can be cast into the quadratic form Eq. (B3).

1. Thermodynamics

Now let us determine thermodynamic state $(\tilde{f}^*, \tilde{y}^*)$ at a given temperature T and external field h. In Fig. 3, the variable $\tilde{f}$ is held constant on the line C while the variable $\tilde{y}$ is varied. Along C the complexity Eq. (B3) is maxized at the point P where $\tilde{y} = 0$. Thus we fined $\tilde{y}^* = 0$. On the other hand $\tilde{f}^*$ is obtained through the condition Eq. (18) which reads as,

$$\frac{1}{T} = \left.\frac{\partial \Sigma}{\partial f'}\right|_{\tilde{f}=\tilde{f}^*, \tilde{y}=0} = -\tilde{f}^* \sqrt{1 - (h\Delta_{\text{eff}})^2} \tag{B7}$$

and the value of the complexity at the saddle point $(f^*, y^* = 0)$ is obtained as $\Sigma^* = c - (\tilde{f}^*)^2/2$.

The saddle point value of the complexity Σ^* becomes 0 when $\tilde{f}^* = -\sqrt{2c}$. Thus the critical temperature T_c is obtained as,

$$T_c(h) = \frac{T_c^0}{\sqrt{1 - (h\Delta_{\text{eff}})^2}} \qquad T_c^0 = \frac{1}{\sqrt{2c}} \tag{B8}$$

Here h dependence comes from the h dependence of (Δ_{eff}) given in Eq. (B4).

In the glass phase $T < T_c$ the saddle point is fixed at $(\tilde{f}^*, \tilde{y}^*) = (-\sqrt{2c}, 0)$. Then we find the total free-energy density f' as

$$(f')^*(h) = -2cT_c(h) \tag{B9}$$

and the equilibrium value of the variable y as

$$y^*(h) = \frac{\Delta^2}{T_c(h)} h. \tag{B10}$$

using Eq. (B5), Eq. (B8) and Eq. (B4). Note that here Δ is the variance of the original Y variable. Taking a derivative of the last equation with respect to h taking into account the h dependence of $T_c(h)$ given by Eq. (B8) one finds,

$$\chi(h) = N\frac{\partial y^*(h)}{\partial h} = N\frac{(\Delta_{\text{eff}})^2}{T_c(h)} \tag{B11}$$

where Δ_{eff} is now the variance of Y given by Eq. (B4).

Taking a derivative of the free-energy $(f')^*$ given in Eq. (B9) with respect to the temperature one finds the well known result [25] that the heat-capacity is zero below T_c,

$$C/N = 0. \tag{B12}$$

2. Replica approach

Here we scketch the construction of the replica approach for this model. The partition function of a given sample is given by

$$Z(T, h, \delta h) = \sum_{i=1}^{M} e^{-\beta N(f_i'(h) - \delta h \tilde{y}_i)} \tag{B13}$$

where i is the label for each metastable state. $f'(h) = f - hy$ is the total free-energy density under external field h. The sum runs over all states whose number is $M = e^{Nc}$ as given in Eq. (B2). We have also included *infinitesimal* probing field δh coupled to the transverse variable $\tilde{y}$ defined in Eq. (B5) which is statistically uncorrelated with the free-energy density f'.

The distribution of the quenched random variables f' and $\tilde{y}$ is specified by the generalized complexity given in Eq. (B3) supplemented by the relation $f' = \sqrt{2c}T_c(h)\tilde{f}$ which follows from Eq. (B5) and Eq. (B8). We obtain sample-averaged replicated free-energy as

$$[\![Z^n]\!] = \sum_{i_1, i_2, \ldots, i_n=1}^{M=e^{cN}} \exp\left[N\left\{c(\beta T_c(h))^2 + \frac{(\beta \delta h)^2}{2}(\Delta_{\text{eff}})^2\right\} \sum_{\alpha, \beta=1}^{n} \delta_{i_\alpha, i_\beta}\right]. \tag{B14}$$

Let us summarize below the analysis of the thermodynamics following [25, 33] which reproduces the results obtained above without using the replica approach. Here we switch off the probing field $\delta h = 0$. Within the replica symmetric ansatz (RS), one assumes that n replicas occupy different states. Then one obtains

$$[\![Z^n]\!] \sim \exp\left[cNn\{1 + (\beta T_c(h))^2\}\right] \tag{B15}$$

from which one obtains the thermodynamic free-energy and entropy as

$$- \beta F_{\mathrm{RS}}/N = \lim_{n \to 0} \frac{[\![Z]\!]^n - 1}{nN} = c\{1 + (\beta T_c(h))^2\} \qquad S_{\mathrm{RS}}/N = c\{1 - (\beta T_c(h))^2\}. \tag{B16}$$

The entropy vanishes as $T \to T_c(h)$ suggesting condensation of the Boltzmann weight. Thus we find again that $T_c(h)$ given in Eq. (B8) is the critical temperature.

Below $T_c(h)$ we expect the 1 step replica symmetry breaking (1 step RSB) ansatz gives physically correct saddle points [25, 33]. It amounts to assume that n replicas are grouped into n/m clusters of size m such that replicas belonging to a common cluster stay at the same state while those belonging to different clusters stay at different states.

In Fig. 11 we show a schematic picture of such a 1RSB solution. Note that there are many 1 step RSB solutions. Each solution is determined by 1) choosing n/m states to be occupied out of M possible states and 2) choosing a partition of n 'atoms' into n/m 'molecules' out of $n!$ possibilities of such partitions. The 1RSB ansatz yields,

$$[\![Z^n]\!] \sim \sum_{\mathrm{SP}} \exp\left[cN\frac{n}{m}\left\{1 + \left(\frac{T_c(h)}{T/m}\right)^2\right\}\right] \tag{B17}$$

where $\sum_{\mathrm{SP}}$ stands for summation over all possible 1RSB solutions explained above. Here the summand is common for all 1RSB solutions so that $\sum_{\mathrm{SP}}$ just yield a multiplicative factor,

$$\sum_{\mathrm{SP}} 1 = \frac{M!}{(M - \frac{n}{m})!} \frac{n!}{(m!)^{n/m}}, \tag{B18}$$

which becomes 1 in $n \to 0$ limit. The 1RSB free-energy is related to the RS free-energy simply as $F_{\mathrm{1RSB}}(T, h) = F_{\mathrm{RS}}(T/m, H)$. Extremization with respect to the parameter m,

$$0 = \frac{\partial F_{\mathrm{1RSB}}}{\partial m} \tag{B19}$$

is formally identical to the condition $S_{\mathrm{RS}}(T/m, H) = 0$ as first noted by Monasson [53]. Then one finds,

$$m = \frac{T}{T_c(h)}. \tag{B20}$$

At $T < T_c(h)$, the thermodynamic free-energy is fixed to

$$F(T, h)/N = -2cT_c(h). \tag{B21}$$

This agrees with Eq. (B9).

APPENDIX C: LOW TEMPERATURE EXPANSIONS OF THE MOMENTS OF THE SUSCEPTIBILITIES

In this appendix we report some details of the computations by the low temperature expansion of the sample-averages of some moments of the thermal cumulants.

1. Accuracy of M-level models

Here we proove that a M-th level model, which only takes into account the lowest M levels, give correct results of the moments up to order $O(T/T_c)^{M-1}$.

We first note that Eq. (45) can be formally expanded as,

$$\left[\!\!\left[\kappa_{k_1}^{p_1}(Y)\kappa_{k_2}^{p_2}(Y)\cdots\right]\!\!\right] = \sum_{l=1}^{M-1}\sum_{0<n_1<n_2...<n_l} C_{n_1,n_2,...,n_l}\left[\!\!\left[\prod_{k=1}^{l} X_k^{n_k}\right]\!\!\right]. \tag{C1}$$

The coefficients $C_{p_1,p_2,...,p_l}$ are to be obtained after averaging over the Y variables, which can be done interdependently of the X variables since they are independent from each other. We remind the readers that we are considering the transverse $\tilde{Y}$ variables.

From the latter we find,

$$\left[\!\!\left[X_k^n\right]\!\!\right] = \int_0^1 (X_k)^n p_k(X_k)dX_k = \frac{k}{n}\frac{T}{T_c(h)}\left[1+\frac{k}{n}\frac{T}{T_c(h)}\right]^{-1}. \tag{C2}$$

which yields,

$$\left[\!\!\left[\prod_{k=1}^{l} X_k^{n_k}\right]\!\!\right] = \left(\frac{T}{T_c(h)}\right)^l \prod_{k=1}^{l}\frac{k}{n_k}\left[1+\frac{k}{n_k}\frac{T}{T_c(h)}\right]^{-1}. \tag{C3}$$

Using Eq. (C3) in Eq. (C1) we notice that $M+1$-level model would give the same results as the M-level model except that it will have additional terms of order $O(T/T_c(h))^M$ (and higher order terms). This in turn certifies that finite M-level model should give correct results up to $O(T/T_c(h))^{M-1}$.

Thus to collect $O(T/T_c(h))$ terms a 2-level model is sufficient. A 3-level model gives only $O(T/T_c(h))^2$ correction terms which take care of rare samples in which three levels happen to become degenerate as shown in Fig. 6.

Let us note that somewhat similar reasoning has been used to justify the phenomenological Imry-Ma type scaling arguments for glassy systems by Fisher and Huse [13, 14] which assume some kinds of schematic low temperature expansions. The class of mean-field models we consider here enable explicit low temperature expansions.

The low temperature expansion can be implemented also to compute the so called participation ratios,

$$\sum_{l=0}^{M-1} W_l^p = \sum_{l=0}^{M-1}\left\{\frac{\prod_{k=1}^{l} X_k}{\sum_{l'=0}^{M-1}\prod_{k=1}^{l'} X_k)}\right\}^p. \tag{C4}$$

Evidently it can be formally expanded in the same way as Eq. (C1). The participation ratios have been computed without the replica method using the exponential distribution of random free-energies Eq. (24) reproducing the replica results [46] in the $M \to \infty$ limit. Our result implies finite M-model gives correct result up to $O((T/T_c(h))^{M-1})$.

2. Linear susceptibility

Following the prescription Eq. (45) the sample-average of 1st moment of the 2nd thermal cumulant $[\![\kappa_2(Y)]\!]^{2-\text{level}}$ is computed within the 2-level model as the following.

$$\begin{aligned}
[\![\kappa_2(Y)]\!]^{2-\text{level}} &= \left[\!\!\left[\left(Y_0 O_0\frac{\partial}{\partial O_0}+Y_1 O_1\frac{\partial}{\partial O_1}\right)^2 \ln Z(O_0,O_1,X_1)\bigg|_{O=1}\right]\!\!\right] \\
&= (\sqrt{N}\Delta_{\text{eff}})^2\left[\!\!\left[\left\{\left(O_0\frac{\partial}{\partial O_0}\right)^2+\left(O_1\frac{\partial}{\partial O_1}\right)^2\right\}\ln(O_0+O_1 X_1)\bigg|_{O=1}\right]\!\!\right] = (\sqrt{N}\Delta_{\text{eff}})^2\int_0^1 dX_1 p_1(X_1)\frac{2X_1}{(1+X_1)^2} \\
&= (\sqrt{N}\Delta_{\text{eff}})^2\left\{\frac{T}{T_c(h)}-2\ln 2\left(\frac{T}{T_c(h)}\right)^2+O\left(\frac{T}{T_c(h)}\right)^3\right\}
\end{aligned} \tag{C5}$$

Here we used Eq. (44) and Eq. (28) to evaluate the sample averages. Then repeating the computation in 3-level model we obtain,

$$
\begin{aligned}
[\![\kappa_2(Y)]\!]^{3-\text{level}} &= \left[\left(Y_0 O_0 \frac{\partial}{\partial O_0} + Y_1 O_1 \frac{\partial}{\partial O_1} + Y_2 O_2 \frac{\partial}{\partial O_2}\right)^2 \ln Z(O_0, O_1, O_2, X_1, X_2)\Bigg|_{O=1}\right] \\
&= (\sqrt{N}\Delta_{\text{eff}})^2 \int_0^1 dX_1 p_1(X_1)\frac{2X_1}{(1+X_1)^2} + (\sqrt{N}\Delta_{\text{eff}})^2 \int_0^1 dX_1 p_1(X_1)\int_0^1 dX_2 p_2(X_2)\left\{\frac{2X_1(1+X_2+X_1 X_2)}{(1+X_1+X_1 X_2)^2} - \frac{2X_1}{(1+X_1)^2}\right\} \\
&= [\![\kappa_2(Y)]\!]^{2-\text{level}} + (\sqrt{N}\Delta_{\text{eff}})^2 \left\{2\ln 2\left(\frac{T}{T_c(h)}\right)^2 + O\left(\frac{T}{T_c(h)}\right)^3\right\} \\
&= (\sqrt{N}\Delta_{\text{eff}})^2 \left\{\frac{T}{T_c(h)} + O\left(\frac{T}{T_c(h)}\right)^3\right\}
\end{aligned}
\tag{C6}
$$

Note that in the 2nd equation we have slipt the integral into two parts, one of which corresponds to that of the 2-level model.

By similar procedure the sample-average of 2nd moment of the 2nd thermal cumulant $\left[\kappa_2^2(Y)\right]^{3-\text{level}}$ is computed within the 3-level model as the following. Following the prescription Eq. (45) the sample-average of 2nd moment of the 2nd thermal cumulant $\left[\kappa_2^2(Y)\right]^{3-\text{level}}$ is computed within the 3-level model as the following.

$$
\begin{aligned}
\left[\kappa_2^2(Y)\right]^{3-\text{level}} &= \left[\left(Y_0 O_{01}\frac{\partial}{\partial O_{01}} + Y_1 O_{11}\frac{\partial}{\partial O_{11}} + Y_2 O_{21}\frac{\partial}{\partial O_{21}}\right)^2 \left(Y_0 O_{02}\frac{\partial}{\partial O_{02}} + Y_1 O_{12}\frac{\partial}{\partial O_{12}} + Y_2 O_{22}\frac{\partial}{\partial O_{22}}\right)^2\right. \\
&\qquad \left. \ln Z(O_{01}, O_{11}, O_{21}, X_1, X_2)\ln Z(O_{02}, O_{12}, O_{22}, X_1, X_2)|_{O=1}\right]_{\text{av}} \\
&= 12(N\Delta^2)^2 \int_0^1 dX_1 p_1(X_1)\frac{X_1^2}{(1+X_1)^4} \\
&\quad + 12(N\Delta^2)^2 \int_0^1 dX_1 p_1(X_1)\int_0^1 dX_2 p_2(X_2)\left\{\frac{X_1^2(1+X_2+X_2^2+X_1 X_2+X_1 X_2^2+X_1^2 X_2^2)}{(1+X_1+X_1 X_2)^4} - \frac{X_1^2}{(1+X_1)^4}\right\}
\end{aligned}
\tag{C7}
$$

In the last equation we have again slip the integral into two parts. The 1st integral corresponds to that of 2-level model which is evaluated as

$$
\int_0^1 dX_1 p_1(X_1)\frac{X_1^2}{(1+X_1)^4} = \frac{1}{12}\frac{T}{T_c(h)} + \left(\frac{1}{24} - \frac{1}{6}\ln 2\right)\left(\frac{T}{T_c(h)}\right)^2 Z + O\left(\frac{T}{T_c(h)}\right)^3
$$

while the 2nd integral corresponds to the contribution due to the 3rd level which is evaluated as,

$$
\begin{aligned}
&\int_0^1 dX_1 p_1(X_1)\int_0^1 dX_2 p_2(X_2)\left\{\frac{X_1^2(1+X_2+X_2^2+X_1 X_2+X_1 X_2^2+X_1^2 X_2^2)}{(1+X_1+X_1 X_2)^4} - \frac{X_1^2}{(1+X_1)^4}\right\} \\
&= \left(-\frac{1}{24} + \frac{1}{6}\ln 2\right)\left(\frac{T}{T_c(h)}\right)^2 + O\left(\frac{T}{T_c(h)}\right)^3
\end{aligned}
$$

Combining the above results we finally obtain Eq. (47),

$$
\left[\kappa_2^2(Y)\right]^{3-\text{level}} = (\sqrt{N}\Delta_{\text{eff}})^4 \left\{\frac{T}{T_c(h)} + O\left(\frac{T}{T_c(h)}\right)^3\right\}.
\tag{C8}
$$

3. Non-linear susceptibility

Using Eq. (45) the sample-average of 2nd moment of the 3rd thermal cumulant $\left[\kappa_3^2(Y)\right]^{3-\text{level}}$ is computed within the 3-level model as the following.

$$
\left[\kappa_3^2(Y)\right]^{3-\text{level}} = \left[\left(Y_0 O_{01}\frac{\partial}{\partial O_{01}} + Y_1 O_{11}\frac{\partial}{\partial O_{11}} + Y_2 O_{21}\frac{\partial}{\partial O_{21}}\right)^3 \left(Y_0 O_{02}\frac{\partial}{\partial O_{02}} + Y_1 O_{12}\frac{\partial}{\partial O_{12}} + Y_2 O_{22}\frac{\partial}{\partial O_{22}}\right)^3\right.
$$

$$
\left.\ln Z(O_{01}, O_{11}, O_{21}, X_1, X_2) \ln Z(O_{02}, O_{12}, O_{22}, X_1, X_2)|_{O=1}\right]_{\text{av}}
$$

$$
= (N(\Delta_{\text{eff}})^2)^3 \int_0^1 dX_1 p_1(X_1) \int_0^1 dX_2 p_2(X_2) F(X_1, X_2). \tag{C9}
$$

where

$$
F(X_1, X_2) \equiv 12X_1^2 \left[10 + 48X_1^2 X_2^2 - 7X_1^2 X_2 - 7X_1 X_2\right.
$$
$$
-7X_1^3 X_2^3 + 10X_1^4 X_2^2 + 10X_1^2 - 20X_1 X_2^3 + 10X_1^2 X_2^4 - 20X_1^4 X_2^3 + 10X_1^4 X_2^4 - 7X_1 X_2^2
$$
$$
\left. -7X_1^2 X_2^3 + 7X_1^3 X_2^4 - 20X_1 + 7X_2 - 7X_1^3 X_2^2 + 7X_1^3 X_2 + 10X_2^2\right] (1 + X_1 + X_1 X_2)^{-6} \tag{C10}
$$

Again the integral can be split into two parts.

$$
\int_0^1 dX_1 p_1(X_1) \int_0^1 dX_2 p_2(X_2) F(X_1, X_2)
$$

$$
= 120 \int_0^1 dX_1 p_1(x_1)\frac{1 - 2X_1 + X_1^2}{(1 + X_1)^6} + \int_0^1 dX_1 p_1(X_1) \int_0^1 dX_2 p_2(X_2)\left\{F(X_1, X_2) - 120\frac{1 - 2X_1 + X_1^2}{(1 + X_1)^6}\right\} \tag{C11}
$$

The 1st integral on the r.h.s corresponds to that of 2-level model which is evaluated as

$$
\int_0^1 dX_1 p_1(x_1)\frac{1 - 2X_1 + X_1^2}{(1 + X_1)^6} = \frac{1}{60}\frac{T}{T_c(h)} - \left(\frac{1}{240} + \frac{1}{30}\ln 2\right)\left(\frac{T}{T_c(h)}\right)^2 + O\left(\frac{T}{T_c(h)}\right)^3
$$

while the 2nd integral on the r.h.s corresponds to the contribution due to the 3rd level which is evaluated as,

$$
\int_0^1 dX_1 p_1(X_1) \int_0^1 dX_2 p_2(X_2)\left\{F(X_1, X_2) - 120\frac{1 - 2X_1 + X_1^2}{(1 + X_1)^6}\right\} = -\left(\frac{3}{2} - 4\ln 2\right)\left(\frac{T}{T_c(h)}\right)^2 + O\left(\frac{T}{T_c(h)}\right)^3
$$

Combining the above results we finally obtain Eq. (48),

$$
\left[\kappa_3^2(Y)\right]^{3-\text{level}} = (N(\Delta_{\text{eff}})^2)^3 \; 2\left[\frac{T}{T_c(h)} - \left(\frac{T}{T_c(h)}\right)^2 + O\left(\frac{T}{T_c(h)}\right)^3\right]. \tag{C12}
$$

4. Other moments

Here we present results of some other moments needed in the present paper using the 3-level model. The 2nd moment of the 1st thermal cumulant is evaluated as,

$$
\left[\kappa_1^2(Y)\right] = \left[\left(Y_0 O_{01}\frac{\partial}{\partial O_{01}} + Y_1 O_{11}\frac{\partial}{\partial O_{11}} + Y_2 O_{21}\frac{\partial}{\partial O_{21}}\right)\left(Y_0 O_{02}\frac{\partial}{\partial O_{02}} + Y_1 O_{12}\frac{\partial}{\partial O_{12}} + Y_2 O_{22}\frac{\partial}{\partial O_{22}}\right)\right.
$$

$$
\left.\ln Z(O_{01}, O_{11}, O_{21}, X_1, X_2) \ln Z(O_{02}, O_{12}, O_{22}, X_1, X_2)|_{O=1}\right]_{\text{av}}
$$

$$
= (\sqrt{N}\Delta_{\text{eff}})^2) \int_0^1 dX_1 p_1(X_1) \int_0^1 dX_2 p_2(X_2)\frac{1 + X_1^2 + X_1^2 X_2^2}{(1 + X_1 + X_1 X_2)^2} = (\sqrt{N}\Delta_{\text{eff}})^2 \left\{1 - \frac{T}{T_c(h)} + \left(\frac{T}{T_c(h)}\right)^3\right\} \tag{C13}
$$

We also need $[\![\kappa_3(Y)\kappa_Y]\!]$ which is evaluated as,

$$
[\![\kappa_3(Y)\kappa_1 Y]\!] = \left[\left(Y_0 O_{01}\frac{\partial}{\partial O_{01}} + Y_1 O_{11}\frac{\partial}{\partial O_{11}} + Y_2 O_{21}\frac{\partial}{\partial O_{21}} \right)^3 \left(Y_0 O_{02}\frac{\partial}{\partial O_{02}} + Y_1 O_{12}\frac{\partial}{\partial O_{12}} + Y_2 O_{22}\frac{\partial}{\partial O_{22}} \right) \right.
$$

$$
\left. \ln Z(O_{01},O_{11},O_{21},X_1,X_2)\ln Z(O_{02},O_{12},O_{22},X_1,X_2)|_{O=1} \right]_{\rm av}
$$

$$
= (\sqrt{N}\Delta_{\rm eff})^4) \int_0^1 dX_1 p_1(X_1 \int_0^1 dX_2 p_2(X_2) \frac{-6X_1(-2X_1+1+X_1^2+X_2-2X_1X_2^2-2X_1^3X_2^2+X_1^3X_2+X_1^3X_2^3+X_1^2X_2^3)}{(1+X_1+X_1X_2)^4}
$$

$$
= -(\sqrt{N}\Delta_{\rm eff})^4 \left\{ \frac{T}{T_c(h)} - \left(\frac{T}{T_c(h)}\right)^2 + O\left(\frac{T}{T_c(h)}\right)^3 \right\} \tag{C14}
$$

APPENDIX D: DISTRIBUTION OF MESOSCOPIC RESPONSE AT $T=0$

In this appendix we compute the distribution function Eq. (51) of the response $\psi \equiv Y(h+\delta h) - Y(h)$ at zero temperature. For our convenience let us introduce some short hand notations,

$$
\int DY_l \ldots \equiv \int \frac{dY_l}{\sqrt{2\pi N\Delta^2}} \exp\left(-\frac{Y_l^2}{2N\Delta^2}\right)\ldots \qquad \int DF_{(l,m)}\ldots \equiv \int d\Delta F_{l,m}\rho_{(l,m)}(\Delta F_{l,m})\ldots . \tag{D1}
$$

where $\rho_{(l,m)}(\Delta F_{l,m})$ is the distribution of the free-energy difference $\Delta F_{l,m}$ between l-th and m-th states under h (See sec. III B 1).

For the two-level model it is easy to find,

$$
p_1(\psi) = \int_{-\infty}^{\infty} DY_0 \int_{Y_0}^{\infty} DY_1 \int_0^{h(Y_1-Y_0)} D\Delta F_{(1,0)}\delta(\psi - (Y_1 - Y_0)) \qquad p_0(\psi) = \delta(\psi)\left(1 - \int_0^{\infty} d\psi' p_1(\psi')\right) \tag{D2}
$$

and thus

$$
p(h,\psi) = \delta(\psi)\left(1 - \int_0^{\infty} d\psi' \frac{e^{-\frac{(\psi')^2}{4N\Delta}}}{\sqrt{4\pi N\Delta^2}}(1 - e^{-\frac{h}{T_c}\psi'})\right) + \frac{e^{-\frac{\psi^2}{4N\Delta}}}{\sqrt{4\pi N\Delta^2}}(1 - e^{-\frac{h}{T_c}\psi}). \tag{D3}
$$

using Eq. (D1),Eq. (28) and Eq. (26). We again remind the readers that we are actually studying the fluctuations of the transverse variable $\tilde{Y}$. Here the 1st and 2nd terms on the r.h.s correspond to $p_0(\psi)$ and $p_1(\psi)$ respectively.

Now we extend the analysis including the 3rd state. Among the diagrams shown in Fig. 7, the cases that the state 1 becomes the ground state appear in 3), 4) and 6-b). Then we can write it as,

$$
p_1(\psi) = \int_{-\infty}^{\infty} DY_0 \int_{Y_0}^{\infty} DY_1 \delta(\psi - (Y_1 - Y_0)) \int_0^{h(Y_1-Y_0)} D\Delta F_{10} \left[\int_{-\infty}^{Y_1} DY_2 \right. \tag{D4}
$$

$$
\left. + \int_{Y_1}^{\infty} DY_2 \int_{h(Y_2-Y_1)}^{\infty} D\Delta F_{21} \right].
$$

Here the 1st term in $[\ldots]$ is the contribution from the case 3) and 4). The 2nd term $[\ldots]$ is due to the case 6-b). Using Eq. (28) and Eq. (26) we obtain,

$$
p_1(\psi) = \frac{e^{-\frac{\psi^2}{4N\Delta^2}}}{\sqrt{4\pi N\Delta^2}}\left(1 - e^{-\frac{h\psi}{T_c}}\right)[1
$$

$$
- \int_{-\infty}^{\infty} \frac{dY_+}{\sqrt{4\pi N\Delta^2}} e^{-\frac{Y_+^2}{4N\Delta^2}} \int_{\frac{Y_++\psi}{2}}^{\infty} \frac{dY_2}{\sqrt{2\pi N\Delta^2}} e^{-\frac{Y_2^2}{2N\Delta^2}}\left(1 - e^{-\frac{h\left(Y_2 - \frac{Y_++\psi}{2}\right)}{2T_c}}\right)] \tag{D5}
$$

in the last equation we introduced new variables $Y_\pm = Y_1 \pm Y_0$ and explicitly integrated over Y_-. The distribution of the scaled variable $\tilde{\psi}$ given in Eq. (54) is obtained as,

$$
\tilde{p}_1(\tilde{\psi}) = \frac{e^{-\frac{\tilde{\psi}^2}{4}}}{\sqrt{4\pi}}\left(1 - e^{-\frac{h}{h_s}\tilde{\psi}}\right)\left[1 - \int_{-\infty}^{\infty} \frac{dz_1}{\sqrt{4\pi}} e^{-\frac{z_1^2}{4}} \int_{\frac{z_1+\tilde{\psi}}{2}}^{\infty} \frac{dz_2}{\sqrt{2\pi}} e^{-\frac{z_2^2}{2}}\left(1 - e^{-\frac{1}{2}\frac{h}{h_s}(z_2 - \frac{z_1+\tilde{\psi}}{2})}\right)\right]. \tag{D6}
$$

where h_{s} is given by Eq. (57).

Next we examine the cases that the state 2 becomes the ground state which can be found 5), 6-a) and 6-b) in the diagrams in Fig. 7 which yield,

$$p_2(\psi) = \int_{-\infty}^{\infty} DY_0 \int_{-\infty}^{Y_0} DY_1 \int_{Y_1}^{\infty} DY_2 \delta(\psi - (Y_2 - Y_0)) \int_0^{h(Y_2 - Y_0)} D\Delta F_{20}$$

$$+ \int_{-\infty}^{\infty} DY_0 \int_{Y_0}^{\infty} DY_1 \int_{Y_1}^{\infty} DY_2 \delta(\psi - (Y_2 - Y_0)) \int_0^{h(Y_2 - Y_1)} D\Delta F_{21} \int_{\Delta F_{21}}^{h(Y_2 - Y_0)} D\Delta F_{20} \tag{D7}$$

The 1st term on the r.h.s. of the above equation is due to the case 5) while the 2nd term is due to the case 6-a) and 6-b). The last two integrals in the 2nd term ensure that both two level crossings $(1,2)$ and $(0,2)$ have took place in 6-a) and 6-b). (The order is reversed in the two cases.)

Using now Eq. (28) and Eq. (26) for the $(0,2)$ level crossing, which is "repulsive", we obtain,

$$p_2(\psi) = \left(1 - 2e^{-\frac{h\psi}{T_c}} + e^{-2\frac{h\psi}{T_c}}\right) \int_{-\infty}^{\infty} \frac{dY_+}{\sqrt{4\pi N\Delta^2}} e^{-\frac{Y_+^2}{4N\Delta^2}} \int_{\frac{Y_+ - \psi}{2}}^{\infty} \frac{dY_2}{\sqrt{2\pi N\Delta^2}} e^{-\frac{Y_2^2}{2N\Delta^2}}$$

$$+ \left(1 - 2e^{-\frac{h\psi}{T_c}} + e^{-2\frac{h\psi}{T_c}}\right) \int_{-\infty}^{\infty} \frac{dY_0}{\sqrt{2\pi N\Delta^2}} e^{-\frac{Y_0^2}{2N\Delta^2}} \int_{Y_0}^{\infty} \frac{dY_1}{\sqrt{2\pi N\Delta^2}} e^{-\frac{Y_1^2}{2N\Delta^2}} \left(1 - e^{-2X}\right)_{X = \frac{h}{T}(\psi - (Y_1 - Y_0))}$$

$$+ \int_{-\infty}^{\infty} \frac{dY_0}{\sqrt{2\pi N\Delta^2}} e^{-\frac{Y_0^2}{2N\Delta^2}} \int_{Y_0}^{\infty} \frac{dY_1}{\sqrt{2\pi N\Delta^2}} e^{-\frac{Y_1^2}{2N\Delta^2}} f(X)_{X = \frac{h}{T}(\psi - (Y_1 - Y_0))} \tag{D8}$$

with

$$f(x) \equiv \left[-(1 - e^{-2X}) + \frac{4(1 - e^{-3X})}{3} - \frac{(1 - e^{-4X})}{2}\right] \tag{D9}$$

In the 1st term on the r.h.s of Eq. (D8) we used $Y_\pm = Y_2 \pm Y_0$ and explicitly integrated over Y_-.

From the above result the distribution of the scaled variable $\tilde{\psi}$ given in Eq. (54) is obtained as,

$$\tilde{p}_2(\tilde{\psi}) = \left(1 - 2e^{-\frac{h}{h_{\mathrm{s}}}\tilde{\psi}} + e^{-2\frac{h}{h_{\mathrm{s}}}\tilde{\psi}}\right) \int_{-\infty}^{\infty} \frac{dz_1}{\sqrt{4\pi}} e^{-\frac{z_1^2}{4}} \int_{\frac{z_1 - \tilde{\psi}}{2}}^{\infty} \frac{dz_2}{\sqrt{2\pi}} e^{-\frac{z_2^2}{2}}$$

$$+ \left(1 - 2e^{-\frac{h}{h_{\mathrm{s}}}\tilde{\psi}} + e^{-2\frac{h}{h_{\mathrm{s}}}\tilde{\psi}}\right) \int_{-\infty}^{\infty} \frac{dz_1}{\sqrt{2\pi}} e^{-\frac{z_1^2}{2}} \int_{z_1}^{\infty} \frac{dz_2}{\sqrt{2\pi}} e^{-\frac{z_2^2}{2}} \left(1 - e^{-2X}\right)_{X = \frac{h}{h_{\mathrm{s}}}(\tilde{\psi} - (z_2 - z_1))}$$

$$+ \int_{-\infty}^{\infty} \frac{dz_1}{\sqrt{2\pi}} e^{-\frac{z_1^2}{2}} \int_{z_1}^{\infty} \frac{dz_2}{\sqrt{2\pi}} e^{-\frac{z_2^2}{2}} \left[-(1 - e^{-2X}) + \frac{4}{3}(1 - e^{-3X}) - \frac{1}{2}(1 - e^{-4X})\right]_{X = \frac{h}{h_{\mathrm{s}}}(\tilde{\psi} - (z_2 - z_1))} \tag{D10}$$

APPENDIX E: COMPUTATIONS OF SAMPLE-TO-SAMPLE FLUCTUATIONS OF THE THERMAL CUMULANTS BY A REPLICA APPROACH

Here we report some details of the computations of the moments of thermal cumulants $\kappa_k(Y)$ using the prescription Eq. (87), which reads as,

$$[\![\kappa_k^p(Y)]\!] = (\sqrt{N}\Delta_{\mathrm{eff}})^{kp} \lim_{n_1, n_2, \ldots, n_p \to 0} \frac{1}{\prod_{r=1}^p n_r} \frac{\partial^k}{\partial x_1^k} \frac{\partial^k}{\partial x_2^k} \cdots \frac{\partial^k}{\partial x_p^k} \sum_{\mathrm{SP}}' \exp\left[\frac{1}{2} \sum_{r,s=1}^p x_r A_{rs} x_s\right]\Bigg|_{x=0}$$

$$= (\sqrt{N}\Delta_{\mathrm{eff}})^{kp} \lim_{n_1, n_2, \ldots, n_p \to 0} \frac{1}{\prod_{r=1}^p n_r} \frac{\partial^k}{\partial x_1^k} \frac{\partial^k}{\partial x_2^k} \cdots \frac{\partial^k}{\partial x_p^k} \left\langle \exp\left[\frac{1}{2} \sum_{r,s=1}^p x_r A_{rs} x_s\right]\right\rangle_{\mathrm{SP}}\Bigg|_{x=0} \tag{E1}$$

where

$$A_{rs} \equiv \sum_{\alpha=(r,1)}^{(r,n_r)} \sum_{\beta=(s,1)}^{(s,n_s)} \delta_{i_\alpha, i_\beta} \tag{E2}$$

In Eq. (E1) the sum $\sum'_{\text{SP}}$ stands for summation over all possible partitions of n_{tot} replicas into n_{tot}/m clusters of size m.

In the 2nd equation $\langle\ldots\rangle_{\text{SP}}$ is the average over the all possible 1 step RSB solutions obtained by permutations of replicas , i.e.,

$$\langle\ldots\rangle_{\text{SP}} \equiv \frac{\sum'_{\text{SP}}\ldots}{\sum'_{\text{SP}}1} \tag{E3}$$

where $\sum'_{\text{SP}}1 = \frac{n!}{(m!)^{n/m}} \xrightarrow{n\to 0} 1$.

The computations of the moments based on the formula Eq. (E1) can be done diagrammatically. For instance let us consider the case of $[\kappa_2^2(Y)]$, i.e $k=2$ and $p=2$. In this case we have 4 derivatives in Eq. (E1) among which 2 of them are associated with the group-1 of replicas and the other 2 are associated with the group-2 of replicas.

1. First we represent them by 'isolated indexes' as in the left hand side of Fig. 13. '1' means that it stands for a derivative associated with the group-1 of replicas and '2' means that it is associated with the group-2 of replicas.

2. All terms generated by the differentiations $\partial/\partial\delta h$ at $\delta h = 0$ in Eq. (E1) can be enumerated by making pairs of indexes as in the right hand side of Fig. 13. As the result we find

$$[\kappa_2^2(Y)] = (N(\Delta_{\text{eff}})^2)^2 \cdot \lim_{n_1,n_2\to 0}\frac{1}{n_1 n_2}(\langle A_{11}A_{22}\rangle_{\text{SP}} + 2\langle A_{12}^2\rangle_{\text{SP}}).$$

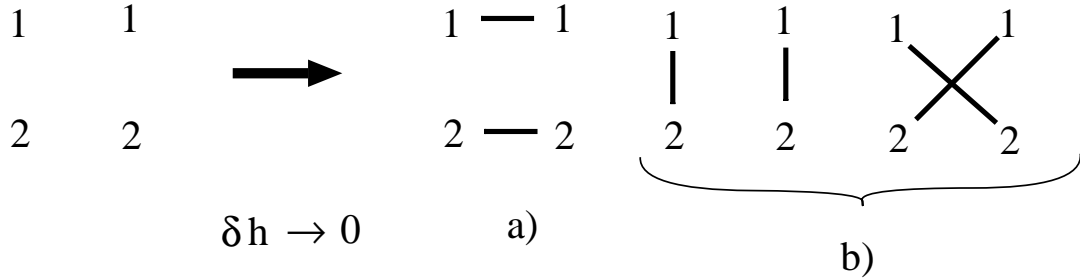Here $A_{11}A_{22}$ is due to the graph a) and $2A_{12}^2$ is due to the two graphs of type b).

FIG. 13: A diagrammatic representation of terms which survive after $\delta h \to 0$ among all terms generated by the differentiations $\partial/\partial h$s in Eq. (E1).

3. Now we have to evaluate $\langle A_{11}A_{22}\rangle_{\text{SP}}$ and $\langle A_{12}^2\rangle_{\text{SP}}$. Let us take the case of $\langle A_{11}A_{22}\rangle_{\text{SP}}$ which is represented by a) in Fig. 13.

Using Eq. (89), $\langle A_{11}A_{22}\rangle_{\text{SP}}$ can be written explicitly as,

$$\langle A_{11}A_{22}\rangle_{\text{SP}} = \sum_{\alpha=(1,1)}^{(1,n_1)}\sum_{\beta=(1,1)}^{(1,n_1)}\sum_{\gamma=(2,1)}^{(2,n_2)}\sum_{\delta=(2,1)}^{(2,n_2)}\langle\delta_{i_\alpha,i_\beta}\delta_{i_\gamma,i_\delta}\rangle_{\text{SP}}.$$

Here replicas α and β belong to the group-1 while γ and δ belong to the group-2.

To proceed further, we classify the terms in the multiple free-sums over replica indexes into some subsets as represented by the diagrams in Fig. 14. Different diagrams represent different ways to contract the indexes. From now on indexes represent replicas *which do not overlap with each other*. Each bond represent a Kronecker-delta. A diagram consists of one or several sets of 'connected bonds'. A sum over replicas is associated with each index, under the constraint that replicas associated with different indexes do not overlap with each other.

Thus the diagrams are identified as follows

$$\text{a)-1} \quad \rightarrow \quad {\sum_{\alpha;\gamma}}' \langle 1 \rangle_{\text{SP}}$$

$$\text{a)-2} \quad \rightarrow \quad {\sum_{\alpha;\gamma,\delta}}' \langle \delta_{i_\gamma,i_\delta} \rangle_{\text{SP}}$$

$$\text{a)-3} \quad \rightarrow \quad {\sum_{\alpha,\beta;\gamma}}' \langle \delta_{i_\alpha,i_\beta} \rangle_{\text{SP}}$$

$$\text{a)-4} \quad \rightarrow \quad {\sum_{\alpha,\beta;\gamma,\delta}}' \langle \delta_{i_\alpha,i_\beta} \delta_{i_\gamma,i_\delta} \rangle_{\text{SP}} \tag{E4}$$

Here α and β belong to group-1 while γ and δ belong to group-2. We use the symbol ${\sum}'$ to mean that the running indexes do not overlap with each other;

$$ {\sum_{\alpha,\beta;\gamma,\delta}}' \ldots \equiv 2 \sum_{\alpha=1}^{n_1} \sum_{\beta=\alpha+1}^{n_1} \cdot 2 \sum_{\gamma=1}^{n_2} \sum_{\delta=\gamma+1}^{n_2} \ldots $$
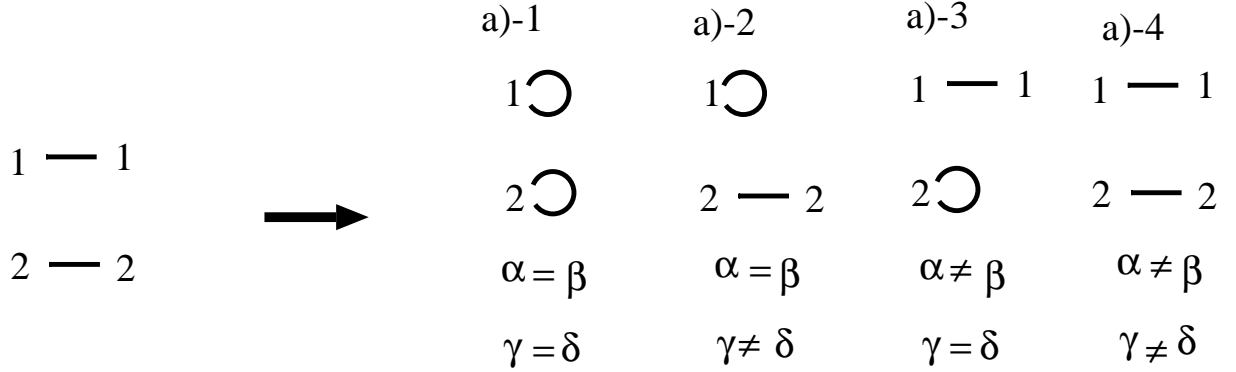

FIG. 14: Classification of the terms in $\langle A_{11} A_{22} \rangle_{\text{SP}}$ represented by the diagram on the left hand side. Indexes on the diagrams a)-1 to a)-4 represent non-identical replicas and their numbers represent the groups to which they belongs to.

4. Now we are left to evaluate expectation values $\langle \ldots \rangle_{\text{SP}}$ (See Eq. (E3)) of the diagrams. An 1RSB solution is represented by a configuration of clusters (See Fig. 11).

Note for instance that $\delta_{i_\alpha,i_\beta}$ is 0 in a solution where α and β belong to different clusters. Thus we just need to count numbers of 1RSB solutions in which all replicas belonging to a set of 'connected bonds' are contained in a common cluster.

For example let us consider the case of a)-4;

$$ {\sum_{\alpha,\beta;\gamma,\delta}}' \langle \delta_{i_\alpha,i_\beta} \delta_{i_\gamma,i_\delta} \rangle_{\text{SP}} $$

There are two possible configurations of clusters which make non-zero contributions, say a)-4-1 and a)-4-2 as shown in Fig. 15.

The case of a)-4-1 is evaluated as follows,

$$ n_1(n_1-1) \times n_2(n_2-1) \times \frac{n_{\text{tot}}}{m} \frac{m(m-1)}{n_{\text{tot}}(n_{\text{tot}}-1)} \times \frac{(m-2)(m-3)}{(n_{\text{tot}}-2)(n_{\text{tot}}-3)} $$
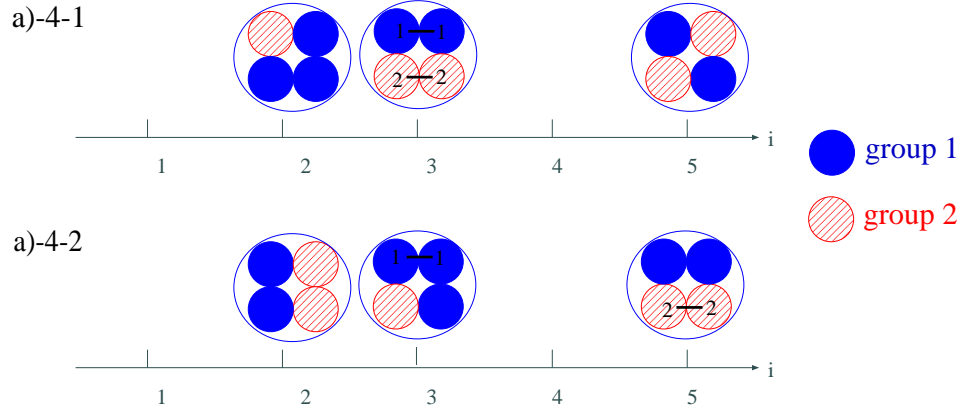
FIG. 15: A schematic representation of some 1RSB solutions. Closed circles represent clusters of the 1RSB solutions. n_1 replicas belong to group 1 (blue) and n_2 replicas belong to group 2 (red). The replicas of the two groups $n_{\text{tot}} = n_1 + n_2$ are mixed together and divided into clusters of size m. Here two kinds of solutions which make non-zero contributions for the diagram a)-4 are shown: the two sets of 'connected bonds' $1-1$' and '$2-2$'are contained in a single cluster a)-4-1 or in different clusters a)-4-2.

The first two factors $n_1(n_1 - 1)$ and $n_2(n_2 - 1)$ represent number of ways to choose the 4 different replicas associated with the 4 running indexes in a)-4: 2 replicas are chosen out of n_1 replicas in group-1 and 2 replicas are chosen out of n_2 replicas in group-2. The last two factors

$$\frac{n_{\text{tot}}}{m} \frac{m(m-1)}{n_{\text{tot}}(n_{\text{tot}}-1)} \times \frac{(m-2)(m-3)}{(n_{\text{tot}}-2)(n_{\text{tot}}-3)}$$

are the probability to have a solution like a)-4-1 in Fig. 15 given n_{tot} replicas.

The probability is obtained by counting the number of such solutions and dividing the result by the total number of solutions $n_{\text{tot}}!$. In the case a)-4-1 all 4 replicas associated with the 'connected bonds' are put in a single cluster. Thus first we note that there are n_{tot}/m possible ways to choose the cluster among n_{tot}/m clusters. Then we note that there are $m(m-1)(m-2)(m-3)$ different ways to choose 4 distinct replicas for the running 4 indexes out of m replicas in the cluster. Last we note that there are $(n_{\text{tot}}-4)!$ ways to choose the rest of replicas. Thus the number of solutions we wanted is $n_{\text{tot}}/m \times m(m-1)(m-2)(m-3) \times (n_{\text{tot}}-4)!$. Then dividing the latter by the total number of solutions $n_{\text{tot}}!$ we obtain the factor displayed above.

The case of a)-4-2 is evaluated in the same way as follows,

$$n_1(n_1-1) \times n_2(n_2-1) \times \frac{n_{\text{tot}}}{m} \frac{m(m-1)}{n_{\text{tot}}(n_{\text{tot}}-1)} \times \left(\frac{n_{\text{tot}}}{m} - 1\right) \frac{m(m-1)}{(n_{\text{tot}}-2)(n_{\text{tot}}-3)}.$$

Here the factor $n_{\text{tot}}/m - 1$ is the number of ways to choose a '2nd cluster'.

Summing up the results of a)-4-1 and a)-4-2 explained above, we obtain

$$\lim_{n_1,n_2 \to 0} \frac{1}{n_1 n_2} \sideset{}{'}\sum_{\alpha,\beta;\gamma,\delta} \left\langle \delta_{i_\alpha,i_\beta} \delta_{i_\gamma,i_\delta} \right\rangle_{\text{SP}}$$

$$= \lim_{n_1,n_2 \to 0} \frac{1}{n_1 n_2} n_1(n_1-1)n_2(n_2-1) \left\{ \frac{n_{\text{tot}}}{m} \frac{m(m-1)}{n_{\text{tot}}(n_{\text{tot}}-1)} \frac{(m-2)(m-3)}{(n_{\text{tot}}-2)(n_{\text{tot}}-3)} \right.$$

$$\left. + \frac{n_{\text{tot}}}{m} \frac{m(m-1)}{n_{\text{tot}}(n_{\text{tot}}-1)} \left(\frac{n_{\text{tot}}}{m} - 1\right) \frac{m(m-1)}{(n_{\text{tot}}-2)(n_{\text{tot}}-3)} \right\}$$

$$= \frac{(1-m)(2-m)(3-m)}{3!} + \frac{m(1-m)^2}{3!}$$

a.   Linear susceptibility

The linear susceptibility is related to the 2nd thermal cumulant as $\chi_1 = \beta \kappa_2(Y)$. In section V B we present the computation of the sample-average of its 1st moment $[\kappa_2(Y)]$.

In the following we describe computation of the 2nd moment $[\kappa_2^2(Y)]$. In the previous subsection sec. V A we have already found that

$$\left[\kappa_2^2(Y)\right] = N(\Delta_{\mathrm{eff}})^2 \cdot \lim_{n_1,n_2 \to 0} \frac{1}{n_1 n_2}(\langle A_{11} A_{22}\rangle_{\mathrm{SP}} + 2 \langle A_{12}^2 \rangle_{\mathrm{SP}}). \tag{E5}$$

This is obtained by analysing possible pairings of the 4 'running indexes' as in Fig. 13. Next $\langle A_{11} A_{22}\rangle_{\mathrm{SP}}$ and $\langle A_{12}^2 \rangle_{\mathrm{SP}}$ must be evaluated.

In the previous section we have evaluated $\langle A_{11} A_{22}\rangle_{\mathrm{SP}}$ to a certain extent. First we noted that it can be considered as sum over contributions from diagrams a)-1 to a)-4 shown in Fig. 14. An important point there is that the multiple 'running indexes' do not overlap with each other. We have evaluated the contribution from diagram a)-4.

In similar ways we obtain contributions from other diagrams a)-1 to a)-3. From diagram a)-1 we simply find

$$\lim_{n_1,n_2 \to 0} \frac{1}{n_1 n_2} {\sum_{\alpha;\gamma}}' 1 = 1.$$

From diagram a)-2 we find,

$$\lim_{n_1,n_2 \to 0} \frac{1}{n_1 n_2} {\sum_{\alpha;\gamma,\delta}}' \left\langle \delta_{i_\gamma, i_\delta} \right\rangle_{\mathrm{SP}}$$
$$= \lim_{n_2 \to 0} \frac{1}{n_2} n_2 (n_2 - 1) \frac{n_{\mathrm{tot}}}{m} \frac{m(m-1)}{n_{\mathrm{tot}}(n_{\mathrm{tot}} - 1)}$$
$$= -(1 - m).$$

From diagram a)-3 we obtain the same result. Summing up these results we obtain,

$$\lim_{n_1,n_2 \to 0} \frac{1}{n_1 n_2} \langle A_{11} A_{22}\rangle_{\mathrm{SP}} = 1 - 2(1 - m) + \left\{ \frac{(1-m)(2-m)(3-m)}{3!} + \frac{m(1-m)^2}{3!} \right\}. \tag{E6}$$

The evaluation of $\langle A_{11}^2 \rangle_{\mathrm{SP}}$ which reads as

$$\left\langle A_{12}^2 \right\rangle_{\mathrm{SP}} = \sum_{\alpha=(1,1)}^{(1,n_1)} \sum_{\beta=(2,1)}^{(2,n_1)} \sum_{\gamma=(1,1)}^{(1,n_2)} \sum_{\delta=(2,1)}^{(2,n_2)} \left\langle \delta_{i_\alpha, i_\beta} \delta_{i_\gamma, i_\delta} \right\rangle_{\mathrm{SP}}.$$

can be done in the same way. Diagrams corresponding to those in Fig. 14 are the diagrams b)-1 to b)-4 shown in
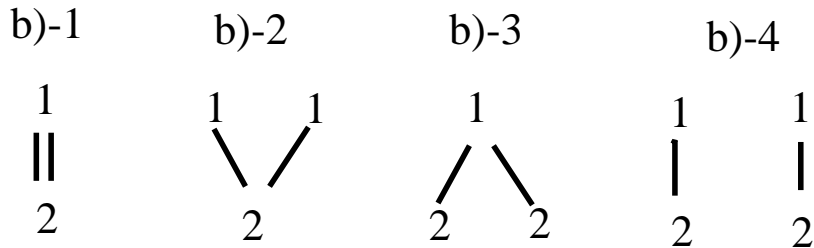

FIG. 16:   Diagrams contributing to $\langle A_{12}^2 \rangle_{\mathrm{SP}}$. Indexes on the diagrams represent non-identical replicas and their numbers represent the groups to which they belongs to.

Fig. 16. The diagrams are evaluated as the following,

b)-1 $\quad\rightarrow\quad$ $\displaystyle\lim_{n_1,n_2\to 0}\frac{1}{n_1 n_2}\sideset{}{'}\sum_{\alpha;\gamma}\langle\delta_{\alpha,\gamma}\rangle_{\mathrm{SP}}=1-m$

b)-2 $\quad\rightarrow\quad$ $\displaystyle\lim_{n_1,n_2\to 0}\frac{1}{n_1 n_2}\sideset{}{'}\sum_{\alpha,\beta;\gamma}\langle\delta_{\alpha,\gamma}\delta_{\beta,\gamma}\rangle_{\mathrm{SP}}=-\frac{(1-m)(2-m)}{2}$

b)-3 $\quad\rightarrow\quad$ $\displaystyle\lim_{n_1,n_2\to 0}\frac{1}{n_1 n_2}\sideset{}{'}\sum_{\alpha;\gamma,\delta}\langle\delta_{\alpha,\gamma}\delta_{\alpha,\delta}\rangle_{\mathrm{SP}}=-\frac{(1-m)(2-m)}{2}$

b)-4 $\quad\rightarrow\quad$ $\displaystyle\lim_{n_1,n_2\to 0}\frac{1}{n_1 n_2}\sideset{}{'}\sum_{\alpha,\beta;\gamma,\delta}\langle\delta_{\alpha,\gamma}\delta_{\beta,\delta}\rangle_{\mathrm{SP}}=\frac{(1-m)(2-m)(3-m)}{3!}+\frac{m(1-m)^2}{3!}$

Note that b)-4 is equivalent to a)-4 so that one must consider two kinds of solutions with different patterns of clustering as those shown in Fig. 15. Summing up the above results we obtain

$$
\begin{aligned}
\lim_{n_1,n_2\to 0}\frac{1}{n_1 n_2}\left\langle A_{12}^2\right\rangle_{\mathrm{SP}} &= 1-m-2\frac{(1-m)(2-m)}{2}+\left\{\frac{(1-m)(2-m)(3-m)}{3!}+\frac{m(1-m)^2}{3!}\right\}\\
&= \frac{1}{3}m(1-m).
\end{aligned}
\tag{E7}
$$

Using Eq. (E6) and Eq. (E7) in Eq. (E5) we finally obtain Eq. (94),

$$
\left[\kappa_2^2(Y)\right]=(N(\Delta_{\mathrm{eff}})^2)^2 m.
\tag{E8}
$$

b. Non-linear susceptibility

The non-linear susceptibility is related to the 2nd thermal cumulant as $\chi_2=(\beta^2/2!)\kappa_3(Y)$. Due to a simple symmetry reason sample-average of the 1st moment $[\kappa_3(Y)]$ is zero. We examine sample-average of the 2nd moment $[\kappa_3^2(Y)]$ below. Following the steps 1,2 in sec. V A we obtain,

$$
\left[\kappa_3^2(Y)\right]=(N(\Delta_{\mathrm{eff}})^2)^3\lim_{n_1,n_2\to 0}\frac{1}{n_1 n_2}(9\left\langle A_{11}A_{12}A_{22}\right\rangle_{\mathrm{SP}}+\left\langle A_{12}^3\right\rangle_{\mathrm{SP}}).
\tag{E9}
$$

First we evaluate,

$$
\begin{aligned}
&\lim_{n_1,n_2\to 0}\frac{1}{n_1 n_2}\left\langle A_{11}A_{22}A_{12}\right\rangle_{\mathrm{SP}}\\
&=\lim_{n_1,n_2\to 0}\frac{1}{n_1 n_2}\sum_{\alpha_1=(1,1)}^{(1,n_1)}\sum_{\alpha_2=(1,1)}^{(1,n_1)}\sum_{\alpha_3=(1,1)}^{(1,n_1)}\sum_{\beta_1=(2,1)}^{(2,n_2)}\sum_{\beta_2=(2,1)}^{(2,n_2)}\sum_{\beta_3=(2,1)}^{(2,n_2)}\left\langle\delta_{i_{\alpha_1},i_{\alpha_2}}\delta_{i_{\beta_1},i_{\beta_2}}\delta_{i_{\alpha_3},i_{\beta_3}}\right\rangle_{\mathrm{SP}}.
\end{aligned}
\tag{E10}
$$

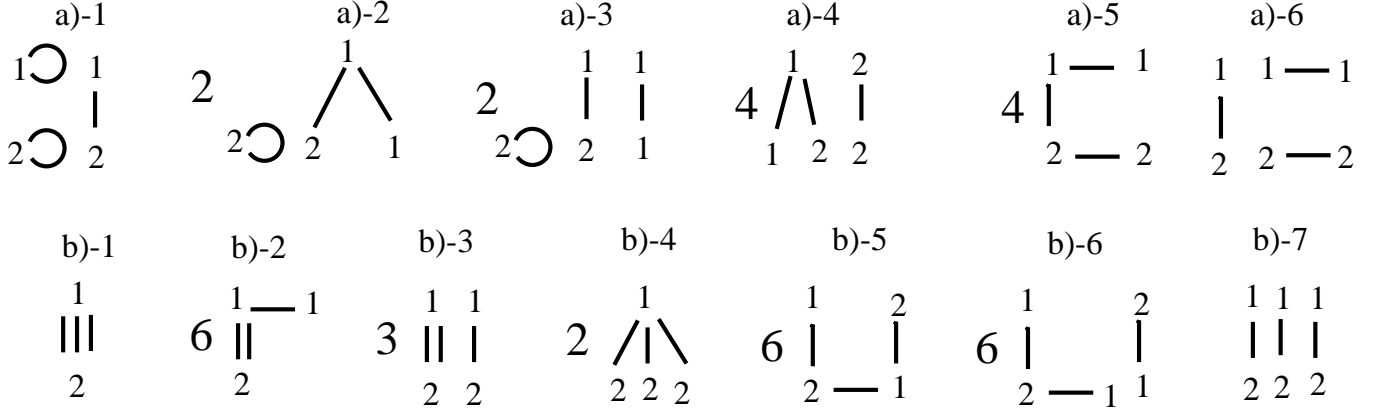Following the step 3 in sec. V A the sum with 6 running indexes can be divided into contributions from the diagrams

a)-1   a)-2   a)-3   a)-4   a)-5   a)-6

b)-1   b)-2   b)-3   b)-4   b)-5   b)-6   b)-7

FIG. 17:   Diagrams contributing to $\left[\kappa_3^2(Y)\right]$. The upper 6 diagrams contribute to $\langle A_{12}A_{22}A_{12}\rangle_{\rm SP}$ and the lower 7 diagrams contribute to $\langle A_{12}^3\rangle_{\rm SP}$. The numbers of the left hand side of the diagrams represent numbers of the graphs of the same geometry.

a)-1 to a)-6 shown in Fig. 17. Then by the step 4 they are evaluated as the following,

$$
\text{a)-1} \quad \rightarrow \quad \lim_{n_1,n_2\to 0}\frac{1}{n_1 n_2}\sideset{}{'}\sum_{\alpha_1,\alpha_2;\beta_1,\beta_2}\langle\delta_{\alpha_2,\beta_2}\rangle_{\rm SP} = \lim_{n_1,n_2\to 0} n_1 n_2 (1-m) = 0
$$

$$
\text{a)-2} \quad \rightarrow \quad \lim_{n_1,n_2\to 0}\frac{1}{n_1 n_2}\sideset{}{'}\sum_{\alpha_1,\alpha_2;\beta_1,\beta_2}\langle\delta_{\alpha_1,\alpha_2}\delta_{\alpha_2,\beta_1}\rangle_{\rm SP} = \lim_{n_1,n_2\to 0} O(n_1) = 0
$$

$$
\text{a)-3} \quad \rightarrow \quad \lim_{n_1,n_2\to 0}\frac{1}{n_1 n_2}\sideset{}{'}\sum_{\alpha_1,\alpha_2,\alpha_3;\beta_1,\beta_2}\langle\delta_{\alpha_1,\alpha_2}\delta_{\alpha_3,\beta_3}\rangle_{\rm SP} = \lim_{n_1,n_2\to 0} O(n_1) = 0
$$

$$
\text{a)-4} \quad \rightarrow \quad \lim_{n_1,n_2\to 0}\frac{1}{n_1 n_2}\sideset{}{'}\sum_{\alpha_1,\alpha_2;\beta_1,\beta_2,\beta_3}\langle\delta_{\alpha_1,\alpha_2}\delta_{\alpha_2,\beta_1}\delta_{\beta_2,\beta_3}\rangle_{\rm SP}
$$
$$
= -2!\left\{\frac{m(1-m)^2(2-m)}{4!} + \frac{(1-m)(2-m)(3-m)(4-m)}{4!}\right\}
$$

$$
\text{a)-5} \quad \rightarrow \quad \lim_{n_1,n_2\to 0}\frac{1}{n_1 n_2}\sideset{}{'}\sum_{\alpha_1,\alpha_2;\beta_1,\beta_2}\langle\delta_{\alpha_1,\alpha_2}\delta_{\alpha_2,\beta_1}\delta_{\beta_1,\beta_2}\rangle_{\rm SP} = \frac{(1-m)(2-m)(3-m)}{3!}
$$

$$
\text{a)-6} \quad \rightarrow \quad \lim_{n_1,n_2\to 0}\frac{1}{n_1 n_2}\sideset{}{'}\sum_{\alpha_1,\alpha_2,\alpha_3;\beta_1,\beta_2,\beta_3}\langle\delta_{\alpha_1,\alpha_2}\delta_{\beta_1,\beta_2}\delta_{\alpha_3,\beta_3}\rangle_{\rm SP}
$$
$$
= (2!)^2\left\{\frac{2!m^2(1-m)^3}{5!} + 3\frac{m(1-m)^2(2-m)(3-m)}{5!}\right.
$$
$$
\left. + \frac{(1-m)(2-m)(3-m)(4-m)(5-m)}{5!}\right\}
\tag{E11}
$$

Next we evaluate,

$$
\lim_{n_1,n_2\to 0}\frac{1}{n_1 n_2}\langle A_{12}^3\rangle_{\rm SP}
$$
$$
= \lim_{n_1,n_2\to 0}\frac{1}{n_1 n_2}\sum_{\alpha_1=(1,1)}^{(1,n_1)}\sum_{\alpha_2=(1,1)}^{(1,n_1)}\sum_{\alpha_3=(1,1)}^{(1,n_1)}\sum_{\beta_1=(2,1)}^{(2,n_2)}\sum_{\beta_2=(2,1)}^{(2,n_2)}\sum_{\beta_3=(2,1)}^{(2,n_2)}\langle\delta_{i_{\alpha_1},i_{\beta_1}}\delta_{i_{\alpha_2},i_{\beta_2}}\delta_{i_{\alpha_3},i_{\beta_3}}\rangle_{\rm SP}.
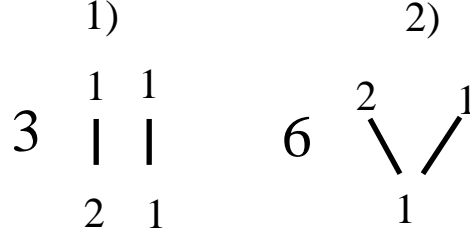\tag{E12}
$$

FIG. 18: Diagrams contributing to $[\![\kappa_3(Y)\kappa_1(Y)]\!]$. The numbers of the left hand side of the diagrams represent numbers of the graphs of the same geometry.

The sum can be divided into contributions from the diagrams b)-1 to b)-7 shown in Fig. 17, which are evaluated as,

$$b)\text{-}1 \qquad \rightarrow \qquad \lim_{n_1,n_2\to 0} \frac{1}{n_1 n_2} {\sum_{\alpha_1;\beta_1}}' \langle \delta_{\alpha_1,\beta_1}\rangle_{\mathrm{SP}} = 1-m$$

$$b)\text{-}2 \qquad \rightarrow \qquad \lim_{n_1,n_2\to 0} \frac{1}{n_1 n_2} {\sum_{\alpha_1,\alpha_2;\beta_1}}' \langle \delta_{\alpha_1,\alpha_2}\delta_{\alpha_1,\beta_1}\rangle_{\mathrm{SP}} = -\frac{(1-m)(2-m)}{2!}$$

$$b)\text{-}3 \qquad \rightarrow \qquad \lim_{n_1,n_2\to 0} \frac{1}{n_1 n_2} {\sum_{\alpha_1,\alpha_2;\beta_1,\beta_2}}' \langle \delta_{\alpha_1,\alpha_2}\delta_{\beta_1,\beta_2}\rangle_{\mathrm{SP}} = \frac{m(1-m)^2}{3!} + \frac{(1-m)(2-m)(3-m)}{3!}$$

$$b)\text{-}4 \qquad \rightarrow \qquad \lim_{n_1,n_2\to 0} \frac{1}{n_1 n_2} {\sum_{\alpha_1;\beta_1,\beta_2,\beta_3}}' \langle \delta_{\alpha_1,\beta_1}\delta_{\alpha_1,\beta_2}\delta_{\alpha_1,\beta_3}\rangle_{\mathrm{SP}} = 2!\frac{(1-m)(2-m)(3-m)}{3!}$$

$$b)\text{-}5 \qquad \rightarrow \qquad \lim_{n_1,n_2\to 0} \frac{1}{n_1 n_2} {\sum_{\alpha_1,\alpha_2;\beta_1,\beta_2}}' \langle \delta_{\alpha_1,\beta_1}\delta_{\alpha_2,\beta_1}\delta_{\alpha_2,\beta_2}\rangle_{\mathrm{SP}} = \frac{(1-m)(2-m)(3-m)}{3!}$$

$$b)\text{-}6 \qquad \rightarrow \qquad \lim_{n_1,n_2\to 0} \frac{1}{n_1 n_2} {\sum_{\alpha_1,\alpha_2,\alpha_3;\beta_1,\beta_2}}' \langle \delta_{\alpha_1,\beta_1}\delta_{\alpha_2,\beta_1}\delta_{\alpha_3,\beta_2}\rangle_{\mathrm{SP}}$$

$$= -2!\left\{ \frac{m(1-m)^2(2-m)}{4!} + \frac{(1-m)(2-m)(3-m)(4-m)}{4!}\right\}$$

$$b)\text{-}7 \qquad \rightarrow \qquad \lim_{n_1,n_2\to 0} \frac{1}{n_1 n_2} {\sum_{\alpha_1,\alpha_2,\alpha_3;\beta_1,\beta_2,\beta_3}}' \langle \delta_{\alpha_1,\beta_1}\delta_{\alpha_2,\beta_2}\delta_{\alpha_3,\beta_3}\rangle_{\mathrm{SP}}$$

$$= 2!\frac{m^2(1-m)^3}{5!} + 3\frac{m(1-m)^2(2-m)(3-m)}{5!}$$

$$+ \frac{(1-m)(2-m)(3-m)(4-m)(5-m)}{5!}. \tag{E13}$$

Summing up the above results we finally obtain Eq. (95),

$$\left[\kappa_3^2(Y)\right] = (N(\Delta_{\mathrm{eff}})^2)^3 2m(1-m). \tag{E14}$$

c. Other moments

Here we present results of some other moments needed in the present paper.

The 2nd moment of the 1st thermal cumulant is evaluated as,

$$
\left[\kappa_1^2(Y)\right] = (\sqrt{N}\Delta_{\text{eff}})^2 \lim_{n_1,n_2\to 0}\frac{1}{n_1 n_2}\frac{\partial}{\partial x_1}\frac{\partial}{\partial x_2}\left\langle \exp\left(\frac{1}{2}\sum_{r,s=1}^2 x_r A_{rs}x_s\right)\right\rangle_{\text{SP}}\Bigg|_{x=0}
$$

$$
= (\sqrt{N}\Delta_{\text{eff}})^2\left\langle A_{12}\right\rangle_{\text{SP}} = (\sqrt{N}\Delta_{\text{eff}})^2\left\langle \sideset{}{'}\sum_{\alpha;\beta}\delta_{i_\alpha,i_\beta}\right\rangle_{\text{SP}}
$$

$$
= (\sqrt{N}\Delta_{\text{eff}})^2(1-m). \tag{E15}
$$

We also need $[\![\kappa_3(Y)\kappa_Y]\!]$ which is evaluated as,

$$
[\![\kappa_3(Y)\kappa_1(Y)]\!] = \quad (\sqrt{N}\Delta_{\text{eff}})^4\lim_{n_1\to 0}\lim_{n_2\to 0}\frac{1}{n_1 n_2}\frac{\partial^3}{\partial x_1^3}\frac{\partial}{\partial x_2}\left\langle \exp\left(\frac{1}{2}\sum_{r,s=1}^2 x_r A_{rs}x_s\right)\right\rangle_{\text{SP}}\Bigg|_{x=0}
$$

$$
= (\sqrt{N}\Delta_{\text{eff}})^4\lim_{n_1\to 0}\lim_{n_2\to 0}\frac{1}{n_1 n_2}3\left\langle A_{11}A_{12}\right\rangle_{\text{SP}}
$$

$$
= -(\sqrt{N}\Delta_{\text{eff}})^4\lim_{n_1,n_2\to 0}\frac{1}{n_1 n_2}\left(3\sideset{}{'}\sum_{\alpha,\beta,\gamma;\delta}\left\langle \delta_{i_\alpha,i_\beta}\delta_{i_\gamma,i_\delta}\right\rangle_{\text{SP}} + 6\sideset{}{'}\sum_{\alpha,\beta;\delta}\left\langle \delta_{i_\alpha,i_\beta}\delta_{i_\beta,i_\delta}\right\rangle_{\text{SP}}\right)
$$

$$
= -(\sqrt{N}\Delta_{\text{eff}})^4 m(1-m). \tag{E16}
$$

The 1st and 2nd terms in the brace $(\ldots)$ in the 2nd equation from below correspond to the two diagrams presented in Fig. 18 which are evaluated as the follwoing. Diagrams corresponding to 1) in Fig. 18 yields,

$$
\lim_{n_1,n_2\to 0}\frac{1}{n_1 n_2}\sideset{}{'}\sum_{\alpha,\beta,\gamma;\delta}\left\langle \delta_{i_\alpha,i_\beta}\delta_{i_\gamma,i_\delta}\right\rangle_{\text{SP}} = 2\frac{(1-m)(2-m)(3-m)}{3!} + 2\frac{m(1-m)^2}{3!}. \tag{E17}
$$

The 1st/2nd term on r.h.s is due to the cases that '1-1' and '1-2' belong to the same/different clusters. On the other hand diagrams corresponding to 2) in Fig. 18 yields,

$$
\lim_{n_1,n_2\to 0}\frac{1}{n_1 n_2}\sideset{}{'}\sum_{\alpha,\beta;\delta}\left\langle \delta_{i_\alpha,i_\beta}\delta_{i_\beta,i_\delta}\right\rangle_{\text{SP}} = -\frac{(1-m)(2-m)}{2!}. \tag{E18}
$$

APPENDIX F: ANALYSIS OF THE CUSP BY A REPLICA APPROACH

The solution can be obtained by closely following the approach of [32] which we outline below. First let us slightly modify how to take the summation over the solutions $\sum_{\text{SP}}$. In our original representation Eq. (99) there are $n/2$ replicas belonging to group '1' and the other $n/2$ replicas belonging to group '2'. Then 1 step RSB solution is given by mixing up all replicas and then dividing them into clusters of size m. We note that it is equivalent to say that there are n/m clusters of size m and 1 step RSB solution is specified by deciding which group ('1' or '2') each replica belongs to. Using this mapping we can rewrite the summation over the solutions in Eq. (99) as,

$$
\sum_{\text{SP}}\exp\left(\frac{1}{2m^2}\sum_{r,s=1}^2\frac{\delta h_r}{h_s}\frac{\delta h_s}{h_s}\sum_{\alpha=(1,1)}^{(1,n/2)}\sum_{\beta=(2,1)}^{(2,n/2)}\delta_{i_\alpha,i_\beta}\right)
$$

$$
= \sideset{}{'}\sum_{\sigma}\exp\left(\frac{1}{2m^2}\sum_{a,b}I_{ab}\left[\frac{1-\sigma_a}{2}\frac{\delta h_1}{h_s} + \frac{1+\sigma_a}{2}\frac{\delta h_1}{h_s}\right]\left[\frac{1-\sigma_b}{2}\frac{\delta h_2}{h_s} + \frac{1+\sigma_b}{2}\frac{\delta h_2}{h_s}\right]\right). \tag{F1}
$$

Here I_{ab} is a standard Parisi's matrix for 1 step RSB which is block-diagonal: block size is m and the elements are $I = 1$ in the block-diagonal part and $I = 0$ for the rest (See Fig. 12). We also introduced 'Ising variables' $\sigma_a = \pm 1$ for $a = 1..n$. The summation $\sum_\sigma$ means to a trace over the Ising variables under the constraint that $\sum_{a=1}^n \sigma_a = 0$.

To simplify notations we introduce $\tilde{h}_1 = \delta h_1/h_{\rm s}$ and $\tilde{h}_2 = \delta h_2/h_{\rm s}$. Using a Hubbard-Stratonovich transformation $e^{\frac{A}{2}\sum_{a,b}\sigma_a\sigma_b} = \int_{-\infty}^{\infty}\frac{d\lambda}{\sqrt{2\pi/A}}e^{-\frac{\lambda^2}{2A}}e^{\sum_a \sigma}$ with $A > 0$, we obtain,

$$
\sideset{}{'}\sum_{\sigma} \exp\left(\frac{1}{2m^2}\sum_{a,b} I_{ab} \left[\frac{1-\sigma_a}{2}\tilde{h}_1 + \frac{1+\sigma_a}{2}\tilde{h}_2 \right] \left[\frac{1-\sigma_b}{2}\tilde{h}_1 + \frac{1+\sigma_b}{2}\tilde{h}_2 \right] \right)
$$

$$
= e^{\frac{n}{m}\frac{(\tilde{h}_1+\tilde{h}_2)^2}{8}} \sideset{}{'}\sum_{\sigma} \prod_{\mathcal{C}=1}^{n/m} \int_{-\infty}^{\infty}\frac{d\lambda_{\mathcal{C}}}{\sqrt{2\pi/A}} \exp\left[-\frac{\lambda_{\mathcal{C}}^2}{2A} + \left(-\frac{\tilde{h}_1^2 - \tilde{h}_2^2}{4m} + \lambda_{\mathcal{C}} \right)\sum_{a\in\mathcal{C}}\sigma_a \right]
$$

$$
= e^{\frac{n}{m}\frac{(\tilde{h}_1+\tilde{h}_2)^2}{8}} \frac{2^{n+1}}{B(-n/2,-n/2)} \int_{-\infty}^{\infty} dy \left[\int_{-\infty}^{\infty}\frac{d\lambda'}{\sqrt{2\pi}} e^{-\frac{\lambda'^2}{2}} \cosh(y+\sqrt{A}\lambda') \right]^{n/m} \tag{F2}
$$

with

$$
A = \frac{(\tilde{h}_1 - \tilde{h}_2)^2}{4m^2}. \tag{F3}
$$

Here $\mathcal{C} = 1, 2, \ldots, n/m$ are the blocks of the block-diagonal matirx I_{ab} and $\sum_{a\in\mathcal{C}}$ denotes a summation over replicas beloging to a block $\mathcal{C}$. To obtain the last equation we used the constraint $\sum_{a=1}^{n}\sigma_a = 0$ and the identity [32],

$$
\sideset{}{'}\sum_{\sigma} e^{\sum_a h_a\sigma_a} = \frac{2^{n+1}}{B(-n/2,-n/2)} \int_{-\infty}^{\infty} dy \cosh(y+h_a). \tag{F4}
$$

Chaging variablies with $\tilde{h} = {\rm sgn}(\tilde{h}_1 - \tilde{h}_2)\lambda'$ and $\mu = e^{-2y}$ we can rewrite the integrals as,

$$
\int_{-\infty}^{\infty} dy \left[\int_{-\infty}^{\infty}\frac{d\lambda'}{\sqrt{2\pi}} e^{-\frac{\lambda'^2}{2}} \cosh(y+\sqrt{A}\lambda') \right]^{n/m} = e^{\frac{n}{m}\frac{(\tilde{h}_1-\tilde{h}_2)^2}{8}} \frac{1}{2^{n+1}} \int_0^{\infty}\frac{d\mu}{\mu}\mu^{-n/2} \left[\int_{-\infty}^{\infty}\frac{d\tilde{h}}{\sqrt{2\pi}} \left\{ e^{-\frac{(\tilde{h}-\tilde{h}_1)^2}{2m}} + \mu e^{-\frac{(\tilde{h}-\tilde{h}_2)^2}{2m}} \right\}^m \right]^{n/m}
$$

Summing up the above results and using $\lim_{n\to 0} nB(n/2,n/2) = 4$ we obtain,

$$
\lim_{T\to 0} \frac{\langle Y(h_0 + \delta h_1) Y(h_0 + \delta h_2) \rangle}{(\sqrt{N}\Delta_{\rm eff}(h_0))^2}
$$

$$
= -\lim_{m\to 0}\lim_{n\to 0} \frac{1}{n} \frac{\partial^2}{\partial\left(\frac{\delta h_1}{h_{\rm s}}\right)\partial\left(\frac{\delta h_2}{h_{\rm s}}\right)} e^{\frac{n}{4m}(\tilde{h}_1^2 + \tilde{h}_2^2)} \int_0^{\infty}\frac{d\mu}{\mu}\mu^{-n/2} \left[\int_{-\infty}^{\infty}\frac{d\tilde{h}}{\sqrt{2\pi}} \left\{ e^{-\frac{(\tilde{h}-\tilde{h}_1)^2}{2m}} + \mu e^{-\frac{(\tilde{h}-\tilde{h}_2)^2}{2m}} \right\}^m \right]^{n/m}
$$

$$
= g_{11} + g_{12} \tag{F5}
$$

with

$$
g_{11} = \sqrt{\frac{2}{\pi}}e^{-\frac{l^2}{8}} \int_0^{\infty} dx \frac{e^{-\frac{x^2}{2}}(x^2 - \frac{l^2}{4})}{e^{-\frac{|l|}{2}}M_0(x - \frac{|l|}{2}) + e^{\frac{|l|}{2}}M_0(-x - \frac{|l|}{2})} = 1 - \frac{3|l|}{2\sqrt{\pi}} + O(|l|^2) \tag{F6}
$$

and

$$
g_{12} = -\frac{|l|}{\pi}e^{-\frac{l^2}{4}} \int_0^{\infty} dx \frac{e^{-x^2}e^{-x|l|}}{\left\{ e^{-\frac{|l|}{2}}M_0(x - \frac{|l|}{2}) + e^{\frac{|l|}{2}}M_0(-x - \frac{|l|}{2}) \right\}^2} = -\frac{|l|}{2\sqrt{\pi}} + O(|l|^2) \tag{F7}
$$

with

$$
M_k(x) = \int_x^{\infty} \frac{dz}{\sqrt{2\pi}} z^k e^{-\frac{z^2}{2}} \tag{F8}
$$

and

$$
l = \frac{\delta h_1 - \delta h_2}{h_{\rm s}}. \tag{F9}
$$

In the above equations we changed the integration variable using $\mu \equiv e^{-x\frac{|l|}{m}}$. For the details of the evaluations of the $m \to 0$ limit of the integrals see [32]. In order to obtain the last equation of Eq. (102), we expanded the integrals by $|l|$ and repeated some partial integrations and some Gaussian integrals.

APPENDIX G: FLUCTUATIONS OF CLUSTERS IN ONE-STEP RSB SOLUTIONS

Let us recalled that a given 1RSB solution is described as a configuration of n replicas grouped into n/m clusters of a unique size m. (See Fig. 11.) Being motivated by a work by Campellone et al [59], we now consider a class of more generic solutions where the sizes of clusters can be inhomogeneous. As noted in sec V this is necessary to evaluate the parameter Δ_{eff} in the generating functional Eq. (85) properly.

The need to take into account the fluctuation of m has been pointed out by several authros. Especially it has been pointed out [57, 58] that if one computes the heat capacity from the thermal fluctuations of energy E via FDT: $(1/N)\beta^2 \left[\langle E^2 \rangle - \langle E \rangle^2\right]$ neglecting fluctuations from the usual 1RSB saddle points, one does not recover the correct thermodynamic heat-capacity that one obtains by taking two time derivatives of the thermodynamic free-energy by temperature T. It has been suggested [57, 58, 59] that one then must consider fluctuations from the saddle point, in particular, the size of clusters m explicitly.

Fluctuations of the size of clusters, seem rather different in nature from the usual small fluctuations [56] of the amplitude of each element of the Parisi matrix. In particular in the case of REM the overlap between the states can be either 0 or 1 by the construction of the model so that fluctuation of the size of clusters amount to very large fluctuations of the amplitudes of the elements of the Parisi matrix [59].

For simplicity we consider below an effective REM with the simple generalized complexity given by Eq. (17).

1. Fluctuations of clusters

In order to obtain some insights let us consider first disorder-average of the replicated partition function given by Eq. (B14),

$$\llbracket Z^n \rrbracket = \sum_{i_1,i_2,\ldots,i_n=1}^{M=e^{cN}} \exp\left[cN(\beta T_{\text{c}}(h))^2 \sum_{\alpha,\beta=1}^{n} \delta_{i_\alpha,i_\beta}\right]. \tag{G1}$$

A given configuration of n replicas of the REM can be viewed as a collection *clusters*. A cluster is a set of replicas sitting on the same microscopic state among $M = e^{cN}$ possible states. We label them as $\mathcal{C}_1,\ldots,\mathcal{C}_l$ where l is the total number of clusters. We denote the size of Ith cluster , namely the number of replicas belonging to C_I, as m_I.

Now using an identity

$$\sum_{\alpha,\beta=1}^{n} \delta_{i_\alpha,i_\beta} = \sum_{I=1}^{l} m_I^2.$$

we can rewrite the replicated partition function as

$$\llbracket Z^n \rrbracket = \sum_l \int cN d\lambda \sum_{\{m_I\}} \frac{n!}{\prod_{I=1}^{l} m_I! l!} e^{-NG(\{m_I\},\lambda,l)} \tag{G2}$$

with

$$-G(\{m_I\},\lambda,l) = c\sum_{I=1}^{l} \left\{1 + (\beta T_{\text{c}}(h))^2 m_I^2 + \lambda m_I\right\} - c\lambda n \tag{G3}$$

here we imposed the constraint

$$\sum_{I=1}^{l} m_I = n \tag{G4}$$

by introducing a Lagrange multiplier λ. The effective action G can be cast into the following form,

$$-\frac{G(\{m_I\},\lambda,l)}{c} = l + (\beta T_{\text{c}}(h))^2 \frac{n}{l}n - \frac{l}{4(\beta T_{\text{c}}(h))^2}(\lambda - \lambda^*(l))^2 + (\beta T_{\text{c}}(h))^2 \sum_{I=1}^{l}(m_I - m^*(\lambda))^2 \tag{G5}$$

with

$$m^*(\lambda) = -\frac{\lambda}{2(\beta T_{\mathrm{c}}(h))^2} \qquad \lambda^*(l) = -\frac{n}{l} 2(\beta T_{\mathrm{c}}(h))^2 \tag{G6}$$

Thus we find

$$[\![Z^n]\!] = \sum_l e^{cN[l+\frac{n}{l}n(\beta T_{\mathrm{c}}(h))^2]} \int cNd\lambda e^{-\frac{cNl}{4(\beta T_{\mathrm{c}}(h))^2}(\lambda-\lambda^*(l))^2} \sum_{\{m_I\}} \frac{n!}{\prod_{I=1}^l m_I!l!} \prod_{I=1}^l e^{cN(\beta T_{\mathrm{c}}(h))^2(m_I-m^*(\lambda))^2}. \tag{G7}$$

Here the order of the summations and integrals is crucial. In order to enforce the constraint Eq. (G4), G must be maximized with respect to λ. On the other hand, G is *minimized* with respect to $\{m_I\}$ at $m_I = m^*(\lambda)$ and $l = l^*$ given by

$$l^* = n\frac{T}{T_{\mathrm{c}}(h)}. \tag{G8}$$

If we disregard fluctuations completely we recover Eq. (78),

$$m_i \simeq m^*(\lambda^*(l^*)) = \frac{T}{T_{\mathrm{c}}(h)} \tag{G9}$$

which is the well known result. Note that usual extremization of the uniform cluster size m (See Eq. (B19) is equivalent here to extremization of the number of clusters l.

In the following we denote fluctuation of the size of cluster $\mathcal{C}_I$ as

$$\delta m_I = m_I - m^*(\lambda). \tag{G10}$$

From Eq. (G7) we find that measure for small fluctuations of the sizes of individual clusters δm_I is given by,

$$\prod_{I=1}^l \int dm_I e^{cN(\beta T_{\mathrm{c}}(h))^2 \delta m_I^2} \dots \tag{G11}$$

The saddle point $\delta m_I = 0$ is the *minimum* which is a strange feature in the $n \to 0$ limit [25, 44].

2. Generating functional for correlation functions of energy

Based on the above observations, let us now construct a generating functional for the correlation functions of energy E. Let us consider p real replicas $r = 1, \ldots, p$, which are replicated further into n_r replicas, at inverse temperatures $\beta + \delta\beta_r$. Here $\delta\beta_r$ is considered as small 'probing fields'. The disorder-averaged partition function of the whole system is given by,

$$[\![Z_1^{n_1} \cdots Z_p^{n_p}]\!] = \sum_{i_{(1,1)},\ldots,i_{(p,n_p)}=1}^{M=e^{cN}} \exp\left[cN\sum_{i=1}^M \left(\sum_{r=1}^p (\beta + \delta\beta_r)T_{\mathrm{c}}(h) \sum_{\alpha=(r,1)}^{(r,n_r)} \delta_{i,i_\alpha}\right)^2\right] \tag{G12}$$

In a given configuration of the system, $n_{\mathrm{tot}} = n_1 + \ldots n_p$ replicas are divided into l clusters of sizes m_I ($I = 1, \ldots, l$). Then we find the exponent in the r.h.s. of the last equation can be expanded as,

$$cN\sum_{i=1}^M \left(\sum_{r=1}^p (\beta + \delta\beta_r)T_{\mathrm{c}}(h) \sum_{\alpha=(r,1)}^{r,n_r} \delta_{i,i_\alpha}\right)^2 = cN(\beta T_{\mathrm{c}}(h))^2 \sum_{I=1}^l m_I^2$$

$$+2cN(\beta T_{\mathrm{c}}(h))\sum_{r=1}^p \delta\beta_r T_{\mathrm{c}}(h) \sum_{\alpha=(r,1)}^{(r,n_r)} m_{I(\alpha)} + cN\sum_{r,s=1}^p (\delta\beta_r T_{\mathrm{c}}(h))(\delta\beta_s T_{\mathrm{c}}(h)) \sum_{\alpha=(r,1)}^{(r,n_r)} \sum_{\beta=(s,1)}^{(s,n_s)} \delta_{i_\alpha,i_\beta} \tag{G13}$$

Here $I(\alpha)$ used in the 2nd term on the r.h.s. denotes the label of the cluster to which the replica α belong to.

Apparently the 3rd term on the r.h.s. of the above equation generates a 2nd order term $O((\delta\beta)^2)$ in the effective action of the generating functional quite similar to the one in Eq. (85). It can yield a spurious finite heat capacity and a spurious temperature-chaos below $T_c(h)$. However we know for sure that $O(N)$ heat capacity is 0 (See Eq. (B12)) and temperature-chaos is absent in REM since temperature-changes cannot induce any level crossings of free-energies in the origianl version of the REM (See [27] for a related discussion). Thus in the present REM the $O((\delta\beta)^2)$ term must be cancelled.

Now we consider effects of fluctuations of the size of clusters. Note that the 2nd term on the r.h.s. of Eq. (G13) can be decomposed as,

$$2cN(\beta T_c(h)) \sum_{r=1}^{p} \delta\beta_r T_c(h) \sum_{\alpha=(r,1)}^{(r,n_r)} m_{I(\alpha)} = 2cN(\beta T_c(h)) \sum_{r=1}^{p} \delta\beta_r T_c(h) n_r m^*(\lambda) + 2cN(\beta T_c(h)) \sum_{I=1}^{l} \delta m_I \sum_{\alpha\in\mathcal{C}_I} \delta\beta_\alpha T_c(h).$$

(G14)

where $\delta\beta_\alpha$ is the *probing field* applied to replica α. Here we find the probing field $\delta\beta_r$ in a cluster C_I is linearly coupled to fluctuation of m_I.

Exponentiating the 2nd term in the r.h.s. of Eq. (G14) and applying the measure for the fluctuation of δm_I given in Eq. (G11) we obtain,

$$\prod_{I=1}^{l} \int d\delta m_I e^{cN(\beta T_c(h))^2 \delta m_I^2} \exp\left[2cN(\beta T_c(h)) \sum_{I=1}^{l} \delta m_I \sum_{\alpha\in\mathcal{C}_I} \delta\beta_\alpha T_c(h)\right]$$

$$= \exp\left[-cN \sum_{I=1}^{l} \sum_{\alpha\in C_I, \beta\in C_I} (\delta\beta_\alpha T_c(h))(\delta\beta_\beta T_c(h))\right] \prod_{I=1}^{l} \int d\delta m_I' e^{cN(\beta T_c(h))^2 (\delta m_I')^2}$$

$$= \exp\left[-cN \sum_{r,s=1}^{p} (\delta\beta_r T_c(h))(\delta\beta_s T_c(h)) \sum_{\alpha=(r,1)}^{(r,n_r)} \sum_{\beta=(s,1)}^{(s,n_s)} \delta_{i_\alpha, i_\beta}\right] \prod_{I=1}^{l} \int d\delta m_I' e^{cN(\beta T_c(h))^2 (\delta m_I')^2} \qquad (G15)$$

in the last equations we changed the integration variable to $\delta m_I' = \delta m_I + \sum_{\alpha\in C_I} \frac{\delta\beta_\alpha}{\beta}$. The last result implies we have another 2nd order term in the action

$$-cN \sum_{r,s=1}^{p} (\delta\beta_r T_c(h))(\delta\beta_s T_c(h)) \sum_{\alpha=(r,1)}^{(r,n_r)} \sum_{\beta=(s,1)}^{(s,n_s)} \delta_{i_\alpha, i_\beta}$$

which exactly cancels the other 2nd order term in the action, i.e. 3rd term on the r.h.s. of Eq. (G13). In another word, the effective variable Eq. (20) of the energies is

$$\Delta_{\text{eff}} = 0. \qquad (G16)$$

As the result we obtain the generating function for the fluctuations of energies as,

$$\left[Z_1^{n_1} Z_2^{n_2} \ldots Z_p^{n_p}\right] = \exp\left[cN \frac{n_{\text{tot}}}{m} \left\{1 + \left(\frac{T_c(h)}{T/m}\right)^2\right\}\right] \sideset{}{'}\sum_{\text{SP}} \exp\left[2cN \sum_{r=1}^{p} \delta\beta_r T_c(h) n_r\right]. \qquad (G17)$$

where the sum $\sum_{\text{SP}}'$ stands for summation over all saddle points where n_{tot} replicas are grouped into n_{tot}/m clusters of size m. Here m is the saddle point value given in Eq. (78) (See also Eq. (G9)). The $O(\delta\beta)$ term in the 2nd exponent is due to the 1st term in the r.h.s. of Eq. (G14).

It can be seen easily that the $O(\delta\beta)$ term in the action generates the correct average energy

$$E/N = \frac{\partial\beta F}{\partial\beta} = -2cT_c(h) \qquad (G18)$$

in agreement with the one obtained from the thermodynamic free-energy (See Eq. (B9)). The absence of the 2nd order term $O(\delta\beta)^2$ in the action means that heat capacity is indeed zero at $O(N)$ and also absence of temperature-chaos, as it should be in REM.

3. Generating functional for correlation functions of Y

Now let us consider fluctuations of the variable Y and construct a generating functional for its correlation functions. We consider again p real replicas $r = 1, \ldots, p$, which are replicated further into n_r replicas, at the same temperature but at slightly different fields $h + \delta h_r$.

$$\left[Z_1^{n_1} \cdots Z_p^{n_p} \right] = \sum_{i_{(1,1)}, \ldots, i_{(p,n_p)}=1}^{M=e^{cN}} \exp\left[cN(\beta T_c^0)^2 \sum_{\alpha, \beta} \delta_{i_\alpha, i_\beta} + \frac{N\Delta^2}{2} \sum_{i=1}^{M} \left(\sum_{r=1}^{p} \beta(h + \delta h_r) \sum_{\alpha=(r,1)}^{(r,n_r)} \delta_{i,i_\alpha} \right)^2 \right] \quad \text{(G19)}$$

Note T_c^0 is the critical temperature at $h = 0$ given by Eq. (B8) and Δ is the variance of the original Y variable.

The 2nd term in the exponent of the r.h.s of the last equation can be expanded as,

$$\frac{N\Delta^2}{2} \sum_{i=1}^{M} \left(\sum_{r=1}^{p} \beta(h + \delta h_r) \sum_{\alpha=(r,1)}^{r,n_r} \delta_{i,i_\alpha} \right)^2 = \frac{N\Delta^2}{2} (\beta h)^2 \sum_{I=1}^{l} m_I^2$$

$$+ N\Delta^2 (\beta h) \sum_{r=1}^{p} (\beta \delta h_r) \sum_{\alpha=(r,1)}^{(r,n_r)} m_{I(\alpha)} + \frac{N\Delta^2}{2} \sum_{r,s=1}^{p} (\beta \delta h_r)(\beta \delta h_s) \sum_{\alpha=(r,1)}^{(r,n_r)} \sum_{\beta=(s,1)}^{(s,n_s)} \delta_{i_\alpha, i_\beta} \quad \text{(G20)}$$

Note that the 2nd term on the r.h.s. of Eq. (G20) can be decomposed as,

$$N\Delta^2 (\beta h) \sum_{r=1}^{p} \beta \delta h_r \sum_{\alpha=(r,1)}^{(r,n_r)} m_{I(\alpha)} = N\Delta^2 (\beta h) \sum_{r=1}^{p} \delta \beta_r n_r m^*(\lambda) + N\Delta^2 (\beta h) \sum_{I=1}^{l} \delta m_I \sum_{\alpha \in \mathcal{C}_I} \beta \delta h_\alpha. \quad \text{(G21)}$$

where δh_α is the probing field applied to replica α. Here again we find the probing field δh_r in a cluster C_I is linearly coupled to fluctuation of m_I.

It can be seen that the coupling between the fluctuations of the size of clusters and δh_r is absent *only* in the special case that the applied external field $h = 0$. Note also that such a situation never happens for the case of energies (See Eq. (G21)) in the whole glass phase $T < T_c(h)$.

Exponentiating the 2nd term in the r.h.s. of Eq. (G21) and applying the measure for the fluctuation of δm_I given in Eq. (G11) we obtain,

$$\prod_{I=1}^{l} \int d\delta m_I e^{cN(\beta T_c(h))^2 \delta m_I^2} \exp\left[N\Delta^2 (\beta h) \sum_{I=1}^{l} \delta m_I \sum_{\alpha \in \mathcal{C}_I} \beta \delta h_\alpha \right]$$

$$= \exp\left[-\frac{N\Delta^4}{4c} \left(\frac{h}{T_c(h)} \right)^2 \sum_{I=1}^{l} \sum_{\alpha \in C_I, \beta \in C_I} (\beta \delta h_\alpha)(\beta \delta h_\beta) \right] \prod_{I=1}^{l} \int d\delta m_I' e^{cN(\beta T_c(h))^2 (\delta m_I')^2}$$

$$= \exp\left[-\frac{N\Delta^4}{4c} \left(\frac{h}{T_c(h)} \right)^2 \sum_{r,s=1}^{p} (\beta \delta h_r)(\beta \delta h_s) \sum_{\alpha=(r,1)}^{(r,n_r)} \sum_{\beta=(s,1)}^{(s,n_s)} \delta_{i_\alpha, i_\beta} \right] \prod_{I=1}^{l} \int d\delta m_I' e^{cN(\beta T_c(h))^2 (\delta m_I')^2} \quad \text{(G22)}$$

in the last equations we changed the integration variable to $\delta m_I' = \delta m_I + \sum_{\alpha \in C_I} \frac{\Delta^2}{2c(\beta T_c(h))^2} (\beta h)(\beta \delta h_\alpha)$. The last result implies we have another 2nd order term in the action

$$-\frac{N\Delta^4}{4c} \left(\frac{h}{T_c(h)} \right)^2 \sum_{r,s=1}^{p} (\beta \delta h_r)(\beta \delta h_s) \sum_{\alpha=(r,1)}^{(r,n_r)} \sum_{\beta=(s,1)}^{(s,n_s)} \delta_{i_\alpha, i_\beta}$$

Combining with the 3rd term on the r.h.s. of Eq. (G20) and using Eq. (B8) we obtain the total $O(\delta h)^2$ term to be,

$$\frac{N(\Delta_{\text{eff}})^2}{2} \sum_{r,s=1}^{p} (\beta \delta h_r)(\beta \delta h_s) \sum_{\alpha=(r,1)}^{(r,n_r)} \sum_{\beta=(s,1)}^{(s,n_s)} \delta_{i_\alpha, i_\beta}$$

with "renormalized variance"

$$\Delta_{\text{eff}} \equiv \frac{\Delta}{\sqrt{1 + (h\Delta)^2}} \tag{G23}$$

Note that this coincides with Eq. (B4).

Now collecting also the 1st term in the r.h.s of Eq. (G21) we finally obtain,

$$\left[Z_1^{n_1} Z_2^{n_2} \ldots Z_p^{n_p} \right] = \quad \exp\left[cN \frac{n_{\text{tot}}}{m} \left\{ 1 + \left(\frac{T_c(h)}{T/m} \right)^2 \right\} \right]$$

$$\sum_{\text{SP}} \exp\left[N\Delta^2 m(\beta h) \sum_{r=1}^{p} \delta\beta_r n_r + \frac{N}{2}(\Delta_{\text{eff}})^2 \sum_{r,s=1}^{p} \beta\delta h_r \beta\delta h_s \sum_{\alpha=(r,1)}^{(r,n_r)} \sum_{\beta=(s,1)}^{(s,n_s)} \delta_{i_\alpha, i_\beta} \right]. \tag{G24}$$

It can be seen easily that the $O(\delta h)$ term in the action generates the average

$$[\![\langle Y \rangle]\!] = -\frac{\partial F}{\partial h} = N\Delta^2 \frac{T}{T_c(h)} \tag{G25}$$

with Δ being the variance of the original Y variable. It agrees precisely with the thermodynamic one Eq. (B10)). Moreover the $O((\delta h)^2)$ generates the average linear susceptibility which also agrees with the thermodynamic one Eq. (B11).

[1] S. Nagata, P. H. Keesom and H. R. Harrison, Phys. Rev B **19**, 1633 (1979).
[2] E. Vincent, J. Hammann, M. Ocio, J.-P. Bouchaud and L.F. Cugliandolo: in *Proceeding of the Sitges Conference on Glassy Systems*, Ed.: E. Rubi (Springer, Berlin, 1996) cond-mat/9607224.
[3] P. Nordblad and P. Svedlindh, in "Spin Glasses and Random Fields", *Series on Directions in Condensed Matter Physics* Vol.12, A.P. Young Editor, World Scient. 1998 pp.1-27 and the references there in.
[4] K. Jonason, E. Vincent, J. Hammann, J.-P. Bouchaud, and P. Nordblad, Phys. Rev. Lett. **81**, 3243 (1998).
[5] E. Vincent, J. P. Bouchaud, D. S Dean, and J. Hammann, Phys. Rev. B **52**, 1050 (1995).
[6] L.C. Struick, Physical Aging in Amorphous Polymers and Other Materials (Elsevier, New York, 1978).
[7] W.K. Waldron, Jr. and G.B. McKenna, M.M. Santore, J. Rheol. 39,471 (1995).
[8] L. Bellon, S. Ciliberto, and C. Laroche, Eur. Phys. J. B **25**, 223 (2002).
[9] K. Fukao and A. Sakamoto, Phys. Rev. E **71**, 041803 (2005).
[10] E. V. Colla , L. K. Chao, M. B. Weissman, and D. D. Viehland, Phys. Rev. Lett. **85** 3033 (2000), E. V. Colla, L. K. Chao, and M. B. Weissman, Phys. Rev. B **63**, 134107 (2001).
[11] A. Levstik, C. Filipic, Z. Kutnjak, I. Levstik, R. Pirc, B. Tadić, and R. Blinc, Phys. Rev. Lett. **66** 2368 (1991).
[12] A. J. Bray and M. A. Moore, Phys. Rev. Lett. **58** 57 (1987).
[13] D. S. Fisher and D. A. Huse, Phys. Rev. **B 38** 386 (1988).
[14] D. S. Fisher and D. A. Huse, Phys. Rev. **B 43** 10728 (1991).
[15] T. R. Kirkpatrick, D. Thirumalai and P. G. Wolynes, Phys. Rev. A **40** 1045 (1989).
[16] M. B. Weissman, Rev. Mod. Phys. **65**, 829 (1993).
[17] K. A. Meyer and M. B. Weissman, Phys. Rev. B **51** 8221 (1995).
[18] C. A. Bolle, V. Aksyuk, F. Hard, P. L. Gammel, E. Zeldov, E. Bucher, R. Boie, D. J. Bishop and D. R. Nelson, Nature **399**, 43 (1999).
[19] E. Vidal Russell and N. E. Israeloff, Nature**408** 695 (2000).
[20] S. Kirkpatrick and A. P. Young, J. Apple. Phys. **52** 1712 (1981).
[21] A. P. Young, A. J. Bray and M. A. Moore, J. Phys. C 17, L149 (1984).
[22] M. Mézard, J. Phys. I. (France) **51** 1831 (1990).
[23] T. Hwa and D.S. Fisher, Phys. Rev. **B 49**, 3136 (1994) .
[24] F. Krzakala and O. C. Martin, Eur. Phys. J. B **28**, 199 (2002).
[25] B. Derrida, Phys. Rev. **B 24** 2613 (1981).
[26] T. Rizzo and H. Yoshino, Phys. Rev. B 73, 064416 (2006).
[27] I. Kurkova, J. Stat. Phys. **111**,112. (2003).
[28] D. J. Thouless, P. W. Anderson and R. G. Palmer, Philosophical Magazine, **35**, (1977) p. 593.
[29] W. Selke, in Phase Transitions and Critical Phenomena vol 15, Academic Press, London (1992).
[30] L. Balents, J. P. Bouchaud and M. Mézard, J. Phys. I. France **6** 1007 (1996).
[31] S. Kida, J. Fluid. Mech. **93** 337 (1979).
[32] J. P. Bouchaud, M. Mézard and G. Parisi, Phys. Rev. E **52**3656 (1995).

[33] J. P. Bouchaud and M. Mézard. J. Phys. **A 30**, 7997 (1997).

[34] S. R. McKay, A. N. Berker, and S. Kirkpatrick, Phys. Rev. Lett. **48**, 767 (1982).

[35] G. Parisi, Phys. Rev. Lett. 50, 1946 (1983).

[36] I. Kondor, J. Phys. A22, L163(1989).

[37] T. Rizzo and A. Crisanti, Phys. Rev. Lett. **90** 137201 (2003).

[38] T. R. Kirkpatrick and D. Thirumalai, Phys. Rev. B **36** 5388 (1987), T. R. Kirkpatrick and P. G. Wolynes, Phys. Rev. A **35** 3072 (1987).

[39] J-P. Bouchaud, L. F. Cugliandolo, J. Kurchan and M. Mézard in *Spin-glasses and random fields*, edited by A. P. Young, (World Scientific, Singapore, 1997)

[40] T. Castellani and A. Cavagna, J. Stat. Mech. 05012 (2005).

[41] L. Balents, P. Le Doussal, Annals of Physics, **315** 213 (2005).

[42] U. Shulz, J. Villain, E. Brézin, and H. Orland, J. of Stat. Phys. bf 51 1 (1988).

[43] A. A. Middleton, P. Le Doussal and K. J. Wiese, Phys. Rev. Lett. **98** 155701 (2007).

[44] D. J. Gross and M. Mézard, Nucl. Phys. **B240** 431 (1984).

[45] C. De Dominicis and A. P. Young, J. Phys. A 16, 2063 (1983).

[46] M. Mézard, G. Parisi, and M.A. Virasoro, "Spin glass theory and beyond", World Scientific (Singapore 1987).

[47] M. Sales and H. Yoshino, Phys. Rev. E **65**, 066131 (2002).

[48] F. Krzakala and JP Bouchaud, Eur. Phys. Lett. **72** 472 (2005).

[49] H. G. Katzgraber, F. Krzakala, Phys. Rev. Lett. **98**, 017201 (2007).

[50] M. Sasaki, K. Hukushima, H. Yoshino, H. Takayama, Phys. Rev. Lett. **95**, 267203 (2005).

[51] P. E. Jönsson, H. Yoshino, P. Nordblad, Phys. Rev. Lett. 89 097201 (2002) and Phys. Rev. Lett. 90 059702 (2003).

[52] P. E. Jönsson, R. Mathieu, P. Nordblad, H. Yoshino, H. Aruga Katori and A. Ito, Phs. Rev. B. **70** 174402 (2004).

[53] R. Monasson, Phys. Rev. Lett. **75** (1995) 2847.

[54] E. Bertin, Phys. Rev. Lett. **95** 170601 (2005).

[55] S. Franz and M. A. Virasoro, J. Phys. A **33** 891 (2000).

[56] T. Temesvari, C. De Dominicis, I. Kondor, J. Phys. A **27** 7569 (1994).

[57] Th. M. Nieuwenhuizen, J. Physique, I **6** 191 (1996).

[58] M. E. Ferrero, G. Parisi and P. Ranieri, J. Phys. A. **29** L569 (1996).

[59] M. Campellone, G. Parisi and M. A. Virasoro, unpublished.

[60] To avoid confusions we should note that the free-energies F_l themselves follow the Gumbell distributions [33, 54].

[61] Note that in the 1) FDT approach, the situation was somewhat simpler since only some finte number of the solutions in the summation $\sum_{\text{SP}}$ remained which could be collected diagramatically.